



VYSOKÉ UČENÍ TECHNICKÉ V BRNĚ
BRNO UNIVERSITY OF TECHNOLOGY



FAKULTA CHEMICKÁ
ÚSTAV FYZIKÁLNÍ A SPOTŘEBNÍ CHEMIE

FACULTY OF CHEMISTRY
INSTITUTE OF PHYSICAL AND APPLIED CHEMISTRY

RHEOLOGY OF HYALURONAN SOLUTIONS

REOLOGIE ROZTOKŮ HYALURONANU

DOKTORSKÁ PRÁCE
DOCTORAL THESIS

AUTOR PRÁCE
AUTHOR

Mgr. HELENA BILEROVÁ

VEDOUCÍ PRÁCE
SUPERVISOR

Prof. Ing. MILOSLAV PEKAŘ, CSc.

BRNO 2012



Vysoké učení technické v Brně
Fakulta chemická
Purkyňova 464/118, 61200 Brno 12

Zadání dizertační práce

Císlo dizertační práce:	FCH-DIZ0058/2011	Akademický rok: 2011/2012
Ústav:	Ústav fyzikální a spotřební chemie	
Student(ka):	Mgr. Helena Bilerová	
Studijní program:	Fyzikální chemie (P1404)	
Studijní obor:	Fyzikální chemie (1404V001)	
Vedoucí práce	prof. Ing. Miloslav Pekař, CSc.	
Konzultanti:		

Název dizertační práce:

Reologie roztoků hyaluronanu

Zadání dizertační práce:

Prostudovat reologické vlastnosti roztoků hyaluronanu v závislosti na molekulové hmotnosti a teplotě.

Termín odevzdání dizertační práce: 30.6.2012

Dizertační práce se odevzdává ve třech exemplářích na sekretariát ústavu a v elektronické formě vedoucímu dizertační práce. Toto zadání je přílohou dizertační práce.

Mgr. Helena Bilerová
Student(ka)

prof. Ing. Miloslav Pekař, CSc.
Vedoucí práce

prof. Ing. Miloslav Pekař, CSc.
Ředitel ústavu

V Brně, dne 30.8.2005

prof. Ing. Jaromír Havlica, DrSc.
Děkan fakulty

ABSTRACT

Present work is focused on rheological properties of hyaluronan solutions. It studies the solutions behavior in dependence on changing Mw and concentration. Also the effect of different solvents and the increasing pH on viscosity of HA solutions is described. In the second part, the effect of increasing temperature is discussed. Finally (but not less important) the dissolving of hyaluronan powder, the time stability of prepared solutions and presence of aggregates are studied. All of these experiments are very useful from the practical point of view, e.g. during the production, sterilization and storage of hyaluronan solution.

KEY WORDS

hyaluronan, rheology, viscosity

ABSTRAKT

Předložená práce se zabývá reologickými vlastnostmi roztoků hyaluronanu. Studuje chování hyaluronanových roztoků v závislosti na jejich Mw a koncentraci. Dále popisuje vliv prostředí několika rozpouštědel a vliv měnícího se pH na viskozitu hyaluronanových roztoků. V druhé části je studován vliv rostoucí teploty na viskozitu roztoků. V neposlední řadě je zkoumána správná příprava roztoků, jejich časová stabilita a tvorba agregátů. Všechny experimenty vycházejí z praktického upotřebení, např. při výrobě hyaluronanu, jeho sterilizaci a následném skladování roztoků.

KLÍČOVÁ SLOVA

hyaluronan, reologie, viskozita

Bilerova H., Rheology of hyaluronan solutions, Brno, 2012, 109 p. The thesis on faculty of chemistry, Brno University of Technology, Institute of Physical and Applied Chemistry. The head of the thesis Prof. Ing. Miloslav Pekař, CSc.

Declaration

I declare that I have developed this thesis independently and that all the literary sources I quoted correctly and completely. The thesis is in terms of content owned by the Faculty of Chemistry, BUT and may be used for commercial purposes only with the agreement of the head of the thesis and the dean of FCH, BUT.

Signature

ACKNOWLEDGEMENT

First and foremost I would like to thank to people whose gave me the opportunity to pursue this topic and write down this thesis, Dr. Vladimír Velebný, CSc. and Prof. Ing. Miloslav Pekař, CSc.

I would like to thank to my colleagues Jaroslav Novotný for particle size measurements and Mgr. Daniela Šmejkalová, PhD. for NMR measurement and discussion of the spectra.

Lastly, I would like to thank to my husband for his help with statistical evaluation of the data, my family for baby-sitting and encouragement and to my daughters, they were such a patient and good girls.

CONTENT

1	INTRODUCTION.....	9
2	THEORETICAL BACKGROUND.....	10
2.1	Chemical structure of hyaluronan	10
2.1.1	Historical perspective	10
2.1.2	Structure of hyaluronan in solid state	12
2.1.3	Structure of hyaluronan in aqueous solutions.....	13
2.2	Polysaccharide hydration	17
2.2.1	Dissolving of HA.....	18
2.2.2	Aggregates.....	19
2.3	Rheology.....	21
2.3.1	Basic terms	21
2.3.2	Rheological instruments for fluids.....	22
2.3.3	Flow of the fluids	26
2.3.4	Rheology of hyaluronan	27
2.4	Particle size measurements	31
2.4.1	Static light scattering	31
2.4.2	Dynamic light scattering	32
2.4.3	The size of particles in HA solutions.....	32
2.5	Surface tension and ionic conductivity.....	33
2.5.1	Ionic conductivity	33
2.5.2	Surface tension	33
3	EXPERIMENTAL PART.....	36
3.1	Materials and methods	36
3.1.1	Chemicals	36
3.1.2	Laboratory aids	37
3.1.3	Instruments	37
3.1.4	Methods	40
3.1.5	Statistical evaluation of experimental data.....	47
4	RESULTS AND DISCUSSION.....	48
4.1	Dissolution of HA powder	48
4.2	Preliminary rheological measurements.....	49

4.2.1	Flow curves.....	49
4.2.2	Temperature ramp	50
4.3	The flow curves.....	53
4.3.1	The effect of Mw and concentration.....	53
4.3.2	HMW HA.....	57
4.3.3	Comparison of VLMW and HMW HA.....	59
4.3.4	The effect of solvent.....	61
4.3.5	The effect of pH.....	62
4.4	The temperature curves	63
4.4.1	LMW HA.....	64
4.4.2	HMW HA.....	66
4.5	Other physical chemical methods.....	71
4.5.1	1D NMR and UV VIS spectra of VLMW HA.....	71
4.5.2	UV-VIS spectra	75
4.5.3	The size of particles in VLMW HA solutions	76
4.6	The time stability of hyaluronan.....	78
4.6.1	Hyaluronan in water	78
4.6.2	Hyaluronan in phosphate buffer	81
4.6.3	Aggregates.....	83
5	CONCLUSION.....	86
6	LIST OF ABBREVIATIONS AND SYMBOLS.....	88
7	LITERATURE.....	90
8	APPENDIX 1 - STATISTICAL EVALUATION OF EXPERIMENTAL DATA.....	98
8.1	Basic principles	98
8.2	Interpretation of analysis of variance table	98
8.3	Flow curves of hyaluronan.....	99
8.4	Temperature curves	105
9	APPENDIX 2 – PUBLICATION ACTIVITY.....	109

1 INTRODUCTION

Hyaluronan is a high molecular weight unbranched glycosaminoglycan, composed of repeating disaccharides (β 1-3 D-N-acetylglucosamine, β 1-4 D-glucuronic acid). It is a widely distributed component of the extracellular matrix of vertebrate tissues.¹

In the last 20 years, scientific attitudes have changed from regarding it only as a molecular cotton wool that fills certain extracellular spaces to ones that also view it as a center around which many matrix macromolecules are organized. A great range of biological functions has been imputed to the molecule, and it has importance from numerous physiological, clinical and diagnostic aspects. Its structural simplicity, span in molecular weight range and unique mode of synthesis mark it as a molecule of distinctive evolutionary significance. To date, no naturally acetylated, sulfated or other modified variants have been discovered.

Hyaluronan has many roles, some requiring its presence in minute quantities (*e.g.*, as a proteoglycan organizer in cartilage) whereas in others, it is the dominant structural entity (*e.g.*, its presence in vitreous, Wharton's jelly or synovial fluid). Thus, hyaluronan function may vary greatly depending on whether its interactions are predominantly with proteins in tertiary and quaternary organizations or with water and ions making viscous solutions or gels.

This work is focused on physical properties of wide range of molecular weight hyaluronan in solution, which means the range of studies Mw is approximately between 10 000 – 2 600 000 g/mol.

In theoretical part, the research on hyaluronan conformation and rheological measurements from the 1934, when the hyaluronan molecule was discovered, to these days is summarized.

The experimental part is concerned with the behavior of HA chains in solution and tries to compare the effect of Mw, concentration and pH of solvent on hyaluronan conformation in the first part. The second part is focused on the temperature stability of hyaluronan aqueous and phosphate solutions. Finally, because of the importance for many applications, the dissolving and time stability studies of HA in solution were done and the presence of aggregates was observed.

2 THEORETICAL BACKGROUND

2.1 Chemical structure of hyaluronan

Hyaluronan (also called hyaluronic acid or hyaluronate) is an anionic, non-sulfated glycosaminoglycan distributed widely throughout connective, epithelial, and neural tissues.

Its name, hyaluronic acid, is derived from hyalos (Greek for vitreous) and uronic acid because it was first isolated from the vitreous humour and possesses high uronic content.

The term hyaluronate refers to the conjugate base of hyaluronic acid. Because the molecule typically exists in vivo in its polyanionic form, it is most commonly referred to as hyaluronan.

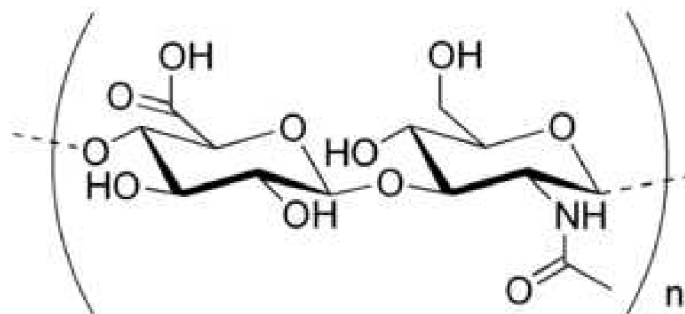


Fig. 1 The repeating disaccharide unit of hyaluronan

Hyaluronan is a polymer of disaccharides, themselves composed of D-glucuronic acid and D-N-acetylglucosamine, linked together via alternating β -1,4 and β -1,3 glycosidic bonds. Hyaluronan can be 25 000 disaccharide repeats in length. Polymers of hyaluronan can range in size from 5 000 to 20 000 g/mol in vivo. The average molecular weight in human synovial fluid is 3-4 million g/mol, and for example hyaluronan purified from human umbilical cord is 3 140 000 g/mol.²

2.1.1 Historical perspective

HA was initially discovered and named hyaluronic acid in a paper published in 1934 in laboratory of Karl Meyer (Fig.2).³ It was isolated from vitreous of the eye as a polysaccharide containing D-glucuronic acid and D-N-acetylglucosamine, but it was not until 20 years later that was completed the determination of its structure and showed that it contained a repeating β 1-3, β 1-4 linked disaccharide. In the meantime, HA was isolated from many tissue sources, including synovial fluid, cock's comb and umbilical cord. Its extraction from tissues was not easy and HA preparations always retained some protein.⁴⁻⁶



Fig.2 Karl Meyer. Photo from⁷

The issue of HA's covalent link to protein as a requirement for biosynthesis was finally resolved with the discovery of the mechanism of biosynthesis of HA⁸ and the subsequent cloning of the HA synthase enzyme,⁹ which showed that HA could be made without any protein primer. HA has thus evolved from quite a different evolutionary origin from the other structurally related glycosaminoglycans, which are synthesized attached to proteins and whose chains are extended by single sugar addition to the non-reducing end of each chain.

From its initial isolation, the physical properties of HA have been the dominant feature that distinguished it from other components of extracellular matrix. In the early work characterizing HA, even including the simple determination of its molecular weight presented great difficulty. The properties of HA provided a challenge to the classical biophysical methods, in which simple analysis was developed for proteins and required that the properties approached those of perfect Newtonian solutes. The behavior of HA in solutions even at low concentration is far from Newtonian or 'ideal', and it presented a challenge in the 1950s and 1960s that some very distinguished researchers took up, notably Sandy Ogston, Torvard Laurent, Endre Balazs and later Bob Cleland.¹⁰⁻¹⁷ Their work established a theoretical and experimental framework that underpins HA research to this day.

The key elements they identified were:

- It was a high molecular weight unbranched polysaccharide, which behaved as a stiffened random coil in solution (Fig. 3)
- It occupied a large hydrated volume and therefore showed solute – solute interactions at unusually low concentration.
- It showed excluded volume effects, as it restricted access to this domain by other macromolecules.
- These properties were compounded by the fact that HA was a polyelectrolyte and therefore the solution properties were also greatly affected by ionic strength.
- HA was also established to be polydisperse and its properties were therefore the aggregate properties of a population of molecules of varying chain length, rather than those of a unique species.

An important early development in this process was the recognition of the need to extrapolate experimental results to vanishingly low concentrations in order to determine intrinsic properties and free the measured parameters from non-ideal effects caused by interaction between adjacent molecules.

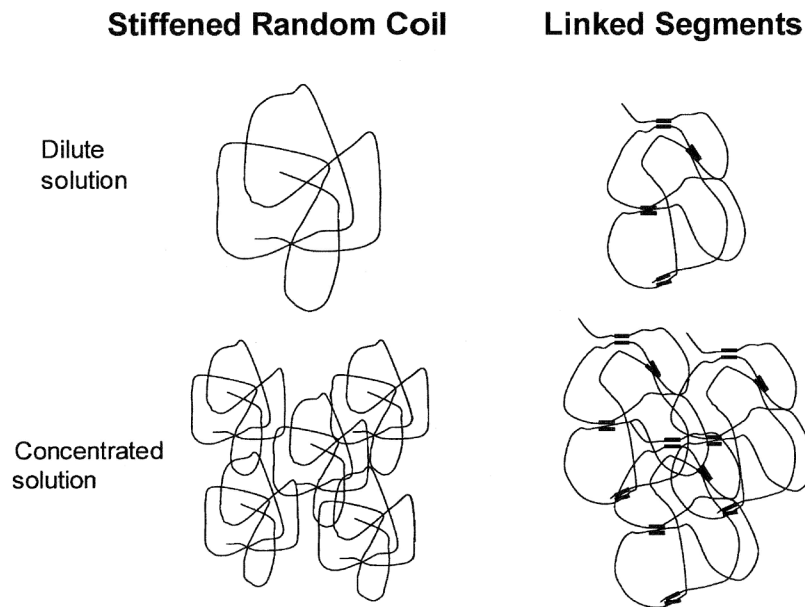


Fig. 3 Models of hyaluronan behavior in solution.

In dilute solution, hyaluronan behaves as a stiffened random coil. The presence of linked segments would act in opposition to chain stiffening in determining the hydrated domain. In concentrated solutions, stiffened random coils show entanglement; they form viscoelastic solutions and retain flow and do not become gels. The presence of linked segments would create a network and lead to gel formation.

2.1.2 Structure of hyaluronan in solid state

Hyaluronan is energetically stable in part because of the stereochemistry of its component disaccharides. Bulky groups on each sugar molecule are in strictly favored positions, whereas the smaller hydrogens assume the less-favorable axial positions.

In the period from 1970 to 1985, a number of X-ray fiber diffraction studies were done on stretched, semi-hydrated fibers and films of different salt forms of hyaluronan. Some 6 different backbone structures were observed, and each of these could be trapped in a variety of packing arrangements.¹⁸ Of these structures, about 8 have been subjected to detailed X-ray refinement. In general, the quality of the data were good, as illustrated by three different diffraction patterns for the potassium salt of hyaluronan (Fig.4).¹⁸ Refinements of some of

these structures gave insight into the preferred chain conformations, molecular packing and ion and water coordination.¹⁹⁻²¹ The origin of these states and how they relate to each other experimentally have been summarized by Sheehan *et al.*¹⁸ Hyaluronan chains are generally found in extended 2-, 3- and 4-fold single helical forms. However, in the presence of the water 'structure-breaking' ions (NH₄, Cs, Rb and K at low pH) antiparallel, intertwining double helices were found.²² Fiber diffraction patterns obtained from potassium hyaluronan at pH 2.0 (a), pH 3-4.5 (b) and pH 5-8 (c). X-ray diffraction in (a) is consistent with an extended 2-fold helix conformation with an axial rise per disaccharide of 0.98 nm, but the structure has never been refined. Diffraction in (b) is consistent with a left - handed 4-fold helix conformation with an axial rise of 0.84 nm per disaccharide. These sinuous chains are organized as two antiparallel double helices in a tetragonal unit cell.²² Diffraction in (c) is consistent with an extended left - handed, 4-fold helix of axial rise 0.95 nm per disaccharide. Two of these chains are packed in a tetragonal unit cell.

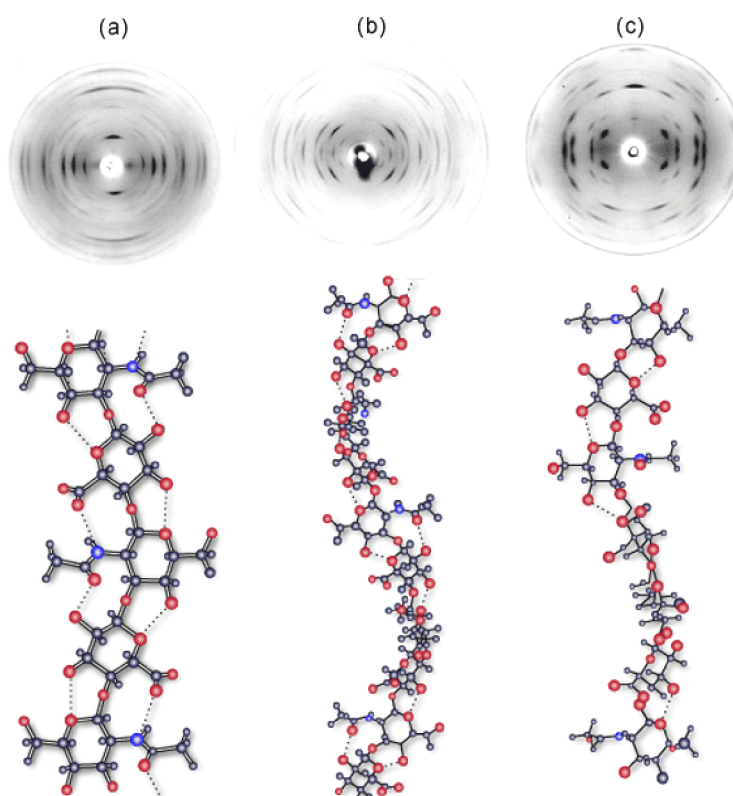


Fig. 4 X-ray fiber diffraction of potassium hyaluronan

2.1.3 Structure of hyaluronan in aqueous solutions

As mentioned above, the solution properties of HA have been investigated for about 60 years, without a clear consensus emerging. HA solutions have pronounced viscoelastic properties and the biophysical basis of its 'non-ideal' behavior has been the sources of much interest and speculation. At neutral pH and physiological ionic strength much of the early

work of the groups of Laurent and Balazs led to the conclusion that HA behaved as a stiffened random coil in solution with considerable local stiffness, and quite large persistence length.^{14,16} (Fig. 3). Later the stiffening was proposed to be at least in part due to hydrogen bonding between adjacent saccharides, combined with some effect from the mutual electrostatic repulsion between carboxyl groups²³⁻²⁶ and these proposals have been substantiated by later results using different techniques.²⁷⁻³⁰

Hascall et al. presented³¹ that in a physiological solution, the backbone of a hyaluronan molecule is stiffened by a combination of the chemical structure of the disaccharide, internal hydrogen bonds, and interactions with solvent. The axial hydrogen atoms form a non-polar, relatively hydrophobic face while the equatorial side chains form a more polar, hydrophilic face, thereby creating a twisting ribbon structure. Consequently, a hyaluronan molecule assumes an expanded random coil structure in physiological solutions which occupies a very large domain (Fig. 5). The actual mass of hyaluronan within this domain is very low, ~0.1% (w/v) or less when the macromolecule is present at a very dilute concentration in saline. This means that the domains of individual molecules would overlap each other at concentrations of 1 mg hyaluronan per ml or higher.

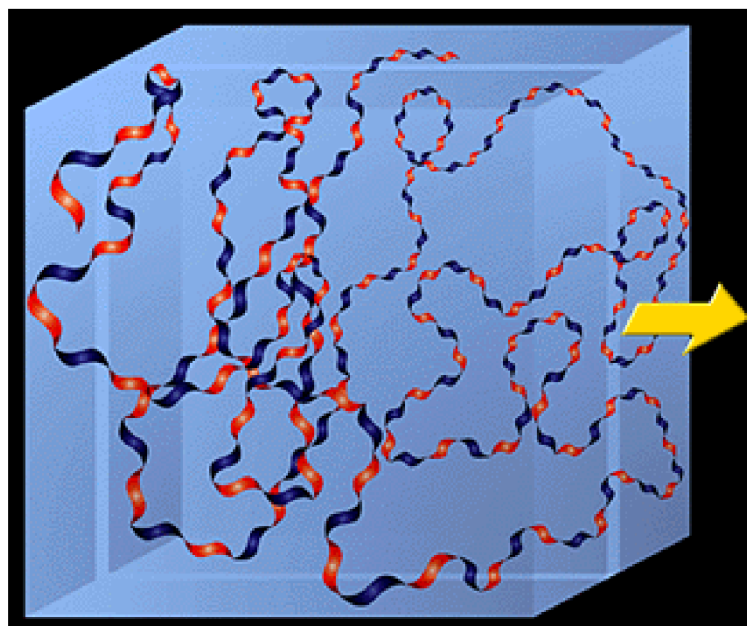


Fig. 5 Model of hyaluronan ribbon in a 3-dimensional domain. The light blue box represents the domain of the molecule in solution. The alternating blue and red strand represents the ribbon structure with blue (hydrophilic) and red (hydrophobic) faces.³¹

The domain structure of hyaluronan has interesting and important consequences. Small molecules such as water, electrolytes and nutrients can freely diffuse through the solvent within the domain. However, large molecules such as proteins will be partially excluded from the domain because of their hydrodynamic sizes in solution.³¹

The concentration of hyaluronan in tissues is often higher than would be expected if individual molecules maintained their expanded domain structures. In many cases the hyaluronan is organized into the extracellular matrix by specific interactions with other matrix macromolecules. However, high molecular weight hyaluronan at high concentration in solution (for example, $5 \cdot 10^6$ g/mol at concentrations above 0.1 mg/ml) can also form entangled molecular networks through steric interactions and self association between and within individual molecules. The latter can occur when a stretch of the hydrophobic face of the ribbon structure of the backbone interacts reversibly with the hydrophobic face on a comparable stretch of hyaluronan on another molecule or in a different region of the same molecule. Such networks exhibit different properties than would isolated hyaluronan molecules. They can resist rapid, short-duration fluid flow through the network, thereby exhibiting elastic properties which can distribute load or shear forces within the network (Fig. 6).³¹ On the other hand, slow fluid flow of longer duration can partially separate and align the molecules, allowing their movement and exhibiting viscous properties. Procedures for introducing covalent cross-links in hyaluronan matrices have been developed to create stable networks and semi-solid materials exhibiting pronounced viscoelastic properties.³¹

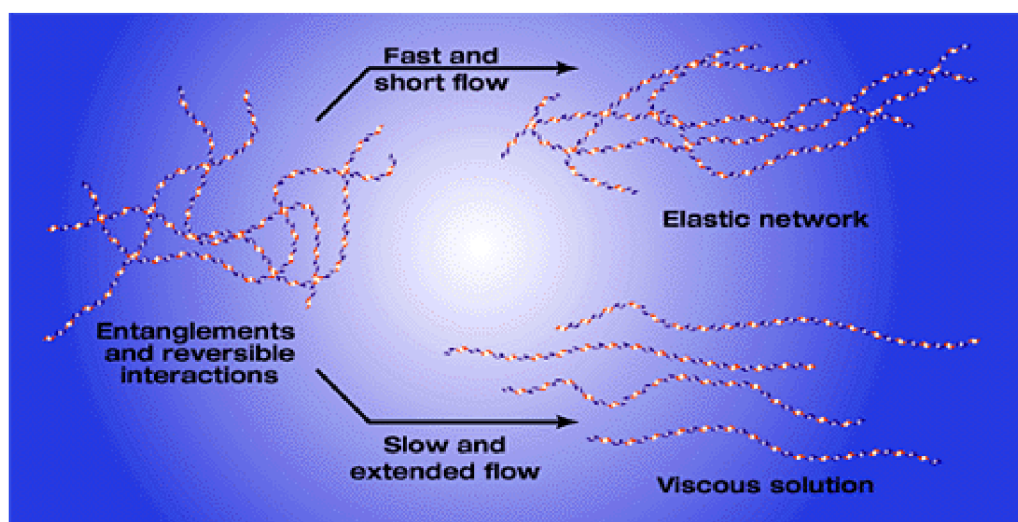


Fig. 6 Model demonstrating the viscous and elastic properties of hyaluronan solutions.³¹

However, this relatively simple model has in recent years been challenged by a proposal that HA chains self-associate and that this dominates the solution properties. The core evidence for this was in two strands. The first was that apparent association between HA chains was visualized in EM preparations and it was interpreted as anti-parallel double helices, bundles and ropes³²⁻³³ and the second was that NMR spectra demonstrated an extended hydrogen-bonded system, a twofold helix with elements of co-operativity that included water bridges between neighboring sugar residues.³⁴⁻³⁵ This structure seemed to account for chain stiffness and also for the observation that the high viscosity of HA reversibly and dramatically decreased at high pH.

However, the principal driver for this model of self-association was the observation that HA in a 2-fold helix could contain hydrophobic patches and these might provide sites for self-

association between chains.²⁷ It was suggested that these patches could be the basis of interactions with lipid membranes and with proteins, and also of self-aggregation.

With the premise that HA may self-associate, but the interactions may be weak and transient, Hardingham et al. investigated HA properties in concentrated solutions and looked for evidence of self-association.³⁶ For this study they used a newly developed technique, confocal-FRAP. An important aspect, and indeed the value, of using confocal-FRAP is that it permitted analysis at concentrations of HA up to and far exceeding the critical concentration at which there is predicted molecular domain overlap.³⁷ This analysis was thus ideally suited to investigations of entanglement and intermolecular chain-chain association, as these would be concentration-dependent and strongly favored at high concentration. Electrostatic and ionic effects on the HA network and its sensitivity to counter-ion type and valence were determined as these are known to greatly affect rheological and hydrodynamic properties.³⁸ The role of hydrogen bonds was investigated by comparing concentration-dependent solution properties in de-ionized water, 0.5 M NaCl and 0.5 M NaOH (Fig.7). The presence of HA chain-chain associations that might involve hydrophobic interactions were investigated under physiological conditions, in solvents of varying polarity and in the presence of chaotropic agents.^{18,36,37,39,40} Intermolecular chain-chain associations were also investigated using HA oligosaccharides as low molecular weight competitors of such interactions.⁴¹⁻⁴²

The results showed that in going from 0.5 M NaOH to de-ionized water, the apparent domains of HA chains were increased by more than 100 times and this most likely resulted from increased electrostatic interactions and hydrogen bond formation.³⁶

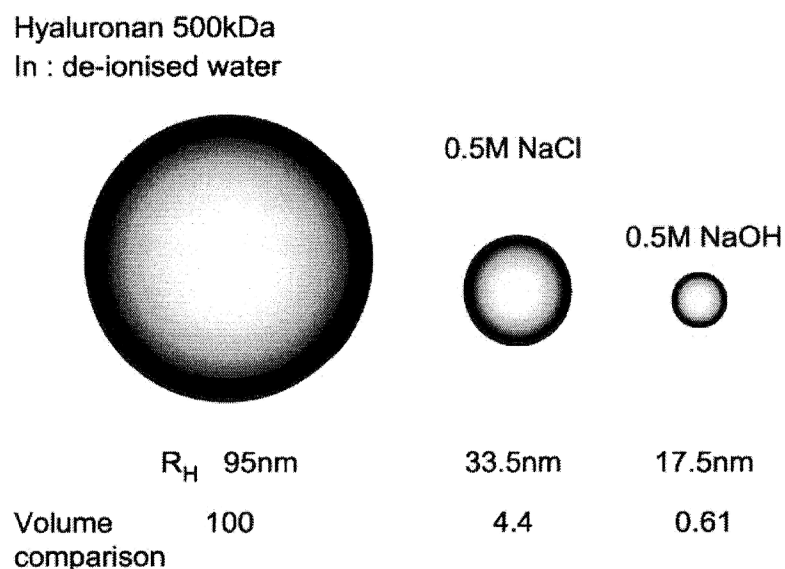


Fig. 7 Comparison of the hydrodynamic radius (R_H) of hyaluronan ($5 \cdot 10^5$ g/mol) in de-ionized water, salt and alkaline solutions.

The authors also suggested^{36,37} that intramolecular hydrogen bonds and polyanionic properties of HA both contribute to provide a highly expanded macromolecular conformation.

However, under physiological conditions of ionic strength the results predict the electrostatic effects to be modest.

To recapitulate it, HA in aqueous solutions exists as an extended random coil at low concentrations (<1 mg/ml),⁴³ allowing for free movement of the polymer chains.⁴⁴ At high concentrations (>1 mg/ml), a transient entanglement network arises where molecules entangle with each other and then disentangle after a period of time. This network is stabilized by hydrogen bonding and non-covalent intermolecular associations.⁴⁵ The network properties of HA at high concentration affect the viscoelasticity of the solution,⁴⁶ giving rise to enhanced viscosity and pronounced non-Newtonian behavior, manifested by a higher extent of shear thinning.^{39,47,48}

Similar effects have been noted as the molecular weight of HA in solution is increased for solutions of the same concentration.³⁹ Solutions of HA of molecular weight of 3 000 000 g/mol showed increased magnitudes of the viscous and elastic components of the complex viscosity, η' and η'' , respectively with frequency compared to solutions with HA of molecular weight of 500 000 g/mol at the same concentration.⁴⁹ However, the increase was more pronounced for the elastic component, η'' .

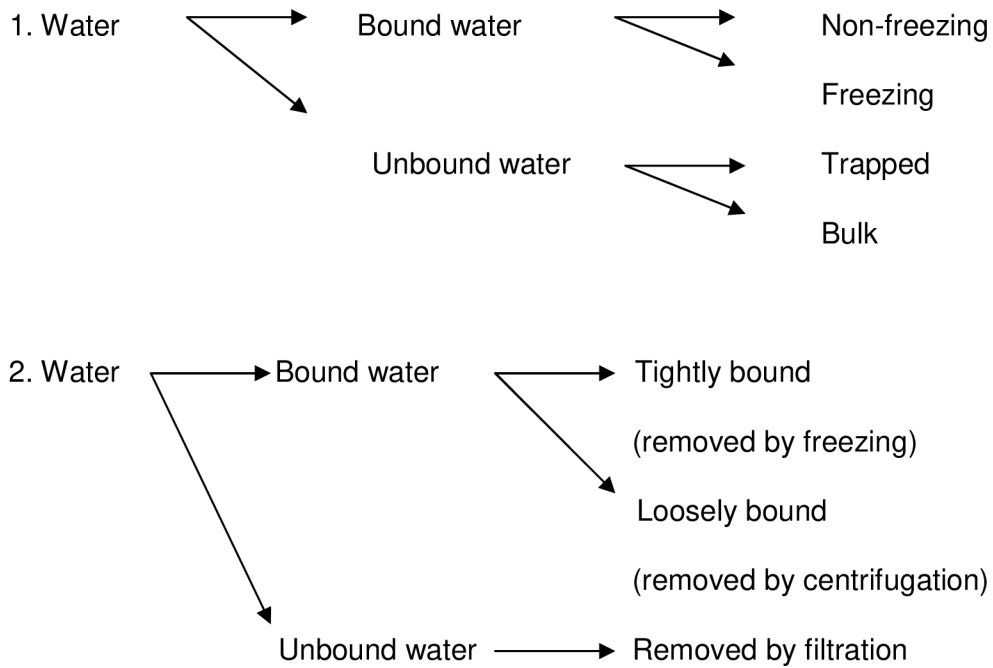
Finally, Kobayashi et al.⁵⁰ indicated that a transient network is formed by entanglements of HA chains at high molecular weight and these entanglements were absent for HA at low molecular weight.

Similar trends were found in studies by Ambrosio et al.,⁴³ who indicated that in the case of high molecular weight HA (1 200 000 g/mol) a network structure is formed from entanglements, as opposed to the low molecular weight HA (150 000 g/mol) where entanglements are absent. The dynamic modulus G' and G'' exhibited cross-over for the higher molecular weight HA, in contrast to the low molecular weight HA that behaved like a viscous fluid throughout the range of frequencies examined.⁵¹ Also, for the higher molecular weight HA, a lower cross-over frequency was observed at higher concentrations of HA. The authors postulated that the cross-over frequency corresponds to the polymer chains' disentanglement rate that is a function of their mobility, which is in turn affected by both the molecular weight and the concentration of HA in solution.

2.2 Polysaccharide hydration

Using a simplistic approach to polysaccharide hydration, water can be divided into 'bound water', subcategorized as being capable of freezing or not, and 'unbound water', subcategorized as being trapped or not.⁵²

Alternatives for defining bound and unbound water:



Scheme 1. Polysaccharide hydration

For alternative 1., the type of water is determined by freezing and meeting calorimetry using the enthalpy of the phase change and thermogravimetry, measuring the weight changes due to absorption from set humidity atmospheres.

For the less precise alternative 2., which is used in dietary fiber area, the firmly held water not removed by centrifugation, gives the water binding capacity whereas the loosely associated water, which is not removed by filtration gives the water holding capacity.

In practical experience, the effects of water on polysaccharide and polysaccharide on water are complex and become even more complex in the presence of other materials, such as salts. Water competes for hydrogen bonding, certainly will determine the carbohydrate's flexibility and may determine the carbohydrate's preferred conformation.⁵³

The effects of dissolved gasses are often ignored. However, they are usually present (even in distilled and de-ionized water), and may have important and varying effects.⁵⁴

2.2.1 Dissolving of HA

In most of the literature, authors do not mention how they dissolved the hyaluronan samples.

The information about the dissolving of HA, which has been found in the literature, are summarized in the following table.

Tab.1 Processes of hyaluronan dissolving known from literature.

Sample (Mw, final concentration)	Solvent	Time of mixing	Type of mixing	Additional step	Ref.
?, ?	Water, buffer	Over night	Turning wheel	Dialysis over water (buffer) for 24 hours	55
?, 1 mg/ml	unbuffered 150mM NaCl	At least 2 days	?	-	56
?, ?	?	25°C at least 12 h *	?	-	57
350 000 - 2200000, 0.11-11.47 mg/ml	pure water	At about 25°C overnight	?	-	58
?, 1.2-2.0 mg/ml	pure water	stirred overnight at 4°C	?	Sonicated in a low-power US **	59

* for the highest concentrations the time required to obtain perfect dissolution was longer than week

** sonication at 30-40°C after several hours of stirring led consistently to increasing diffusion coefficients

From the table, it can be clearly seen, that many authors make a little account of perspicuous description of HA dissolving. In the papers, the specification of Mw, concentration and type of mixing have been often omitted.

2.2.2 Aggregates

One of the earliest works dealing with hyaluronan aggregates was paper written by Schurz et al.⁶⁰ They found evidence for microgels in relatively fresh bovine vitreous humor hyaluronate samples in pure water, which, remarkably, they stored for two years and subsequently measured by light scattering. After this lapse of time they reported that the microgels had fallen apart into a low molecular weight species.

Also Ribitzsch et al. studied the HA aggregates by light scattering.⁵⁵ They observed that the light scattering curves develop an oscillatory fine structure on a time scale of days for rooster comb hyaluronate in a variety of solvents. They concluded that the scattering form factor curves represented random-coil structure hyaluronate molecules with the superimposed oscillatory fine structure representing spherical aggregates of hyaluronate. In other words: hyaluronic acid in water exhibits a non-monotonous scattering function, which is explained in terms of multimerization leading to gel-like supermolecular particles. This tendency is highest in water, lower in buffer, and lowest in isotonic NaCl-solution + NaN_3 . It means that ions have the tendency to suppress the aggregation. The aggregates are also disturbed by mechanical movement.

The possibility that HA associates in NaCl and CaCl_2 but not in KCl was suggested by the light scattering studies of Sheenan et al.,⁶¹ but has been disputed by Månsson et al.⁶²

Welsh et al. have discussed the possibility of breaking the aggregates by addition of shorter chains (about 60 disaccharide units). Longer or very short chains have no effect on it.⁶³

The behavior of HA from two sources (bacterial and cock's combs) have been also studied by atomic force microscope (Fig. 8).⁶⁴ Long unbranched chains with evident intramolecular interactions have been observed on mica base.

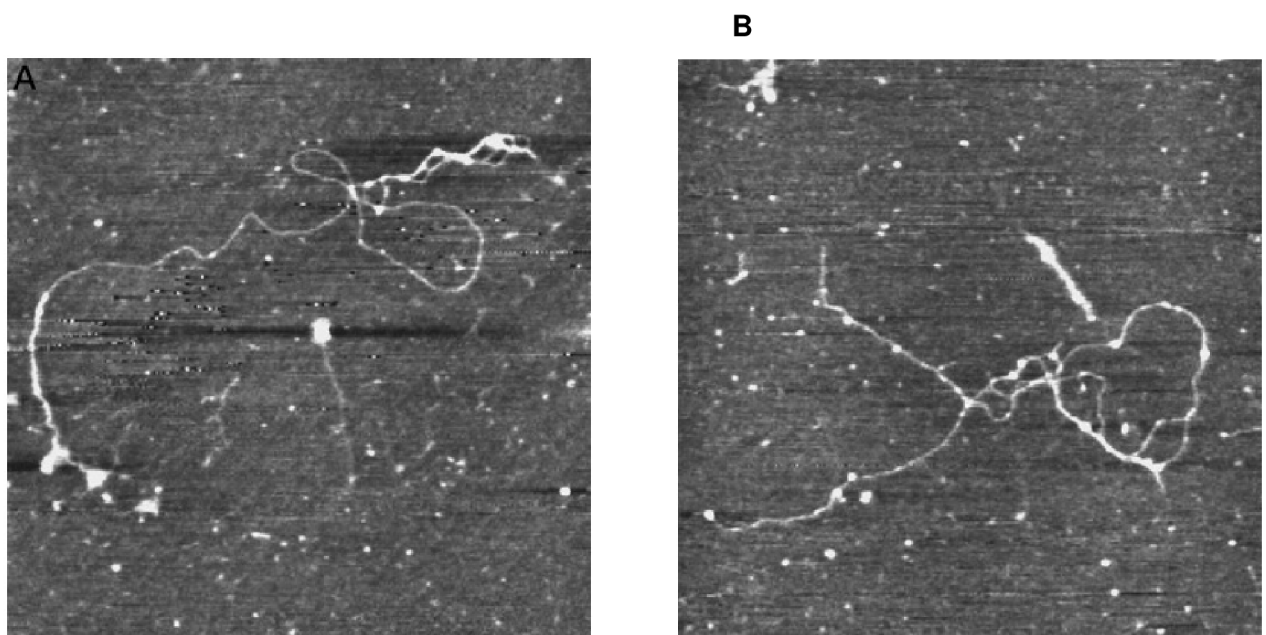


Fig.8 TMAFM image of an HA chain with extensive intramolecular self-association leading to a A) fenestrated structure B) meshwork structure

On the other hand, Gribbon et al. have found intramolecular association unimportant⁶⁵ and they have asserted that the behavior of concentrated solutions of HA is given by hydrodynamics and its chains entanglements. They have found no evidence for chain-chain

association by mechanism such as hydrophobic patches contributing to the network properties. Even at high concentration of HA in solution, the chains are still mobile without any gelation.

Ghosh et al. have found aggregates in HA solutions, which were possible to filter out using 0.45 μm filter or remove it by centrifugation.⁶⁶

2.3 Rheology

2.3.1 Basic terms

Rheology has been properly defined as the study of the flow and deformation of materials, with special emphasis being usually placed on the former.⁶⁷

Shear rate ... $\dot{\gamma}$ is the gradient of velocity in the direction at right angles to the flow, with the unit s^{-1} . The force per unit area creating or produced by the flow is called the *shear stress* ... σ , unit is Pa.

In fig. 9, there are visible a hypothetical layers, between them occur the fluid friction that causes the viscosity of the liquid.

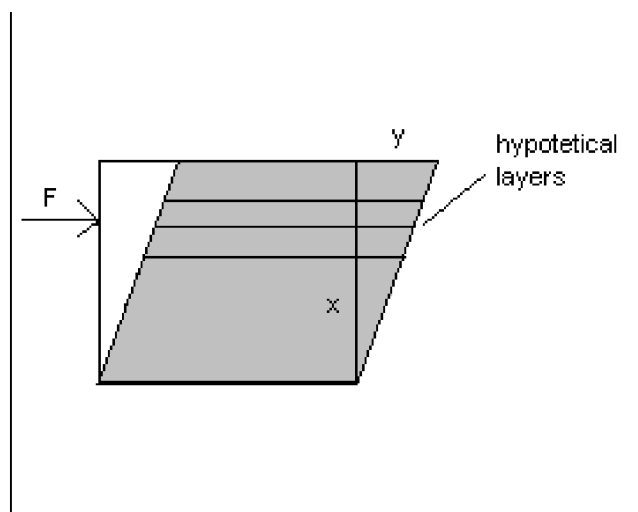


Fig.9 Hypothetical layers in shear flow

Dynamic viscosity is given by

$$\eta = \frac{\sigma}{\dot{\gamma}}, [\text{Pa}\cdot\text{s}] \quad (\text{eq.1})$$

Kinematic viscosity

$$\nu = \frac{\eta}{\rho} [\text{cm}^2/\text{s} = \text{St}] \quad (\text{eq.2})$$

Relative viscosity

$$\eta_{rel} = \frac{\eta}{\eta_s}, \quad (\text{eq.3})$$

where η_s is viscosity of solvent.

Specific viscosity

$$\eta_{sp} = \frac{\eta_p}{\eta_s} = \frac{(\eta - \eta_s)}{\eta_s} = \eta_{rel} - 1 \quad (\text{eq.4})$$

Reduced viscosity

$$\eta_{red} = \frac{\eta}{c} [\text{ml/g}] \quad (\text{eq.5})$$

Intrinsic viscosity

$$[\eta] = \frac{(\eta_{rel} - 1)}{c} [\text{m}^3/\text{kg}] \quad (\text{eq.6})$$

2.3.2 Rheological instruments for fluids

Common instruments, capable of measuring fundamental rheological properties of fluids, may be placed into two general categories:

1. Rotational type

- Parallel plate
- Cone and plate
- Concentric cylinder
- Mixer

2. Tube type

- Glass capillary
- High pressure capillary
- Pipe

Rotational instruments may be operated in the steady shear (constant angular viscosity) or oscillatory (dynamic) mode. Rotational systems are generally used to investigate time-dependent behavior because tube systems only allow one pass of the material through the apparatus.

There are advantages and disadvantages associated with each instrument. Gravity operated glass capillaries are only suitable for Newtonian fluids because the shear rate varies during discharge. Cone and plate systems are limited to moderate shear rates, but calculations (for small cone angles) are simple. Pipe and mixer viscometers can handle much larger particles than cone and plate, or parallel plate, devices.

The following description is focused only on rotational viscometers, because only this type was used in experimental work.

2.3.2.1 Flow in rotational viscometers⁶⁸

A measuring system consists of two parts:

- a. the fixed member (stator)
- b. the second part is attached to the driving motor spindle (geometry)

Geometries are usually constructed from stainless steel, aluminum or plastic.

The simplest possible flows are those where the shear rate is more or less the same everywhere in the following liquid.

Narrow-gap concentric-cylinder geometry⁶⁸

The circular flow is between closely-fitting, narrow gap concentric-cylinder that is why the shear rate is almost the same everywhere. Concentric cylinder systems are generally used for lower viscosity samples. If the inner cylinder is stationary and the outer cylinder is rotated, the shear rate in the contained liquid is given by

$$\dot{\gamma} = \frac{a_2 \cdot \omega}{a_2 - a_1}, \quad (\text{eq.7})$$

where a_1 ...radius of inner cylinder [cm]

a_2 ... radius of outer cylinder [cm]

ω ...rotation rate of outer cylinder [rad/s]

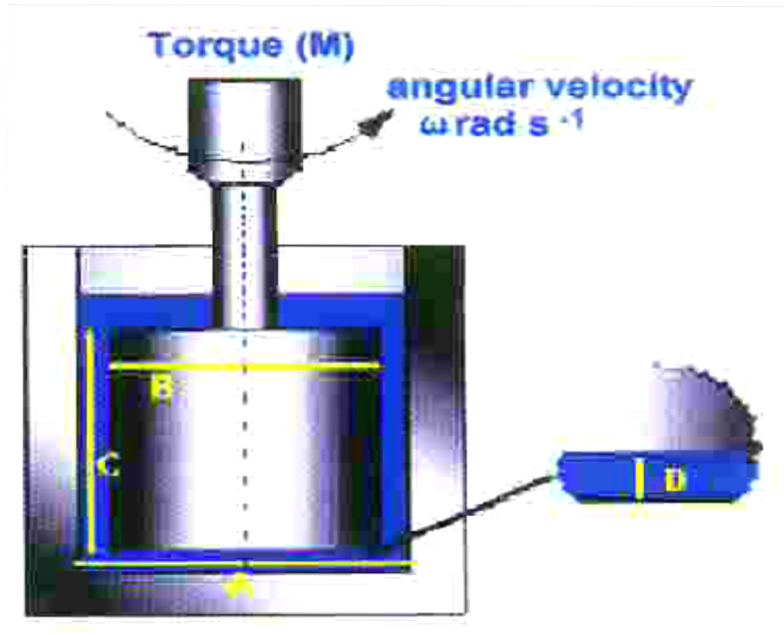


Fig. 10 Concentric cylinder measuring system

The shear stress is given by the force per unit area of inner cylinder

$$\sigma = \frac{T}{2\pi a_1^2 H}, \quad (\text{eq.8})$$

where T... torque on the inner cylinder [Nm]
 H...cylinder height [cm]

Double gap concentric cylinder geometry⁶⁸

The double gap concentric cylinder is a special case of concentric cylinder geometries that can be used for samples with very low viscosity

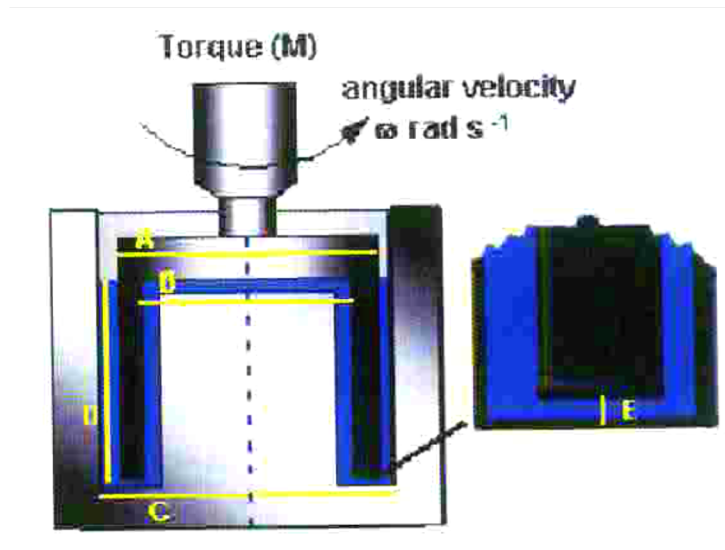


Fig. 11 Double gap concentric cylinder measuring system

Small-angle cone and plate geometry⁶⁸

The second simple geometry is flow in a rotating cone and plate (or plate and plate) geometry. Schematics of a cone and plate and two parallel plates systems are shown below in Fig. 12.

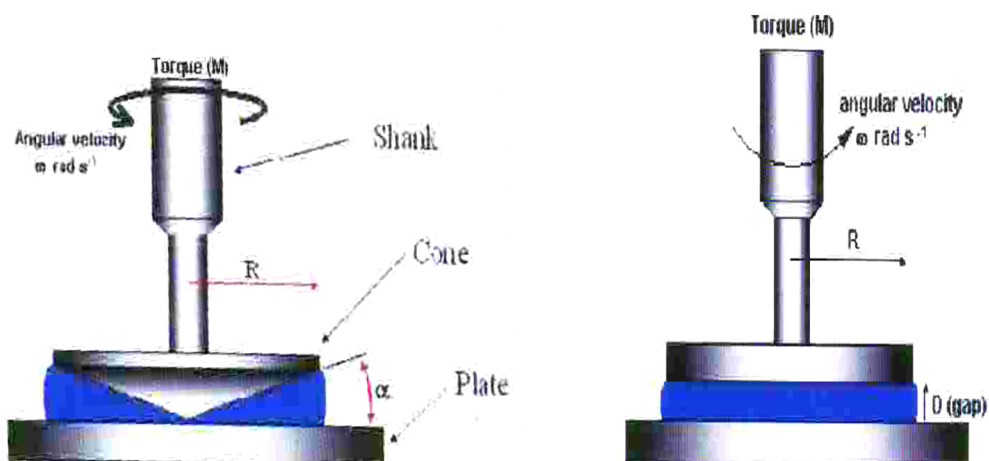


Fig. 12 Cone and plate and parallel plates measuring systems

Cone and plate geometries are generally used for single-phase homogenous samples or samples with submicron particles. On the other hand, the parallel plate system allows samples containing particles to be effectively measured.

Shear rate is given by

$$\frac{\omega}{\Phi}, \tag{eq.9}$$

where

Φ ...the angle between the cone and plate [rad].

Shear stress is given by

$$\frac{3T}{2\pi a^3}, \tag{eq.10}$$

where

a...radius of the plate [cm].

2.3.3 Flow of the fluids

2.3.3.1 Newtonian fluids

Newtonian liquid (for example water, mineral oils) is one for which the viscosity - although varying with temperature and pressure - does not vary with deformation rate or time (Fig.13).⁶⁷

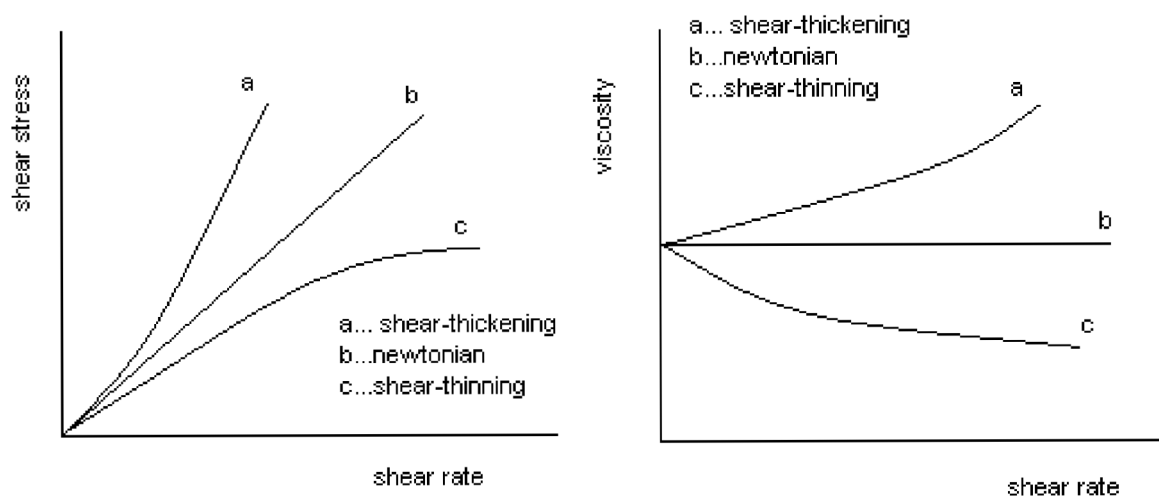


Fig.13 Typical shear stress–shear rate and viscosity–shear rate variations

2.3.3.2 Shear-thinning fluids

At low-enough shear rates or shear stress, the viscosity is constant (with a value η_0), but at some point it begins to decrease, and usually enters a straight-line region on a logarithmic plot, which indicates power-law behavior. If data at a high-enough shear rate or shear stress is available, then a second constant viscosity region (with value η_∞), is usually seen (Fig. 14).⁶⁷

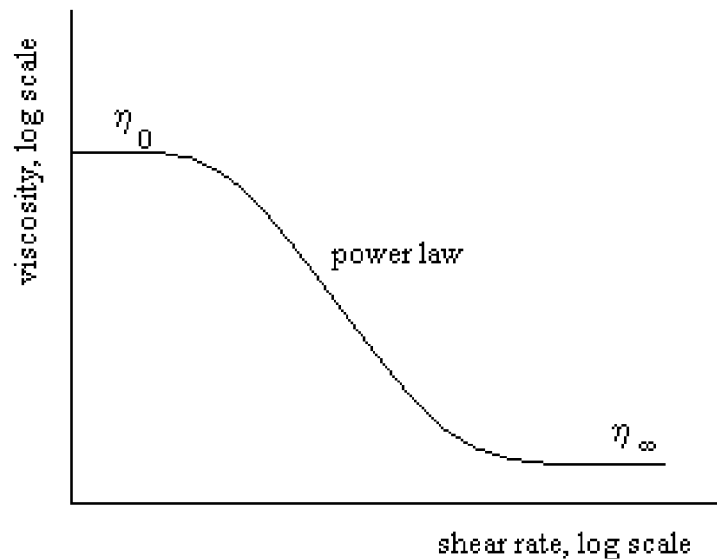


Fig.14 Viscosity versus shear rate for shear-thinning liquid, logarithmic scale

This is, the case of HA - as the shear rate increases, the viscosity decreases – a phenomenon called „shear-thinning,“ and a property named pseudoplasticity.

Rheology may be a good way how to study conformation changes of HA in solution. From relationship between the shear stress and deformation of the sample it is possible to get the dynamic viscosity (η , Pa.s). By fitting this viscosity versus shear rate, a flow curve is obtained. After extrapolation this curve to zero shear rates, the zero-shear viscosity is earned.⁶⁸ And this values of HA water, PBS or PB solution samples have been often compared in following experimental part.

2.3.4 Rheology of hyaluronan

The first rheological measurements of HA were done by Gibbs et al ⁶⁹ who measured the dynamic viscoelastic properties of its sodium salt over the frequency range. The effects of varying temperature, HA concentration, pH and ionic strength on the dynamic shear module were studied. It was shown that HA behaves as a non-Newtonian liquid.

Hyaluronate solutions at neutral pH and physiological ionic strength show high viscosity at relatively low concentrations, and also display substantial solid-like character, which is called viscoelastic behavior of hyaluronan solutions.⁷⁰ The influence of salt addition was studied and it was shown that according to increasing ionic strength, the electrostatic repulsions are suppressed and it may cause enhanced coupling. Increase in viscosity, at sufficiently high polymer concentration, was by the same authors also observed.

Rheological properties of hyaluronan solutions are related not only to the molecular weight or concentration, but also to the origin of the sample.⁷¹ HA chains are free to move individually in dilute solution, but entangle with each other and form a temporary network in concentrated solutions. The overlap (critical) concentration C^* of HA was reported to be about 1 mg/ml, and it is dependent on ionic strength, molecular weight and concentrations.^{44,72,73}

The rheological properties of sodium hyaluronate in phosphate-buffered saline were studied by Krause et al.⁴⁷ It behaved as a typical polyelectrolyte in the high-salt limit and there were no strong associations between NaHA chains under physiological conditions.

Effect of metal ions on flow profile of NaHA was studied by Knill et al.,⁷⁴ who obtained a result, that as the atomic number (atomic mass) of the metal ion increased, the Williamson zero shear viscosity decreased.

In Maleki et al. work, they have reported some novel findings about the influence of steady shear flows on intermolecular association in dilute and semidilute aqueous solutions of hyaluronic acid.⁷⁵ Their main results can be summarized in the following way:

(1) A pronounced shear thinning behavior was found for semidilute solutions of HA at high shear rates, and no hysteresis effects were observed upon the subsequent return to low shear rates. In the case of dilute solutions, the shear-induced decrease of the viscosity may be related to the alignment of polymer chains.

(2) The results from the AFFFF experiments showed no tendency of mechanical degradation of HA, even if the sample is exposed to a high shear rate (1000 s^{-1}) for 10 min.

(3) When the temperature was changed from $10 \text{ }^\circ\text{C}$ to $45 \text{ }^\circ\text{C}$ for a 1 wt % solution, the low shear rate viscosity decreased by ca. 40 %.

(4) When a low fixed shear rate (0.001 s^{-1}) was applied on a dilute HA solution, a significant viscosification was occurred in the course of time. They deduced that the growth of stronger association structures at lower HA concentrations, was probably due to an easier reorganization of the chains. The conjecture is that the shear-induced alignment and stretching of polymer chains favor the formation of hydrogen-bonded structures, where cooperative zipping of stretched chains yields an interconnected network.

(5) At a higher constant shear rate (0.1 s^{-1}), the polymer chains in a dilute solution were aligned and the viscosity decreased as time went. In this case, the higher shear flow perturbation obstructs the chains from building up association complexes.

(6) When HA solutions were exposed to increasing shear rate perturbations during a short period of time, the network structures broke down, but they were restored upon return to the low shear rate.

Zero Shear Viscosity, MW and Concentration

As shear rate approaches zero, a maximum viscosity number – zero shear viscosity – is reached. Zero shear rate viscosity has gained popularity in its use as a standard measure for the comparison of various HA products, especially those for ophthalmic use.⁷⁶ Zero shear viscosity is a function of MW and concentration. Bothner and Wik⁷⁷ studied the relation between zero shear viscosity of HA, and the product of HA concentration (mg/ml) x HA MW. Within the range of MW ($1-4 \cdot 10^6$ g/mol) and concentrations (10 and 20 mg/ml) investigated, there appeared to be a linear relation between their logarithmic functions. The authors concluded that a twofold increase in HA concentration or MW would result in a 10-fold increase in the zero shear viscosity (Fig.15).

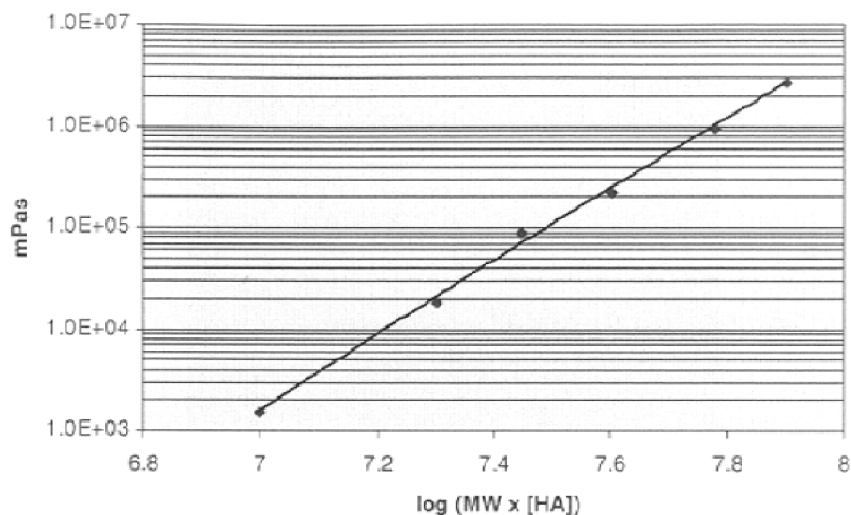


Fig. 15 The log of zero-shear viscosity plotted against the log of HA MW x [HA].

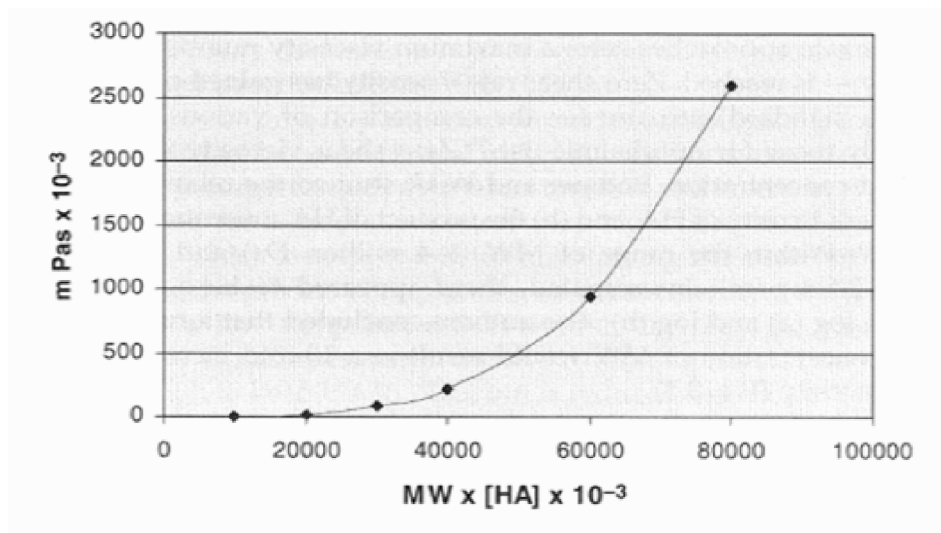


Fig. 16 Zero-shear viscosity of HA – a power function of HA MW x [HA]

Alternatively, if the zero shear rate viscosity is directly plotted against MW x [HA] without taking a logarithm, the viscosity appears to be a power function of MW x [HA]. It is not difficult to envision from the chart that a moderate increase of either MW or [HA] would greatly increase the zero shear viscosity (Fig.16).

Welsh et al. observed an interesting phenomenon that offered evidence that the intermolecular of HA is specific, rather than random entanglement.⁷⁸ It was found in their experiments that the dynamic viscosity of HA polymer (3500 disaccharide units) was decreased by an order of magnitude when an equal amount of HA oligosaccharides (60 disaccharide units) was added. This is incompatible with the „entanglement coupling“ theory for synthetic polymers, according to which the additional polymers should have increased the viscosity. The existence of cooperative interchain (interhelical) association and competitive inhibition of interchain (interhelical) binding of HA was therefore suggested. The HA segments were considered as occupying the binding junctions without contributing to the network.⁵⁷

The viscous properties of hyaluronan solutions of various average molecular weights and concentrations are shown in Figs. 16 and 17.⁵⁷ The viscous properties depend on the concentration of the hyaluronan in solution and on the average molecular weight of the molecules, as well as on the solvent and the shear rate at which the measurement is made.

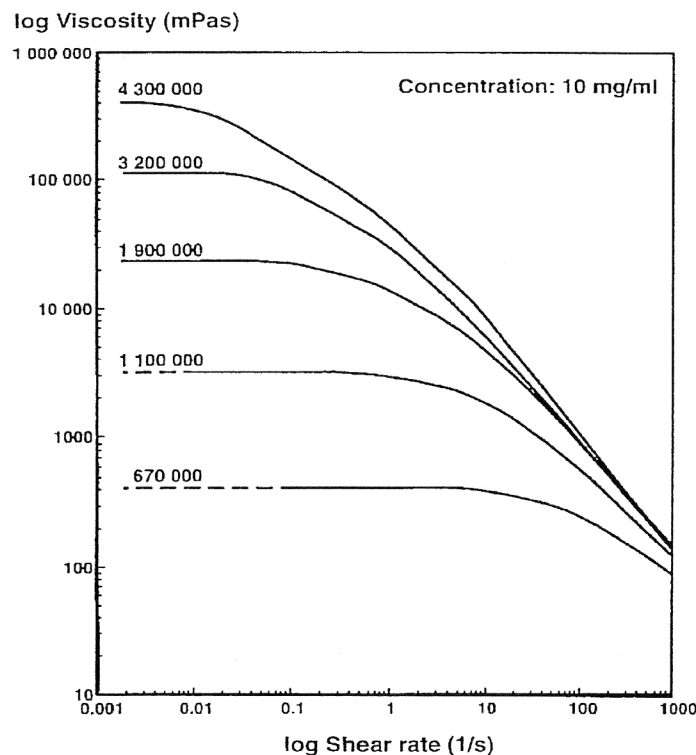


Fig. 17 Shear dependence of the viscosity of hyaluronan solution (10 mg/ml, dissolved in 0.15 N NaCl solution). Five hyaluronan preparations with average molecular weights of 0.67, 1.1, 1.9, 3.2 and 4.3 · 10⁶ g/mol are shown.⁵⁷

When the concentration decreases and the molecules are not crowded or when the average molecular weight is very low, the frequency dependence of the viscosity drastically decreases. This is the reason why hyaluronan in blood, lymph and the aqueous of the eye is not viscous.

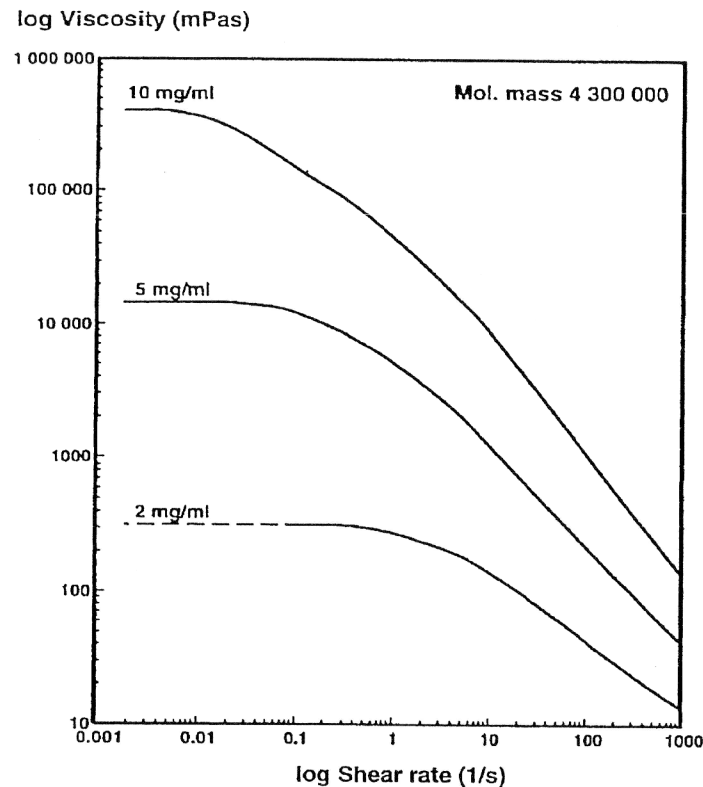


Fig. 18 Shear dependence of the viscosity of hyaluronan solutions (average molecular weight $4.3 \cdot 10^6$ g/mol) of 2, 5 and 10 mg/ml concentrations (solvent: 0.15 N NaCl).⁵⁷

2.4 Particle size measurements

Light scattering offers new insight on properties of particles and molecules in the size range between 10^{-10} and 10^{-6} meters. This method is suitable to observe the changes of particle size during the time period (dissolution, aggregation, degradation). Light scattering can be static or dynamic and the basic principles are described in next statements.

2.4.1 Static light scattering

The physiological and physical-chemical properties of HA are characterized by its molecular mass. When a solution of macromolecules is illuminated with a beam of light at

wavelength λ , the polymer chains will scatter light in direct proportion to their weight-average molecular mass (M_w). LS concern the interaction of light with matter in the specific case with macromolecules in solution. In a SLS experiments (also known as elastic or total or Rayleigh scattering) is measured the intensity of the scattering. In this case, is assumed that the scattered light has the same wavelength and polarization of the incident light.^{79,80}

2.4.2 Dynamic light scattering

The disperse particles or macromolecules suspended in a liquid medium undergo Brownian motion which causes the fluctuations of the local concentration of the particles, resulting in local inhomogeneities of the refractive index. This turn results in fluctuations of intensity of the scattered light. Since the size of the particles influences their Brownian motion, analysis of the scattered light intensity yields a distribution of the size(s) of the suspended particles.⁸¹

2.4.3 The size of particles in HA solutions

Ribitzsch et al. studied the HA aggregates by light scattering.⁵⁵ They observed that the light scattering curves develop an oscillatory fine structure on a time scale of days for rooster comb hyaluronate in a variety of solvents. They concluded that the scattering form factor curves represented random-coil structure hyaluronate molecules with the superimposed oscillatory fine structure representing spherical aggregates of hyaluronate. In other words: hyaluronic acid in water exhibits a non-monotonous scattering function, which is explained in terms of multimerization leading to gel-like supermolecular particles. This tendency is highest in water, lower in buffer, and lowest in isotonic NaCl-solution + NaN_3 . It means that ions have the tendency to suppress the aggregation. The aggregates are also disturbed by mechanical movement.

The possibility that HA associates in NaCl and CaCl_2 but not in KCl was suggested by the light scattering studies of Sheenan et al.³⁸, but has been disputed by Månsson et al.⁸²

Welsh et al. have discussed the possibility of breaking the aggregates by addition of shorter chains (about 60 disaccharide units). Longer or very short chains have no effect on it.⁶³

2.5 Surface tension and ionic conductivity

2.5.1 Ionic conductivity

In ionic conductors, the current is transported by ions moving around (and possibly electrons and holes, too). In contrast to purely electronic current transport, there is always a chemical reaction tied to the current flow that takes place wherever the ionic current is converted to an electronic current - i.e. at the contacts.⁸³ Ionic conductivity is defined for ionic species B by:⁸⁴

$$\lambda = |z_B| F u_B , \quad (\text{eq.11})$$

where

z_B is the charge number of the ionic species B

F is the Faraday constant

u_B is the electric mobility of species B.

In most current practice z_B is taken as unity, i.e. ionic conductivity is taken as that of species such as Na^+ , $\text{Ca}^{2+}/2$, $\text{La}^{3+}/3$ etc.

2.5.2 Surface tension

Surface tension, measured in Newton per meter ($\text{N}\cdot\text{m}^{-1}$), is represented by the symbol σ or γ or T and is defined as the force along a line of unit length perpendicular to the surface, or work done per unit area. Surface tension is caused by the attraction between the molecules of the liquid, due to various intermolecular forces. In the bulk of the liquid each molecule is pulled equally in all directions by neighboring liquid molecules, resulting in a net force of zero. At the surface of the liquid, the molecules are pulled inwards by other molecules deeper inside the liquid, but there are no liquid molecules on the outside to balance these forces. All of the molecules at the surface are therefore subject to an inward force of molecular attraction which can be balanced only by the resistance of the liquid to compression. Thus the liquid squeezes itself together until it has the lowest surface area possible.⁸⁵



Fig.19 Surface tension is an effect within the surface layer of a liquid that causes the layer to behave as an elastic sheet. It is the effect that allows insects (such as the water strider) to walk on water.

Influence of temperature on surface tension

There is only empirical equation by Eötvös:

$$\gamma \cdot V^{2/3} = k(T_c - T) \quad (\text{eq.12})$$

where

V is the molar volume of that substance

T_c is the critical temperature

k is a constant for each substance

Influence of solute concentration on surface tension

Solutes can have different effects on surface tension depending on their structure:

- No effect, for example sugar
- Increase of surface tension, inorganic salts
- Decrease surface tension progressively, alcohols
- Decrease surface tension and, once a minimum is reached, no more effect, surfactants

Josiah Willard Gibbs proved that:

$$\Gamma = -\frac{1}{RT} \left(\frac{\partial \gamma}{\partial \ln C} \right)_{T,P}, \quad (\text{eq.13})$$

where

Γ is known as surface concentration (represents excess of solute per unit area of the surface over what would be present if the bulk concentration prevailed all the way to the surface [mol/m^2])

C is the concentration of the substance in the bulk solution

R is the gas constant

T is the temperature

3 EXPERIMENTAL PART

3.1 Materials and methods

3.1.1 Chemicals

The summary of used chemicals with their batch numbers and producers are described in Table 2.

Tab. 2 Summary of used chemicals.

Chemicals	Batch number	Mw [g/mol]	Producer
Deuterium oxide 99.9%	MKBB2315		Aldrich
Sodium azide p.a.	42305090		Fluka
Sodium hyaluronate	verela T9001/070709	16 000	Contipro
	VLMW 080708-P1	39 900	Group
	HYA 141007	86 600	
	VLMW 190707-E1	102 600	
	verela 070909	133 000	
	verela 200409-E2	175 300	
	verela 251109/209-079	275 600	
	HA 250205-D1	750 000	
	HA 250205	1 400 000	
	HA 060306	1 690 000	
	HMW 160505	2 612 000	
Sodium chloride	K38062004 745		Merck
Sodium hydrogenphosphate dihydrate p.a.	0001434476		Sigma-Aldrich
Sodium dihydrogenphosphate dehydrate p.a.	PP/2009/10133		Lachner
Sodium hydroxide	SZBA0560UN1823		Sigma-Aldrich

3.1.2 Laboratory aids

Beakers (25, 50, 100 ml)

Volumetric flasks (250, 500 ml)

Magnetic stirrer RO 10 power

Pipette (25, 50 ml)

Plastic disposable pipettes

pH meter Ionolab

Ultrasound bath

3.1.3 Instruments

3.1.3.1 Rheology

AR G2 magnetic bearing rheometer (Fig. 20) developed by TA Instruments is a combined motor and transducer (CMT) instrument. The lower component of the measuring system is fixed, the upper component is attached to a shaft that can rotate by a torque produced by an induction motor. The constraint on the low torque performance of such an instrument is the friction between the rotating and the stationary components. An induction motor is therefore used not only because of the rapidity and stability of its response, but more specifically to minimize the friction. But the rotating shaft has to be supported in some way, and this requires a bearing: another source of friction.



Fig. 20 AR-G2 rotational rheometer

Until now, all high performance commercial CMT rheometers have used air bearings, either of the jet or the diffusion type. AR-G2 is equipped with magnetic bearing, which had previously been used for research instruments used only in creep. The advantages of this type of bearing over an air bearing are mainly produced by the much wider gaps above and below the thrust plate. On the AR-G2 these are around half a millimetre, for an air-bearing they would be of the order of microns. This leads not only to less friction, but also to smoother operation, allowing more accurate mapping of the slight fluctuations in the friction as the bearing rotates.

- used geometry:

Double gap concentric cylinder - sample volume: 7.8 ml

Cone and plate (60 mm, 1°) - sample volume: 1.0 ml

- used software:

for the instrument:

Rheology Advantage Instrument Control AR, product version V5.7.0

for data analysis:

Rheology Advantage Data Analysis, product version V5.7.13

3.1.3.2 Particle size:

Zetasizer Nano ZS is unique equipment that enables to measure static light scattering (SLS) and also dynamic light scattering (DLS) to provide characterization of HA.



Fig.21 Zeta Sizer Nano ZS

DLS experiments were performed by Zetasize Nano ZS equipment with a helium neon laser operating at 633 nm with power 4.0 mW and avalanche photodiode detector, a computer-controlled and a temperature controlled sample cell. The temperature was 25 ± 0.1 °C.

The data were analyzed with DTS (Nano) 4.2 software by method of cumulants and CONTIN to obtain an average particles size and an approximate particle size distribution.

3.1.3.3 NMR

1D NMR spectra were measured by Bruker Avance III 500 MHz Ultrashield plus.



Fig.22 NMR spectrometer Bruker Avance III 500 MHz

3.1.3.4 UV-VIS

UV-VIS spectra were measured by UV-VIS spectrophotometer Shimadzu UV-2401 PC.

3.1.3.5 Density

The density was measured by the digital densitometer Anton Paar DMA 4500. Each sample was degassed and measured at least two times at temperature 25°C.

3.1.3.6 Conductivity

The conductivity was measured by InoLab Cond 720 using the measuring cell TetraCon 325. The cell is composed of four graphite electrodes and its constant is $0,475 \text{ cm}^{-1}$ with a relative error $\pm 1.5 \%$.

3.1.3.7 Surface tension

The surface tension was measured by the Digital Tensiometer K9 using Wilhelmy Plate Method, which is an universal method especially suited to check surface tension over long time intervals. A vertical plate of known perimeter is attached to a balance, and the force due to wetting is measured.



Fig.23 Tensiometer K9

3.1.4 Methods

3.1.4.1 Preparation of HA solutions for the effect of Mw, c, solvent and T (chap. 4.2-4.4)

All solutions were prepared by dissolving appropriate amount of hyaluronan powder in the proper solvent at ambient temperature during mechanical stirring for at least 6 hours. During the night, the samples were stored in the fridge at temperature about 4°C .

0.1 M Phosphate buffer, pH = 5, 6, 7, 8

0.1M solutions of sodium dihydrogenphosphate dihydrate and sodium hydrogenphosphate dodecahydrate were prepared in demineralised water. After dissolving, the solution of

sodium hydrogenphosphate dodecahydrate was added dropwise to the solution of sodium dihydrogenphosphate dihydrate (or conversely) until the pH reached the require value. The pH was measured at the ambient temperature 25°C by pH meter Inolab.

Physiological solution

Physiological solution is 0.9% (w/v) solution of NaCl and was prepared by dissolving of a calculated amount of NaCl in demineralised water. The solution was stirred for at least one hour and stored in a fridge.

3.1.4.2 Preparation of HA solutions for other physical chemical methods (chap. 4.5)

Samples for zeta sizer

Sample concentration for DLS was 10.0 g.l⁻¹. Solutions were measured after filtration through the 0.2 µm Fisher Brand, mixed esters of cellulose membranes of syringe filters. For measurements, 1 ml of sample was putted into disposable sizing cuvette.

Samples for NMR

The samples for NMR were prepared by dissolving 10 mg of HA powder in 0.75 ml of D₂O (99.9%) and were stirred overnight.

Samples for UV-VIS

Sample concentration for measuring UV-VIS spectra was 10.0 g.l⁻¹ and only one solvent - HA in PBS (pH 7) was chosen.

Samples for dissolving and time-stability studies (chap. 4.1 and 4.6)

A special attention was paid to preparation samples for dissolving studies.

Preparation of solutions

All solutions were prepared by dissolving hyaluronan powder in distilled water at ambient temperature during mechanical stirring for at most 72 hours. The additions of powder samples to the solvents were done under strictly controlled conditions. The injection water was filtered throw the 0.22 µm filter. The solutions were placed on a mechanical stirrer and were mixed at room temperature at 300 rpm.

0.1 M Phosphate buffer, pH = 7.0

15.6 g of sodium dihydrogenphosphate dihydrate was dissolved in 1000 ml of demineralised water and 71.6 g of sodium hydrogenphosphate dodecahydrate was dissolved in 2000 ml of demineralised water. After dissolving, the solution of sodium

hydrogenphosphate dodecahydrate was added dropwise to the solution of sodium dihydrogenphosphate dihydrate until the pH reached 7.00. The pH was measured at the ambient temperature 25°C by pH meter Inolab.

Ultrasound degradation

The 1% solutions of HA in phosphate buffer or demineralised water with addition of NaN_3 were immersed into ultrasound bath. The power of the ultrasound was 72 W and samples stand in the bath for 10, 20 and 30 minutes.

Samples for zeta sizer

Sample concentration for DLS was 1.0 g.l^{-1} . It was prepared before measurement by dilution the stock solution after investigation, that was continuously stirred (10 g.l^{-1}), in water or phosphate buffer solution with addition of sodium azide. Dissolution was necessary for providing Brownian motion in solution. Solutions were measured after filtration or not filtered. Filtration was performed by $0.2 \mu\text{m}$ Fisher Brand, mixed esters of cellulose membranes of syringe filters. For measurements 1 ml of sample was putted into disposable sizing cuvette.

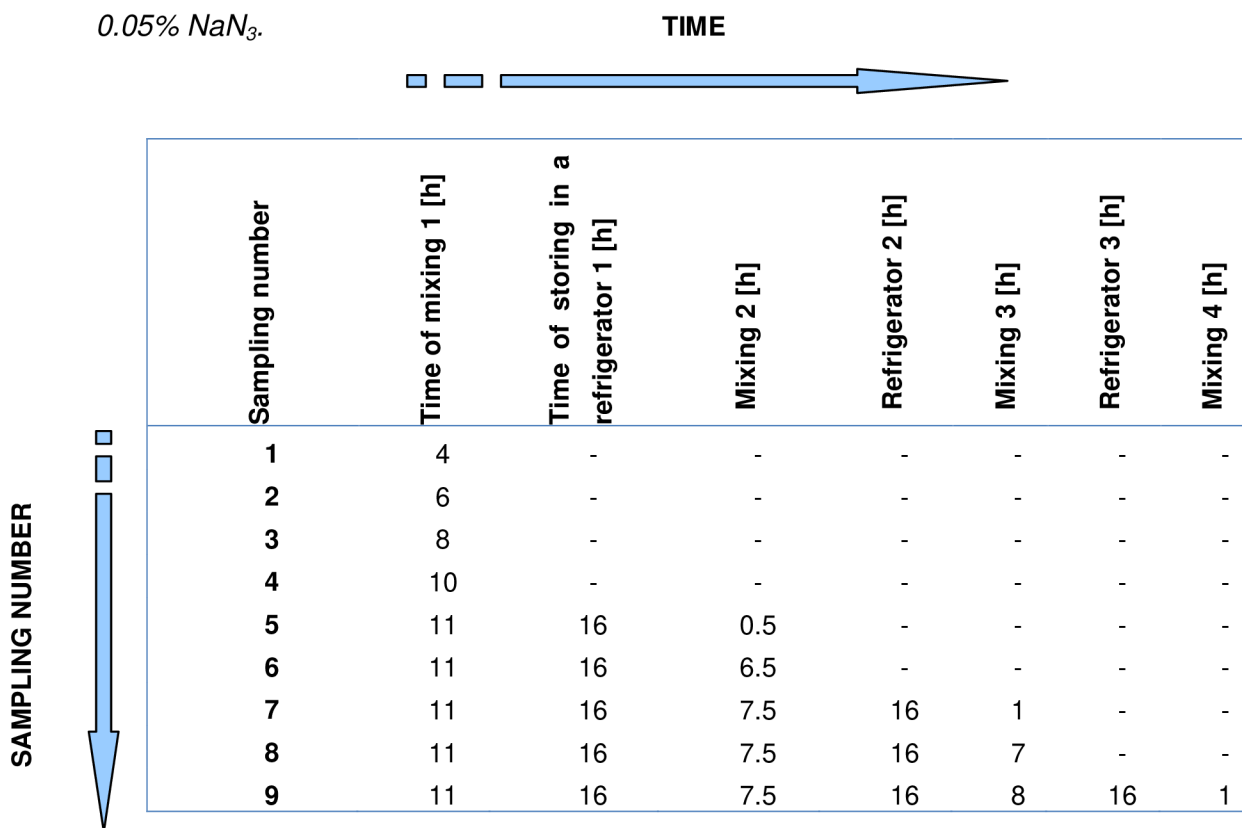
Process of dissolving

The solutions were prepared as was mentioned above and the samples were taken in predetermined time period (Tabs. 3-5).

Tab.3 The mixing process of 0.15% aqueous solution HA 060306 with addition of 0.02% NaN_3 .

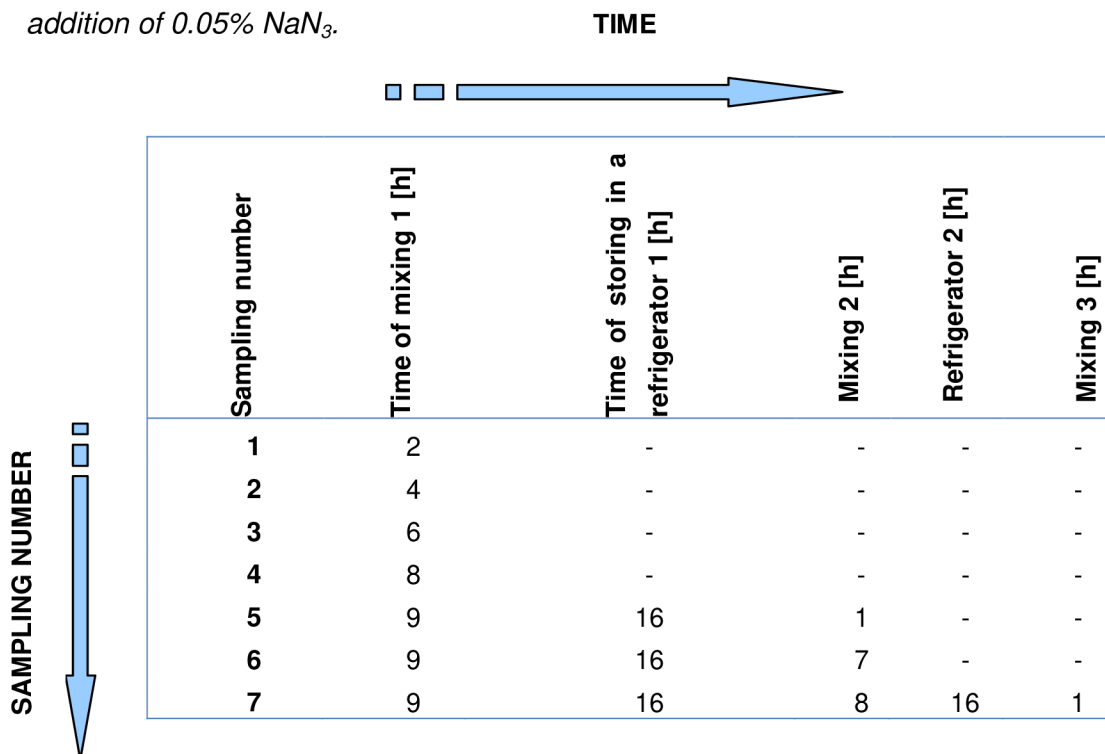
	Time of mixing 1 [h]	Time of storing in a refrigerator 1 [h]	Mixing 2 [h]	Refrigerator 2 [h]	Mixing 3 [h]	Refrigerator 3 [h]	Mixing 4 [h]
1	1.5	-	-	-	-	-	-
2	3.5	-	-	-	-	-	-
3	5.5	-	-	-	-	-	-
4	8.5	-	-	-	-	-	-
5	8.5	16	1	-	-	-	-
6	8.5	16	2	-	-	-	-
7	8.5	16	5	-	-	-	-
8	8.5	16	9	15	1	-	-
9	8.5	16	9	15	15	-	-
10	8.5	16	9	15	8	16	1
11	8.5	16	9	15	8	16	5

Tab.4 The mixing process of 1.0% aqueous solution HA 250205-D1 with addition of 0.05% NaN_3 .



Sampling number	Time of mixing 1 [h]	Time of storing in a refrigerator 1 [h]	Mixing 2 [h]	Refrigerator 2 [h]	Mixing 3 [h]	Refrigerator 3 [h]	Mixing 4 [h]
1	4	-	-	-	-	-	-
2	6	-	-	-	-	-	-
3	8	-	-	-	-	-	-
4	10	-	-	-	-	-	-
5	11	16	0.5	-	-	-	-
6	11	16	6.5	-	-	-	-
7	11	16	7.5	16	1	-	-
8	11	16	7.5	16	7	-	-
9	11	16	7.5	16	8	16	1

Tab.5 The mixing process of 1.0% solution HA 250205-D1 in 0.1M phosphate buffer with addition of 0.05% NaN_3 .



Sampling number	Time of mixing 1 [h]	Time of storing in a refrigerator 1 [h]	Mixing 2 [h]	Refrigerator 2 [h]	Mixing 3 [h]
1	2	-	-	-	-
2	4	-	-	-	-
3	6	-	-	-	-
4	8	-	-	-	-
5	9	16	1	-	-
6	9	16	7	-	-
7	9	16	8	16	1

3.1.4.3 Rheology

Each sample was measured at least three times and the average value of zero shear viscosity was calculated

Used methods

1. Stepped flow - applies successive shear values, data are sampled at the end of each value.

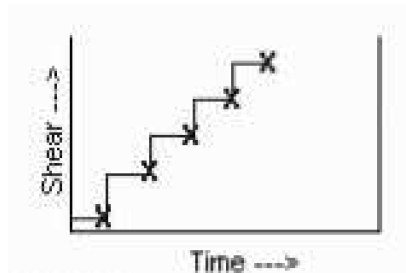


Fig. 24 Scheme of Stepped flow method

2. Temperature ramp – holds the shear constant while ramping the temperature, samples at defined intervals.

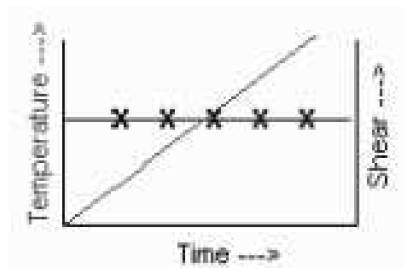


Fig. 25 Scheme of the Temperature ramp method

Used rheological models

The basic rheological equations, used for describing hyaluronan solutions flow, are mentioned below.⁵³

Newtonian model

This model describes the simplest type of flow behavior, namely that where the materials viscosity is constant, independent of applied shear. The model is expressed in terms of the shear stress/shear rate relationship.

$$\sigma = \eta \cdot \dot{\gamma} \quad (\text{eq.14})$$

Power Law model

Since most materials are non-Newtonian, non-linear models are needed to describe the change in viscosity as a function of shear. The power law equation is the simplest of the available models. The viscosity (either Newtonian or apparent) is replaced by a consistency coefficient, K. Based upon the index, n, the power law model describes three basic types of flow:

$$\sigma = k \cdot \dot{\gamma}^n \quad (\text{eq.15})$$

n =1 Newtonian behavior

n <1 Shear thinning (or pseudoplastic)

n >1 Shear thickening

The Cross model

To obtain a model for a general flow curve, over a wide range of shears, requires a equation with at least four parameters. The Cross model is a good example of this type of equation. It predicts behavior consisting of low and high shear plateau's, with a shear thinning region between in. The Cross model uses shear rate as the independent variable. The Ellis model can be used as an equivalent using shear stress. The viscosity of many suspensions could be described by the equation of the form:

$$\frac{\eta - \eta_{\infty}}{\eta_0 - \eta_{\infty}} = \frac{1}{1 + (K \cdot \dot{\gamma})^m}, \quad (\text{eq.16})$$

where η_0 and η_{∞} are the dynamic viscosity of the solution [Pa.s] at very low and high shear rates, respectively. K and m are constant parameters, generally called as consistency and flow index, respectively. K is constant expressed in seconds and m is dimensionless constant. The reciprocal, 1/K give us a critical shear rate that proves a useful indicator of the onset shear rate for shear thinning. K and m can be related to texture, application properties, pumping, mixing and pouring characteristics and many other everyday flow processes which often occur in the shear thinning region the fluid's flow behaviour.

The Williams model

This is another Cross-like model, which uses the stress rather than the shear rate as the independent variable. This model can often be used with data generated at low shear rates (where the power law model fails.)

$$\eta = \frac{\eta_{\infty}}{(1 + (k \cdot \dot{\gamma})^n)} \quad (\text{eq.17})$$

3.1.5 Statistical evaluation of experimental data

Nearly 600 samples were measured to have enough of high-quality data, presented in this work. Each of the samples was measured at least for three times, more often for five times. All data mentioned in the Experimental part are the medians from three – five measurements. The maximum relative mistake of flow measurements is 1.5%, maximum relative mistake of temperature measurements is little higher, about 3%. More detailed statistical evaluation is enclosed in Appendix 1.

4 RESULTS AND DISCUSSION

This part is divided into 6 chapters. In the beginning, to be sure the solutions are good, the dissolution of HA powder is studied, while this topic is not discussed in the literature. The second chapter deals with the best conditions and adjustment of rheometer for the next rheological measurements. In following chapters the effect of concentration of the solution, Mw of HA, pH, type of the solvent and temperature on HA viscosity is described step by step. To confirm HA quality, other physical methods, such as particle size measurements, NMR, UV-VIS, were used. Finally, the time stability of HA solutions and presence of aggregates is study in the last part.

4.1 Dissolution of HA powder

The dissolution of any polysaccharide and especially of hyaluronic acid is not as easy as it would be expected. The dissolution depends on many factors, for example temperature, speed of rotation, concentration of final solution, Mw of the polysaccharide, the way of adding the powder sample, the size of solution surface and a few others.

The dissolution of HA powder and preparation of HA solutions generally is not satisfactorily described in literature (Tab. 1), it was studied at the beginning of present work, to be sure to have good solutions without any aggregates or not dissolves particles. Three molecular weights and two solvents (demineralised water and 0.1M PBS, pH 7) were tested and the solutions were prepared according to procedure described earlier.

To study dissolving of HA, flow curves of HA solutions were measured in fixed time and the dependence of zero shear viscosity on time was observed (Fig. 26). From the graph it can be clearly seen that in first day (20 hours) the zero-shear viscosity decreases rapidly, the second day (50 hours) it decreases slightly and the decrease stops after 50 hours.

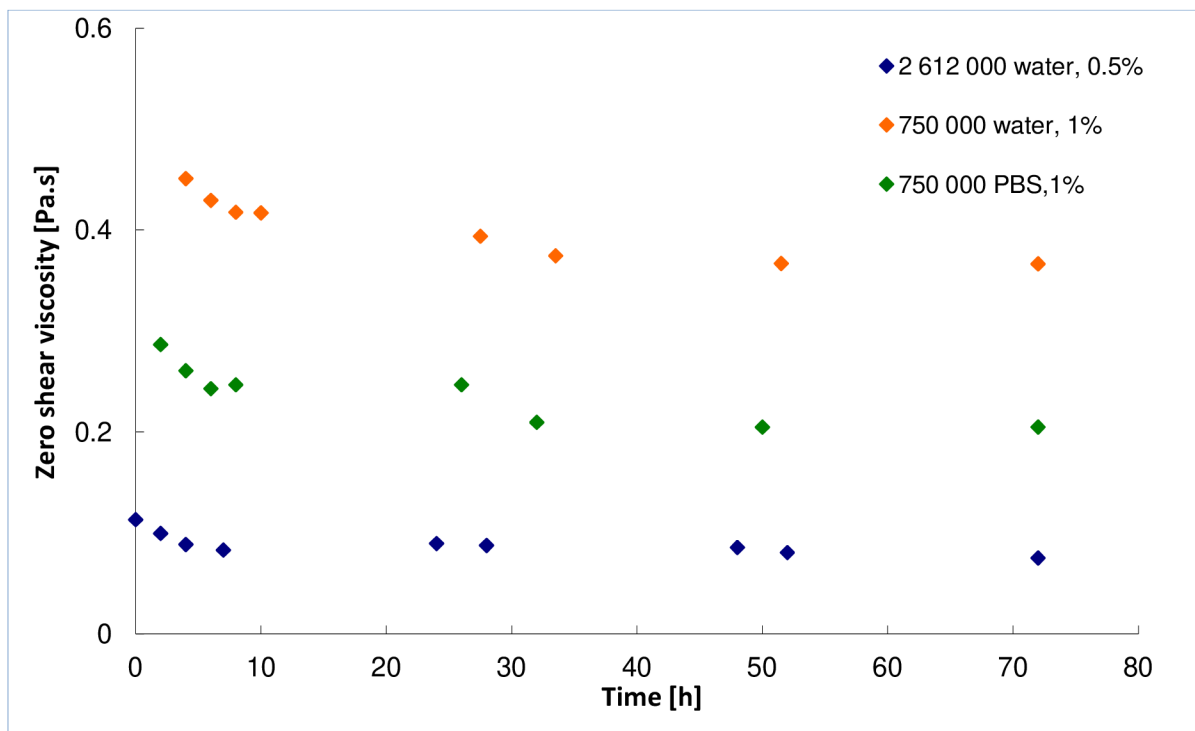


Fig. 26 Plot of changing zero shear viscosities in time for two MW of HA and two solvents.

These results were taken into consideration during preparation of all solutions that were mixed at least 24-48 hours in dependency on their MW. More detailed study, using particle size measurements, conductivity and surface tension, is at the end of present work in Chap. 4.6.

4.2 Preliminary rheological measurements

4.2.1 Flow curves

The range of acceptable shear rates was determined by testing one HA sample (Mw 86 600 g/mol), Fig. 27. When the shear rate was too low, no relevant points were detected. On the other hand, at too high shear rates, the sample flowed out of the rheometer sensor and the data were also incorrect. Consequently, the range of measured shear rates was chosen (depending up the measured Mw) from 0.1 – 10 000 s⁻¹.

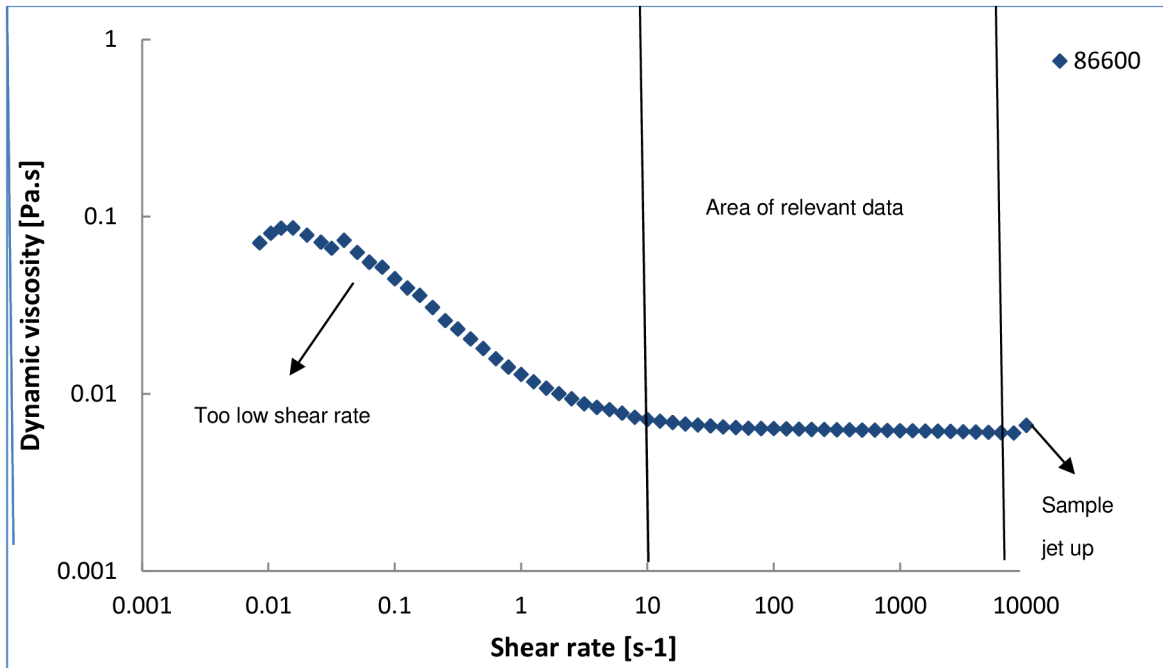


Fig.27 The flow curve of 1% aqueous solution of HYA 141007 (Mw 86 600 g/mol) at temperature 25°C.

4.2.2 Temperature ramp

According to the temperatures commonly used in the production of hyaluronan, the temperature range was chosen from 15 to 90 °C. This is also the maximum range in which the dynamic viscosity of hyaluronan solutions can be measured by the AR-G2 rotational rheometer, because it is very difficult to reach the lower temperature and above 90°C it is close in quick evaporation of the solvent. There was a question about the ideal temperature ramp during those experiments. It means how many degrees the temperature should increase in one minute. The experiment with 1% aqueous solution of HYA 141007 (Mw 86 600 g/mol) was done (Fig. 28)

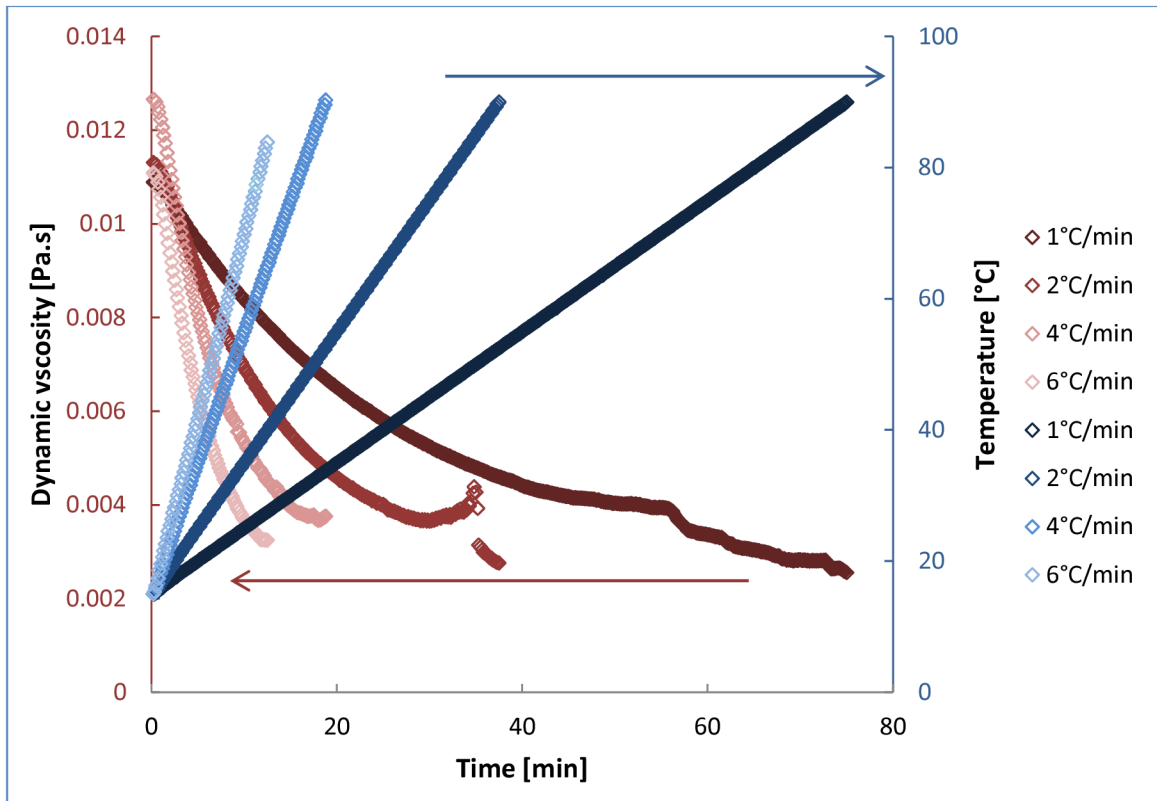


Fig.28 The temperature ramp curves for 1% aqueous solution of HYA 141007 (Mw 86 600 g/mol) with different temperature ramps. CS mode, shear rate 100s^{-1}

From the Fig 28, it can be clearly seen that in case of the ramp $6^\circ\text{C}/\text{min}$, the increase of temperature is too quick and the sample is not able to warm up in the same speed. That is why the measurement has finished earlier than the solution reached temperature of 90°C . The ramp of 1 and 2°C took a long time so as the best ramp for next temperature measurements was chosen $4^\circ\text{C}/\text{min}$.

Also the best shear rate for the temperature ramp was found with the same sample of HYA. The shear rate should be chosen from the first Newtonian plateau that is for this sample in range $5\text{-}1000\text{ s}^{-1}$ (Fig. 29).

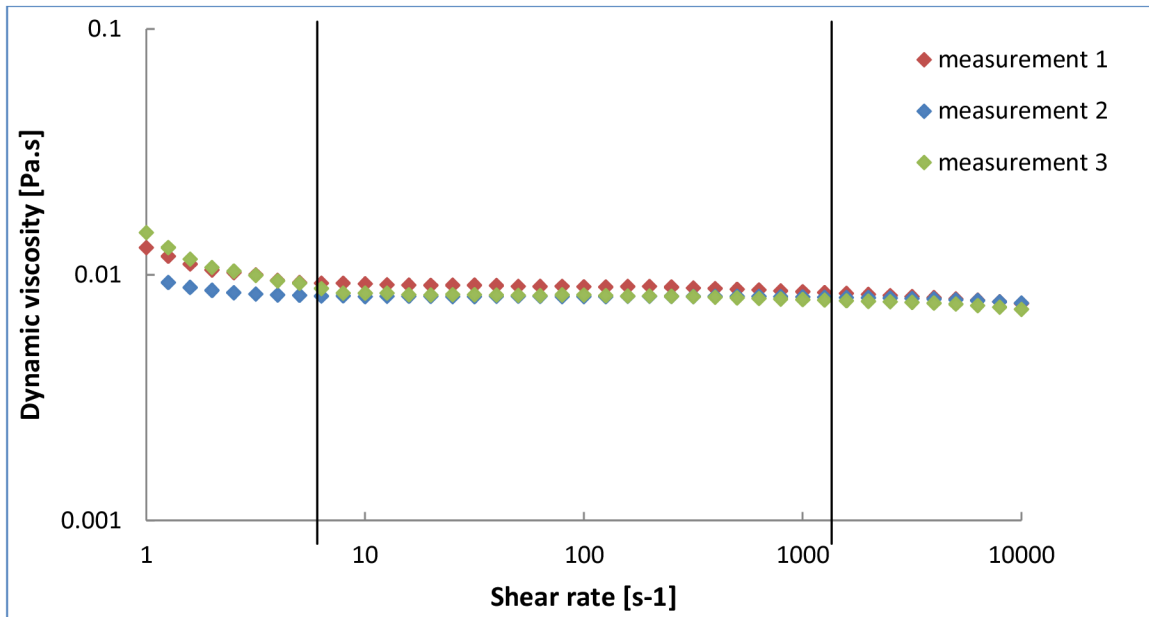


Fig. 29 The first Newtonian region of 1% aqueous solution of HYA 141007 (Mw 86 600 g/mol). Temperature 25°C.

Three measurements with the shear rates of 10, 100 and 1000 s^{-1} were done (Fig. 30). The shear rate of 10s^{-1} was too low to get relevant data. On the other hand, shear rate 1000 s^{-1} caused the decrease of viscosity because of the degradation of the sample by too high shear, not only because of the increasing temperature. This implied that the shear rate 100s^{-1} would be the best for our measurements.

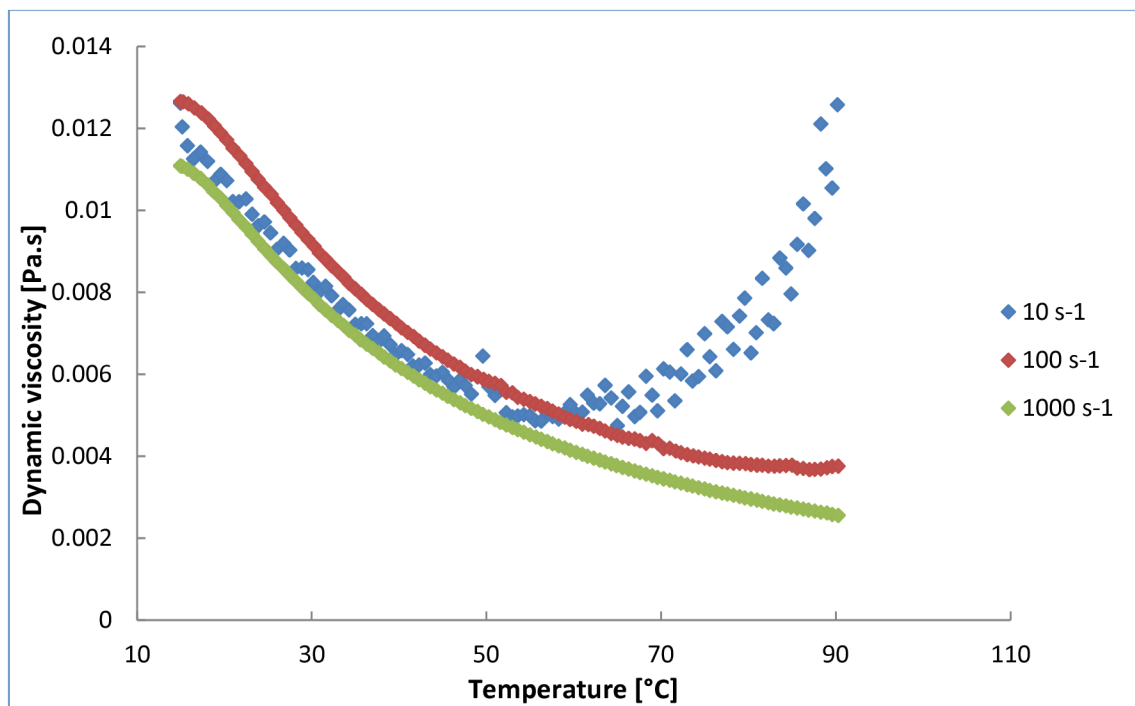


Fig. 30 The temperature ramp curves for 1% aqueous solution of HYA 141007 (Mw 86 600 g/mol) with different shear rates.

4.3 The flow curves

This chapter includes the main results of the present work, the flow curves measurements. It means dependence of dynamic viscosity on increasing shear rate of hyaluronan samples was studied. Always one from the chosen parameters was variable (concentration, Mw, solvent, pH), while the temperature was always constant (25°C).

4.3.1 The effect of Mw and concentration

The effect of Mw and concentration on dynamic viscosity of hyaluronan solution was studied. The range of Mw of measured HA samples was 16 000 – 2 612 000 g/mol. For all those measurements 0.1M PBS, pH 7.00 was used as a solvent.

4.3.1.1 VLMW HA

Figure 31 shows the rheological flow behavior of 1% VLMW HA in range of molecular weight 16 000 – 275 600 g/mol in 0.1M PBS at pH = 7.00. Up to the 102 600 g/mol, hyaluronic acid exhibited essentially Newtonian characteristics throughout all the shear rate range analyzed.

Pseudoplastic behavior (shear thinning) was observed for higher molecular weight HA, from 133 000 g/mol. At shear rate lower than 1000 s⁻¹, the viscosity is almost constant decreasing slightly with the shear rate (Newtonian plateau). At shear rate greater than 1000 s⁻¹ the viscosity decreases. At higher shear rate, sharply drops with the shear rate (thinning in an S-shaped fashion) and a second plateau should be expected.

The rheological behavior of these solutions is typical of entangled networks. In these networks, the rheological response is controlled by the rate of entanglement formation and disruption. At low shear rate, the two rates are comparable and the total number of active entanglement is almost constant. As the shear rate increases, the rate of disruption becomes predominant leading to the thinning. ⁴³

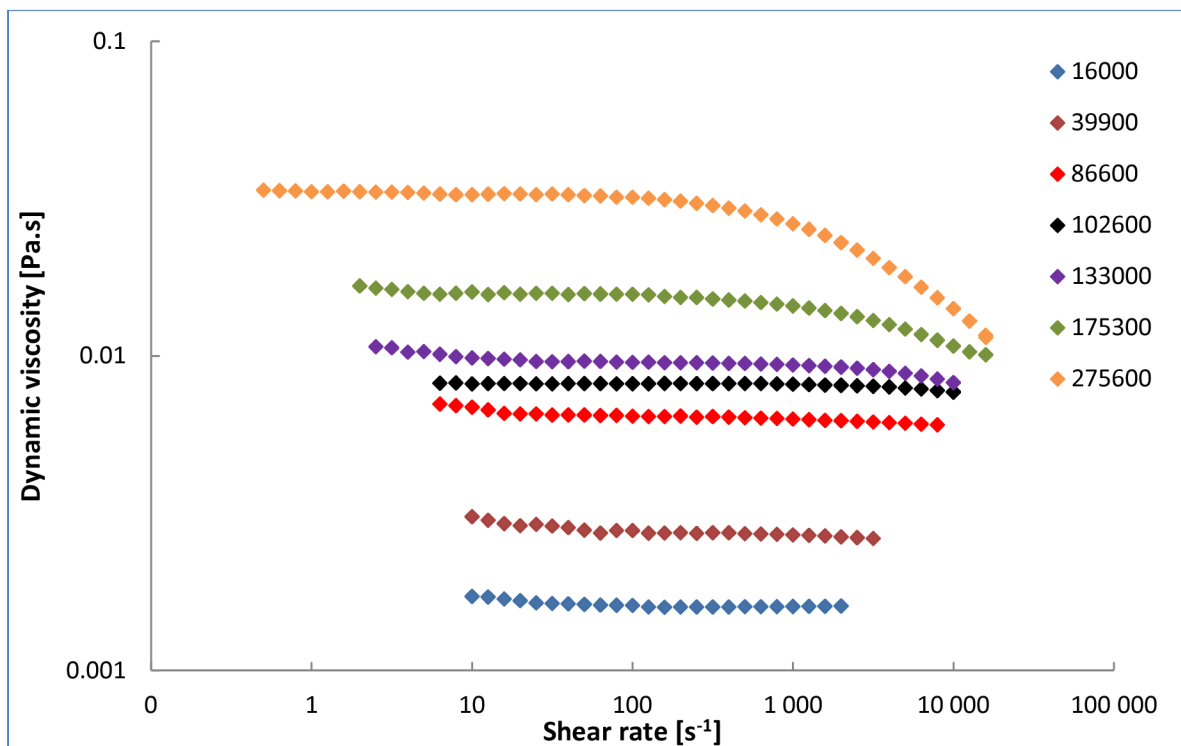


Fig. 31 The flow curves of 1% VLMW HA in range of Mw 16 000 – 275 600 g/mol in 0.1 M PBS, pH = 7.00, T=25°C

From the flow curves, the zero shear viscosities (η_0) were calculated using the relevant rheological model (Tab. 6). Such a practice was applied for all measurements (different solvents, pH and concentrations of HA).

Tab. 6 The zero shear viscosities of 1% VLMW HA in 0.1M PBS (pH = 7.00) calculated from the flow curves by using of the appropriate rheological model.

Molecular weight [g/mol]	Rheological model	Zero shear viscosity [Pa.s]	Consistency [s]	Rate constant
16 000	Newtonian	0.00159	-	-
39 900	Newtonian	0.00264	-	-
86 600	Newtonian	0.00508	-	-
102 600	Newtonian	0.00619	-	-
133 000	Cross	0.0127	3.04*10 ⁻⁵	0.58
175 300	Cross	0.0169	8.24*10 ⁻⁵	0.62
275 600	Cross	0.0329	2.36*10 ⁻⁴	0.68

To study the effect of concentration and Mw on zero shear viscosity of VLMW HA, seven different molecular weight (16 000 – 275 600 g/mol) and five different concentrations (1-5%,w/w) of HA were chosen. All these measurements were done in PBS, pH 7.00.

The zero shear viscosity of HA is highly dependent on its Mw and concentration (Fig. 32). With increasing both, concentration and Mw, the zero shear viscosity strongly increases. The increase of zero shear viscosity by increasing only concentration is dependent on Mw. So for example: by increasing the concentration 5 times for sample with Mw 16 000 g/mol, the zero shear viscosity increases about 4 times. But by increasing the concentration 5 times for sample with Mw 102 600 g/mol, the zero shear viscosity increases about 36 times and for sample with Mw 275 600 g/mol, the zero shear viscosity increases even more than 177 times. That explains the necessity of logarithmic scale in these graphs. The curves of two highest MW samples show folding dependence. The explanation may be in the interaction and entanglement of longer chains that causes the increase of viscosity, whereas the viscosity of shorter chains increases only as a result of increasing concentration.

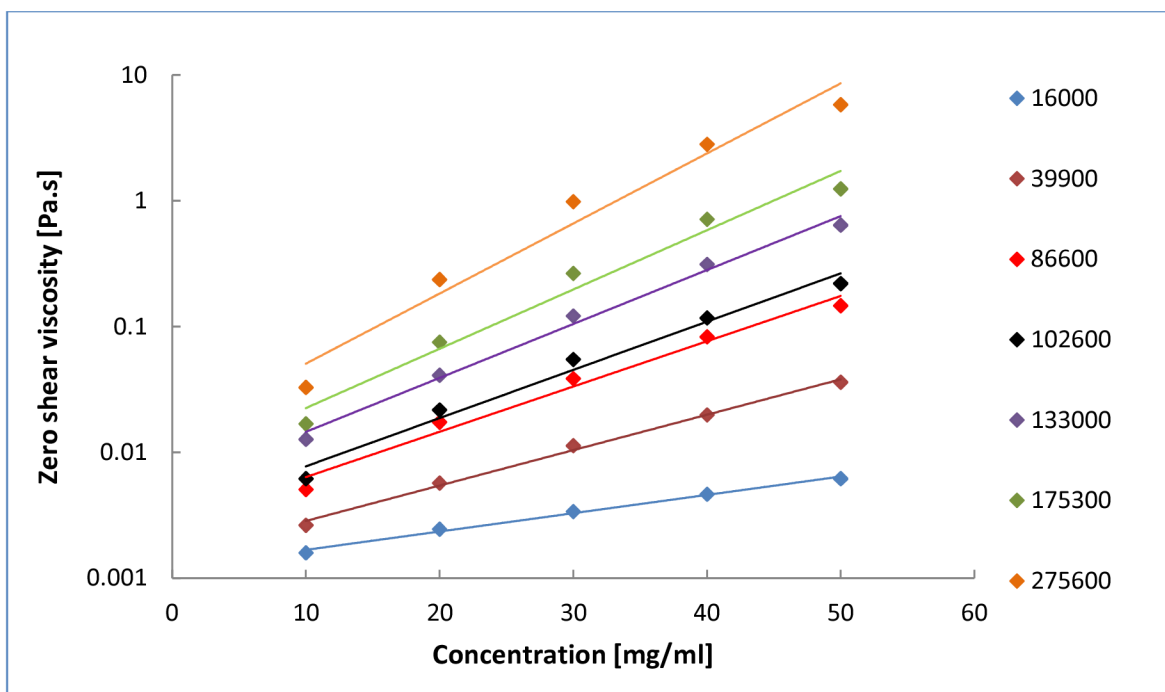


Fig. 32 The effect of Mw and concentration on zero shear viscosity of VLMW HA in 0.1 M PBS, pH = 7.00.

The specific viscosity versus $Mw \cdot c$ dependence of all measured samples in PBS, pH 7.00 is summarized in Fig. 33. Also the same curve of aqueous solutions is added to make a complete notion of this dependence.

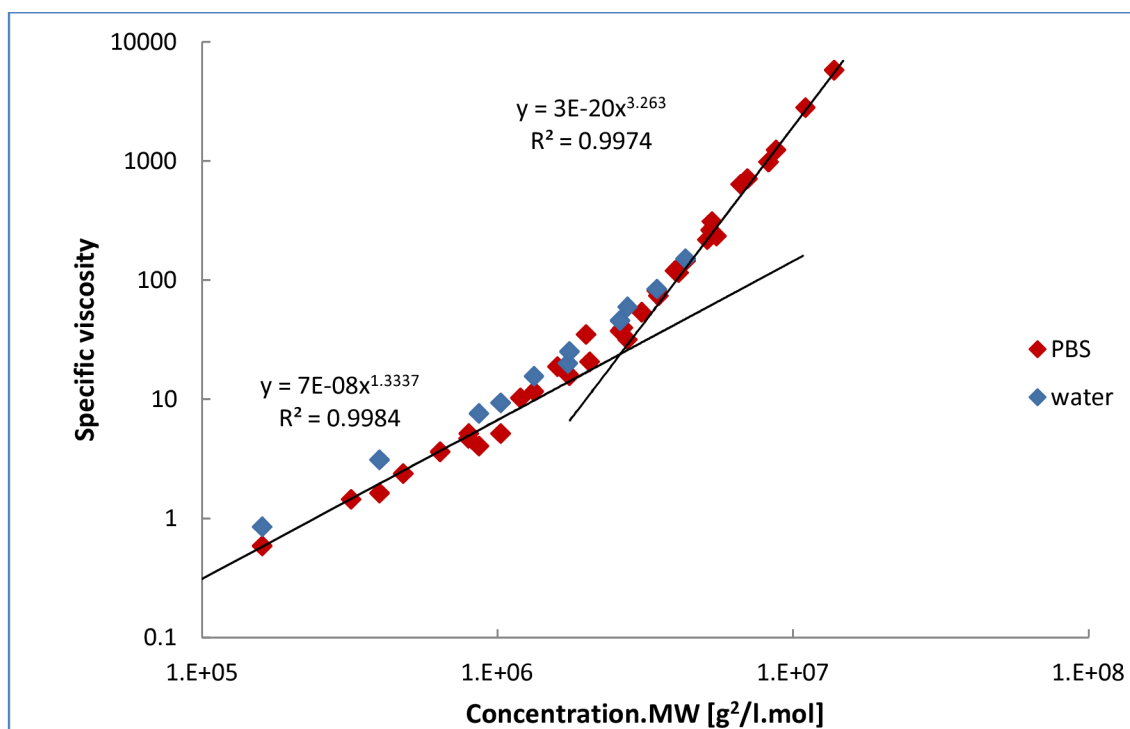


Fig. 33 The dependence of specific viscosity on $Mw \cdot c$ of VLMW HA in 0.1 M PBS, $pH = 7.00$ and water.

The data span two decades in $Mw \cdot c$ and crossovers from the dilute to the semidilute entangled regime, that are observed as changes in slope. In dilute solution, viscosity should be proportional to concentration ($\eta_{sp} \sim c$) for polyelectrolytes in the high salt limit (as well as neutral polymers in good solvent).⁸⁶ This study found $\eta_{sp} \sim c \cdot Mw^{1.33}$ in dilute solution, in excellent agreement with the results in literature. For example Krause et al. who measured only one sample of HA with $Mw 1.5 \cdot 10^6$ g/mol in phosphate buffer saline mix ($pH 7.4$, 0.138 M NaCl, 0.0027 M KCl).⁴⁷ Their study found $\eta_{sp} \sim c^{1.1}$. The overlap concentration was determined to be $c^* = 0.59$ mg/ml, and the entanglement concentration c_e which characterizes the end of the semidilute unentangled regime and the beginning of the entangled regime was determined to be $c_e = 2.4$ mg/ml.

Briefly, the specific viscosity η_{sp} , measured for homogeneous well-behaved HA solutions at very low or zero shear rate is a simple function of the concentration, c , and average molecular weight of the HA, described in terms of its intrinsic viscosity⁸⁷

$$\eta_{sp} = c[\eta] + k' (c[\eta])^2 + \frac{(k')^2}{2!} (c[\eta])^3 + \dots \quad (\text{Eq.18})$$

where the value of k' , the Huggins constant, is explicitly 0.4, based on its derivation from the Stokes–Einstein equation for the viscosity of a suspension of spheres. Presented measurements of the zero shear viscosity for HA in neutral salt solution as a function of

concentration and molecular weight are in excellent agreement with the simple predictions of the four-term interaction equation (Eq. 18).

In dilute solution, when the product $c[\eta]$ is less than about 1, the specific viscosity is apparently dependent on $c[\eta]$ to a little more than the first power. The data are often expressed in the literature in terms of the molecular weight, M , rather than $[\eta]$. Cowman and Matsuoko in their review⁸⁴ recall that $[\eta]$ is proportional to $M^{0.80}$ for the spherical HA conformation, and can easily interconvert the variables. The actual range of exponents observed (probably strongly dependent on the exact range of $c[\eta]$ used in the data fit) show that η_{sp} depends on $c^{0.8-1.6} M^{1.0-1.5}$ in dilute solution, with exponents near 1.2 for c and 1.0 for M most commonly found. This corresponds to $c^{1.2} \eta^{1.25}$ and shows that both the first and second power terms contribute in dilute solution.

In more concentrated solutions, when $c[\eta]$ is greater than about 10, the specific viscosity has been found to depend on $c^{3.8-4.1} M^{3.3-4}$ equivalent to $c^{3.8-4.1} \eta^{4.1-5}$. The values are summarized from eight articles and together are reported in Cowman and Matsuoko work.⁸⁴

4.3.2 HMW HA

Also the flow curves of different concentrations of HMW HA solutions were measured in 0.1M PBS solution, pH 7.00 (Fig. 34). The concentration range was 0.1 – 1% (w/w), except the highest concentration of HA with Mw 2 612 000 was only 0.75 %, because higher concentration was too viscous to prepare it.

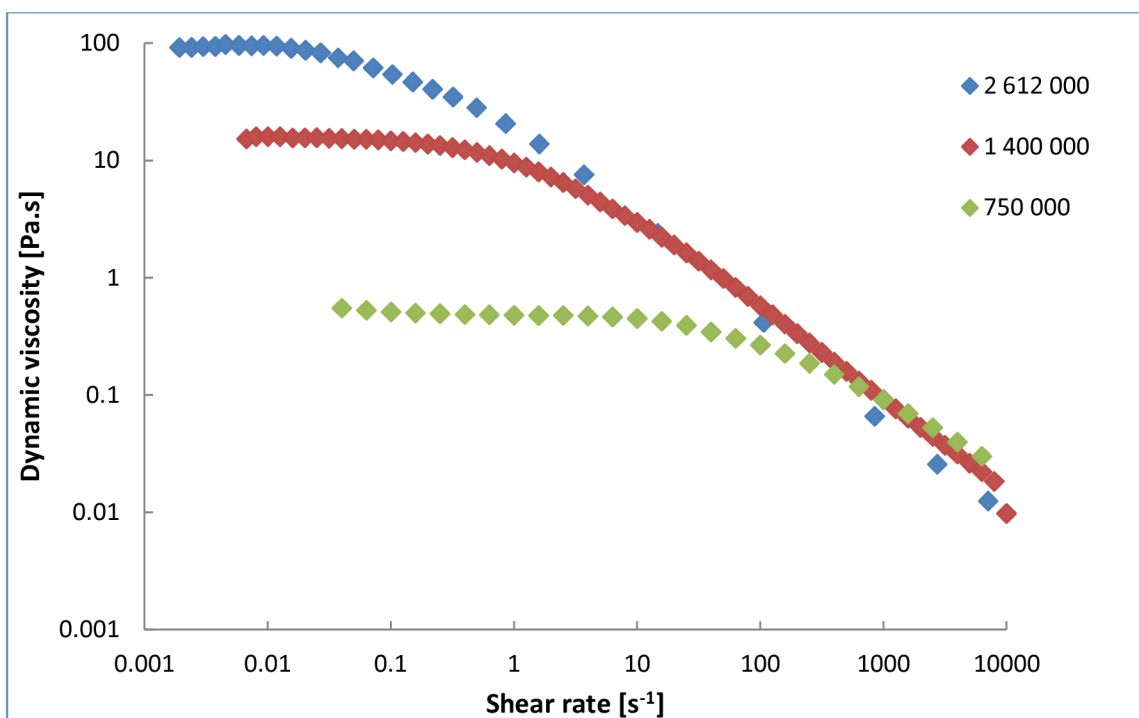


Fig. 34 The flow curves of HMW HA in range of Mw 750 000 – 2 612 000 g/mol in 0.1 M PBS, pH = 7.00.

Tab. 7 The zero shear viscosities of 1 (0.75)% HMW HA in 0.1M PBS (pH = 7.00) calculated from the flow curves by using of the appropriate rheological model.

Molecular weight [g/mol]	Rheological model	Zero shear viscosity [Pa.s]	Consistency [s]	Rate constant
750 000	Cross	0.6693	$8.29 \cdot 10^{-3}$	0.74
1 400 000	Cross	15.33	$6.60 \cdot 10^{-1}$	0.82
2 612 000*	Cross	98.80	2.29	0.86

*concentration is only 0.75 % (w/w)

Whereas the viscosity of HMW sample is too high that it is impossible to measure 1% HA in PBS solution, by decreasing the Mw less than twice, the zero shear viscosity of 1% solution is about 15 Pa.s and by another decrease (approximately 3,5x) the viscosity of 1% aqueous solution is only about 0,5 Pa.s. On the other hand, a critical shear $\dot{\gamma}^*$, which is the shear rate when the curve pass from the linear region to the shear–thinning region, increases with the decreasing molecular weight and concentration of HA.

As mentioned above, the viscosity is strongly dependent on concentration and molecular weight of HA. At any molecular weight of HA, the viscosity increases by $\sim 10^3$ for a 10-fold increase in concentration and at concentration of 10 mg/ml the viscosity varies from 1 to 100 Pa.s as the molecular weight is increased (Fig. 35).

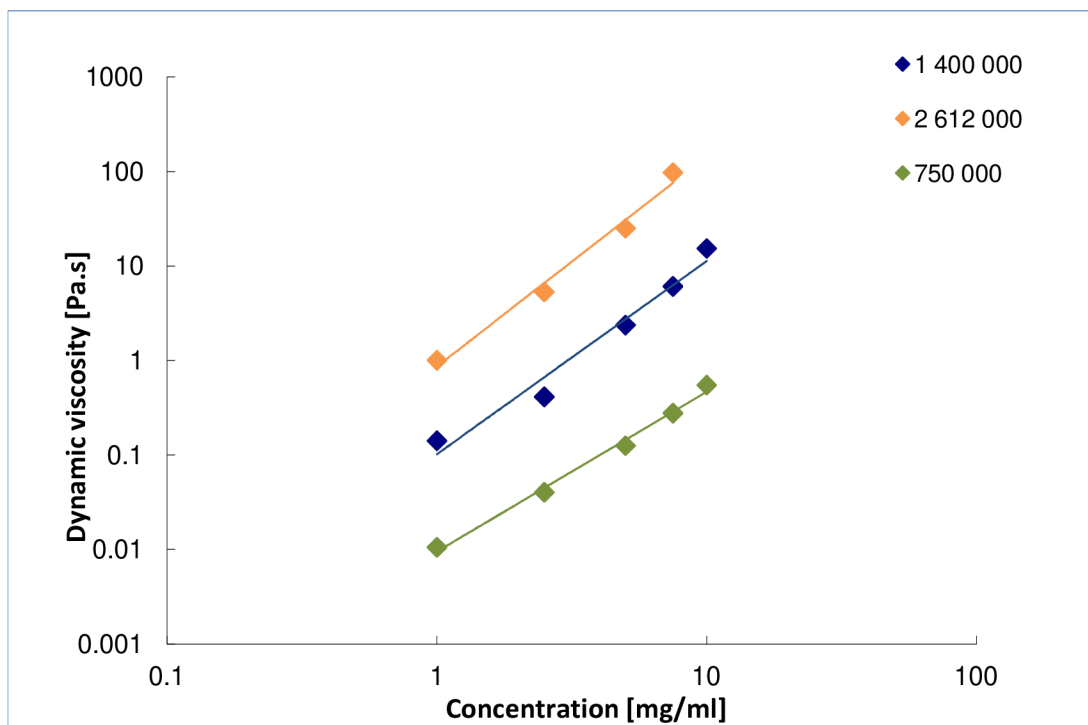


Fig. 35 The log-log plot of zero shear viscosity, η_0 , as a function of solution concentration for HA at three molecular weights, 0.1M PBS, pH 7.

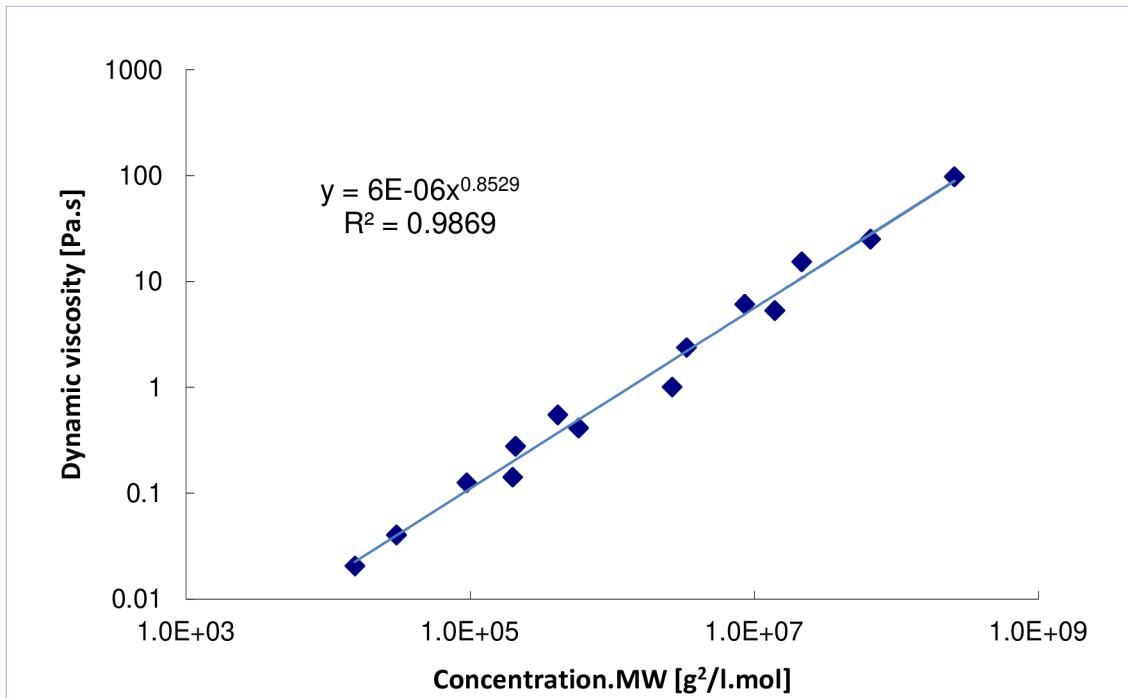


Fig. 36 The log of zero shear viscosity plotted versus the log of the (concentration · molecular weight) for HMW HA, 0.1M PBS, pH 7.

For these data (Fig. 36), η_0 correlates very well with HA (concentration · molecular weight) and the HA solution η_0 can be predicted from the relationship: $\eta_0 = 6 \cdot 10^{-6} (c \cdot Mw)^{0.853}$. This equation also matches the previous results, which are known from the literature.⁸⁴ Cowman and Matsuoka wrote down a review informing about the research on hyaluronan structure to the year 2005. For the high molecular weight region, results of a parameter from Mark-Hoving equation were reported from 0.73 to 0.92.⁸⁴ This equation is valid only for limited range of molecular weights. It is requisite to make a new curve for smaller or higher values of molecular weights, because this dependence is not strictly linear and the deviations in lower and upper parts of the curve may be inconsiderable.

4.3.3 Comparison of VLMW and HMW HA

To compare previous results of LMW and HMW HA solutions, the double-logarithmic plot of specific viscosity versus molecular weight for LMW HA (MW 16000-275600 g/mol) and HMW HA (MW 750000-2612000 g/mol) in 0.1M PBS is shown in Fig. 37.

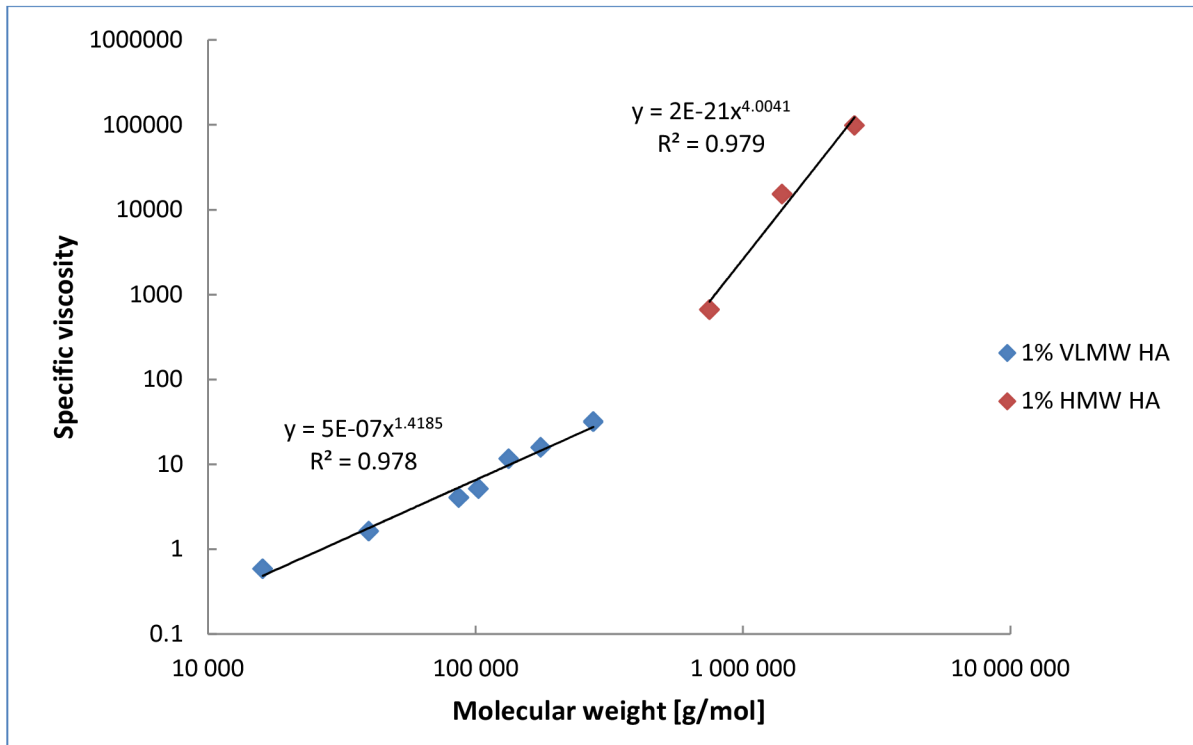


Fig. 37 Variation of specific viscosity at concentration 1% (w/w) with the weight average molecular weight of hyaluronan samples in 0.1 M PBS at 25°C.

The results are in good agreement with analogous measurement done by Foussiac et al., who measured different molecular weight of hyaluronan in dilute and semi-dilute regions ($c = 5 \cdot 10^{-4}$ and 10^{-2} g/ml), whereas they used 0.15M NaCl as a solvent.⁵⁸ Their results reveals that the molecular weight dependence of η_{sp} in 0.1 M NaCl solutions is given by $\eta_{sp} \sim M^4$ in the more concentrated regime and $\eta_{sp} \sim M$ in the dilute regime. They have checked that these exponents do not depend on the concentrations chosen in the different regimes for their determination.

3.1.1. Kinematic viscosity

Also kinematic viscosities, which are often used in many publications, were calculated. The kinematic viscosity is also an important parameter during the produce of hyaluronan as a quick orientation test of viscosity and it is useful for approximate determination of molecular weight of produced batch. As was mentioned in previous chapters, the viscosity of hyaluronan is strongly dependent on shear rate. That is why the zero shear viscosity values were appointed in to the calculation. The fractions of zero shear viscosities and densities of proper samples, were calculated for 1% samples of LMW HA in PBS, pH 7.00. Kinematic viscosity is given by:

$$\nu = \frac{\eta}{\rho} \text{ [cm}^2\text{/s]} \quad (\text{eq.19})$$

Because the density of all measured samples was not different from 1 g/cm³, the values of zero shear viscosities and kinematic viscosities are nearly identical (Tab.8). This implies that for approximately determination, it is not necessary to measured both, kinematic and dynamic viscosity. This is important information from the practical point of view, because some studies are focused on the dynamic viscosity of HA, some on the kinematic viscosity.

Tab. 8 Kinematic viscosity of 1% VLMW HA samples in 0.1M PBS, pH 7.00

Molecular weight [g/mol]	Zero shear viscosity [Pa.s]	Density [g/cm³]	Kinematic viscosity [cm²/s]
16 000	0.00159	1.01290	0.00157
39 900	0.00264	1.01271	0.00261
86 600	0.00508	1.01250	0.00502
102 600	0.00619	1.01276	0.00611
133 000	0.01270	1.01292	0.01254
175 300	0.01690	1.01306	0.01668
275 600	0.03290	1.01268	0.03249

4.3.4 The effect of solvent

Three different types of solvent, demineralised water, physiological solution and phosphate buffer solution, were used at the pH 7.00 and the concentration of HA was always 1% (w/w). The viscosity of HA in water is always higher than in PB or PBS, which is caused by the conformation of chains in a given solvent (Fig. 38). While in water, HA chains are more extended and that is why the viscosity is higher, in presence of ions HA forms more rigid entanglements.³⁶ The structure of chains in PB and PBS is more compact and there is no big difference in viscosity between them.

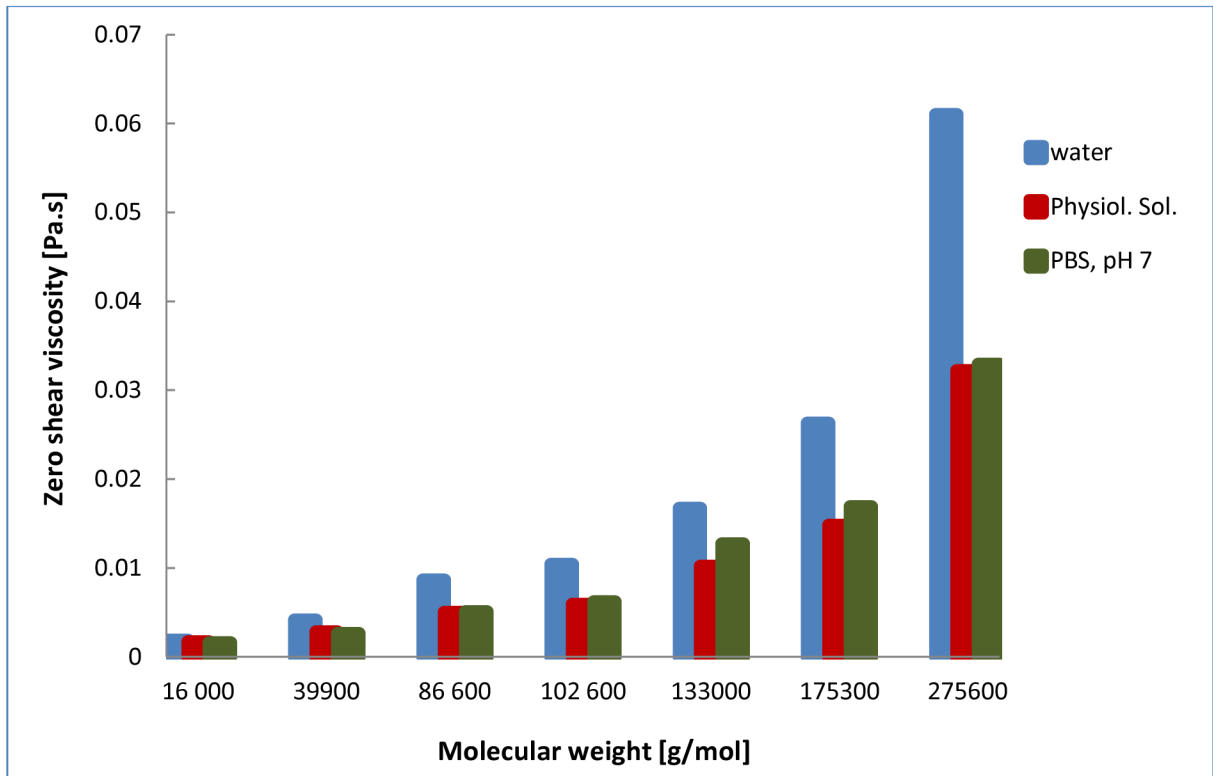


Fig. 38 The effect of solvent on zero shear viscosity of 1% (w/w) VLMW HA.

4.3.5 The effect of pH

Phosphate buffer solution of pH 5.00, 6.00, 7.00 and 8.00 was chosen to study the effect of pH on zero shear viscosity of 1% (w/w) VLMW HA (Fig. 39). Because the values of zero shear viscosities are comparable for each sample, molecular weight of HA is not degraded and also the conformation does not change in this range of pH. It's known that HA degradation is significant when the pH is very low (less than 3) or on the other hand very high (higher than 10). The effect of pH would be probably more evident for HA with higher molecular weight, but in case of VLMW HA is insignificant.

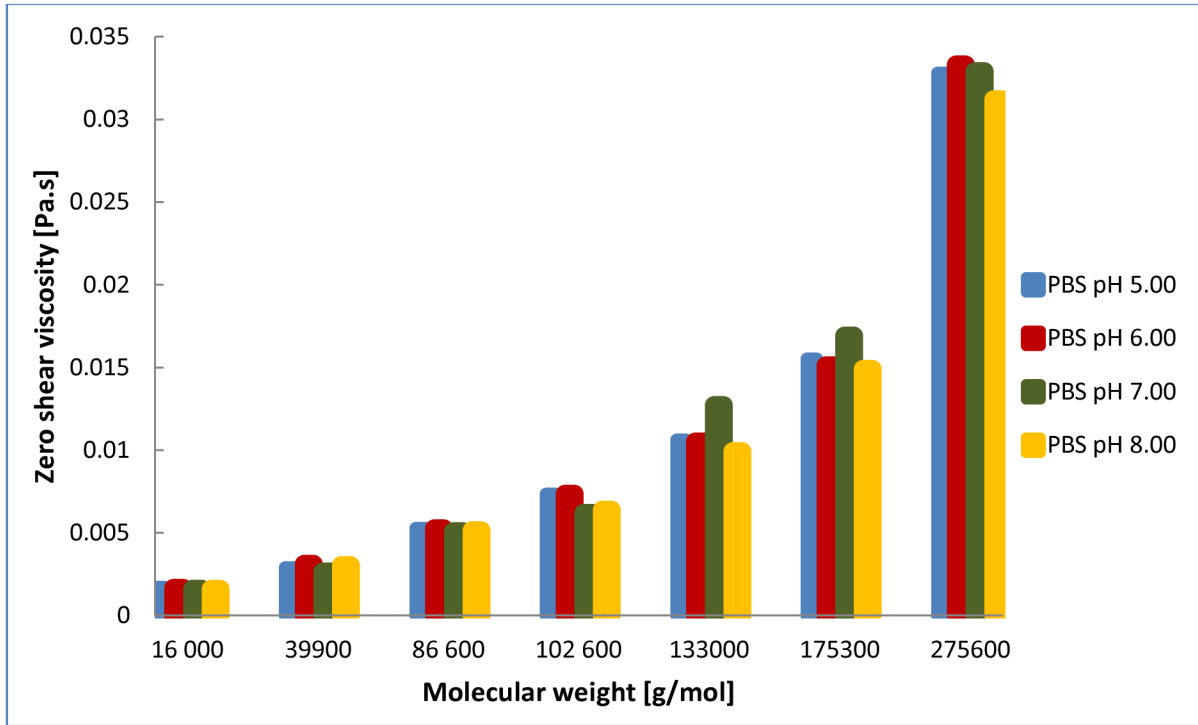


Fig. 39 The effect of pH on zero shear viscosity of 1% (w/w) VLMW HA.

A surprising pH-dependent transition, near neutral pH, was reported by Barrett and Harrington.⁸⁸ Using potassium phosphate buffers in the pH range 6.0–8.5 at an ionic strength of 0.1, these authors observed a dramatic drop in zero shear intrinsic viscosity as pH was decreased from 7.5 to 7.0. It should be noted that the concentration range used to extrapolate the reduced viscosity to zero concentration was quite high, opening the possibility that a small change in bulk viscosity due to aggregation could result in an erroneous estimation of the intrinsic viscosity. The phenomenon was reexamined by Balazs et al.,⁸⁶ but no change in intrinsic viscosity between pH 6 and 8 in potassium phosphate under the same conditions was observed. That is also coincident with results presented in this work.

4.4 The temperature curves

The temperature dependence of liquid viscosity is the phenomenon by which liquid viscosity tends to decrease (or, alternatively, its fluidity tends to increase) as its temperature increases.

To evaluate the temperature curves, Arrhenius model has been used. The model is based on the assumption that the fluid flow obeys the Arrhenius equation for molecular kinetics:

$$\mu(T) = \mu_0 \exp\left(\frac{\eta}{RT}\right) \quad (\text{eq. 20})$$

where T is temperature

μ_0 is a coefficient

η is the viscosity

R is the universal gas constant.

4.4.1 LMW HA

The effect of increasing temperature on dynamic viscosity of HA was studied according to evaluated method (Chap. 4.2.2.). It means shear rate was 100 s^{-1} and the temperature ramp was always $4^\circ\text{C}/\text{min}$. 1% sample concentration and two types of solvent, demineralised water and PBS pH 7.00, were used for these measurements. It is evident (Figs. 40 and 41) that with increasing temperature the viscosity decreases. This phenomenon is due to the changes of chain conformation and at higher temperatures (more than 60°C), the degradation process of HA starts.

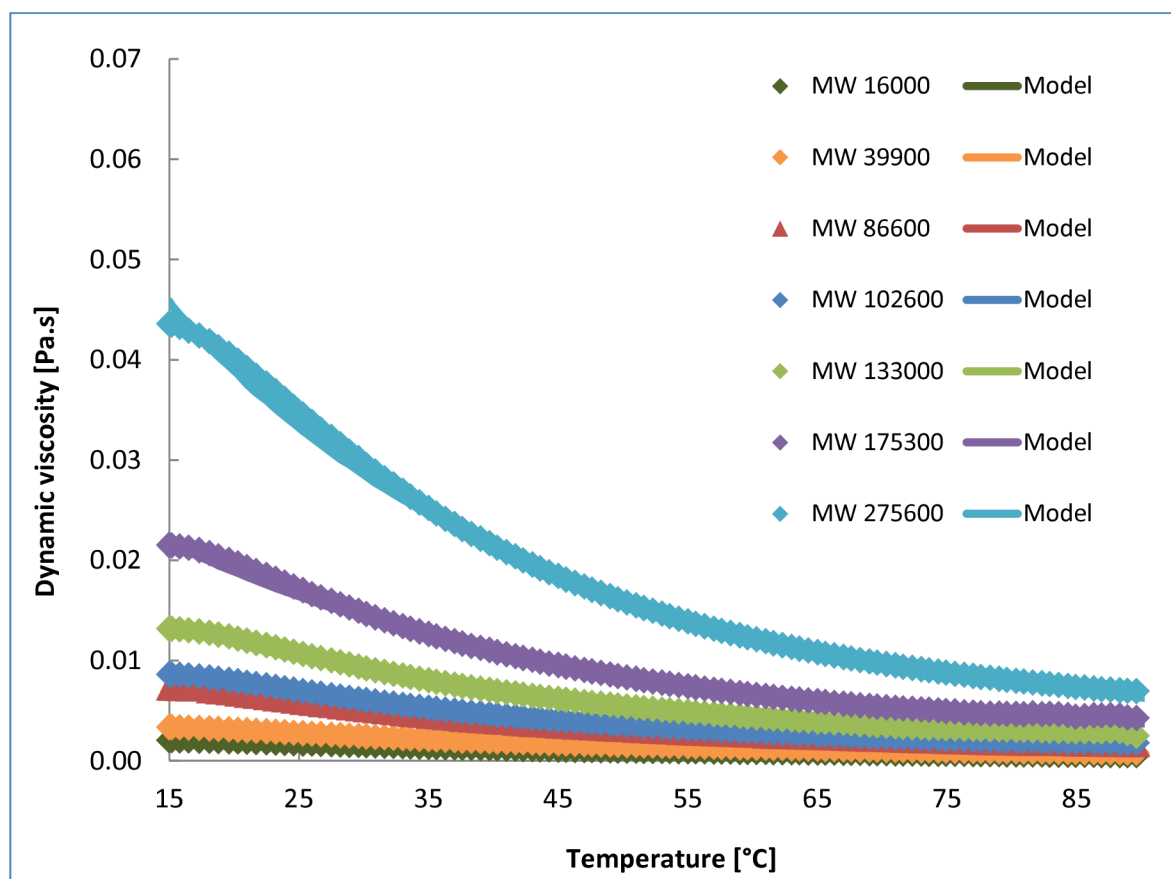


Fig. 40 The temperature ramp curves of 1% VLMW HA with different molecular weight in phosphate buffer solution, pH = 7.00. Shear rate 100s^{-1} , temperature ramp $4^\circ\text{C}/\text{min}$.

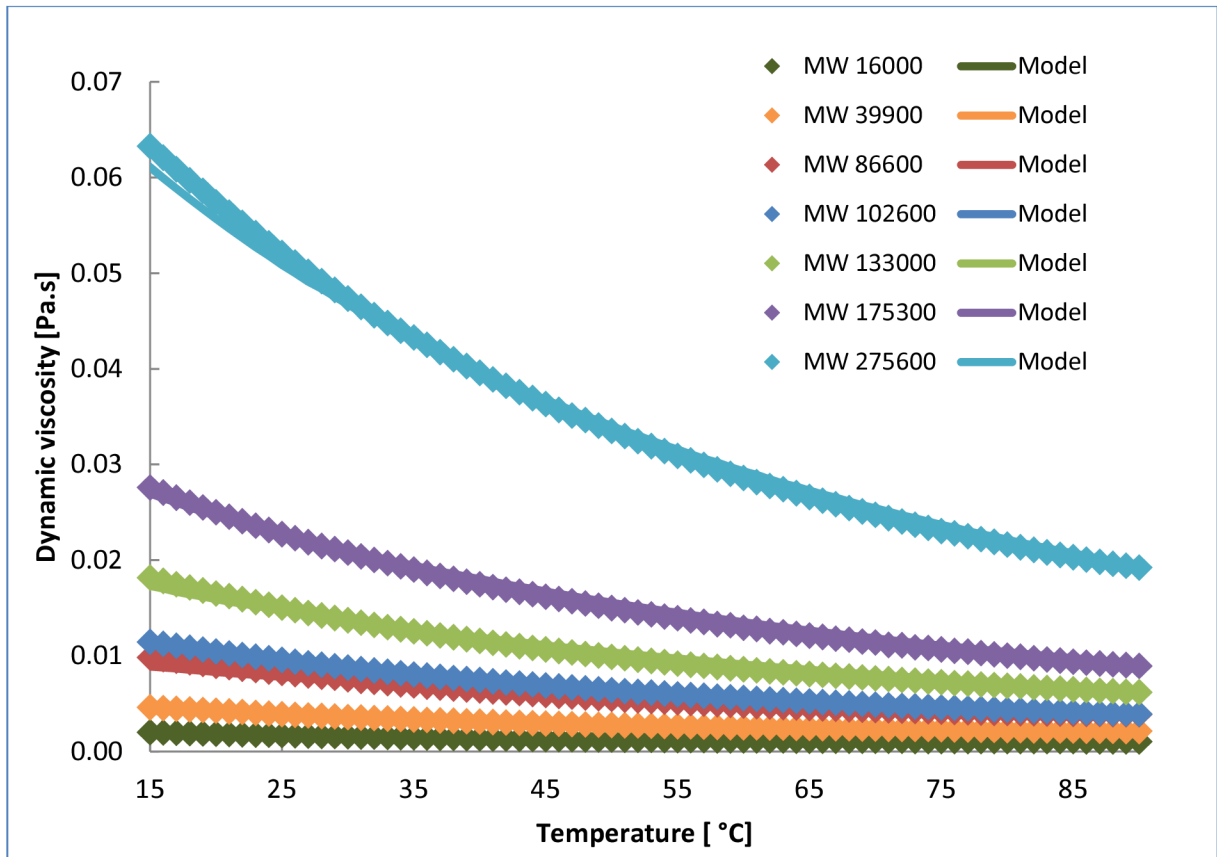


Fig. 41 The temperature ramp curves of 1% VLMW HA with different molecular weight in demineralised water. Shear rate $100s^{-1}$, temperature ramp $4^{\circ}C/min$.

An interesting phenomenon is observed when comparing the decrease of viscosity in demineralised water and in PBS, pH 7.00 (Fig. 42). While in case of PBS the decrease of viscosity is nearly linear (in log scale) during the whole range of temperatures, in case of water a little increase of viscosity at higher temperatures can be observed. Because the double gap concentric cylinders were used for all these measurements, the effect of chosen geometry is impossible. The surface that solution occupies in this type of geometry is very small and so the effect of different evaporation of PBS and water is also improbable. Maybe in water at temperatures higher than $60^{\circ}C$ some organized structure, which is the cause of viscosity increase, is formed. With another increase of temperature, the viscosity would probably decrease again. However, it is impossible to verify, because of near boiling point of water.

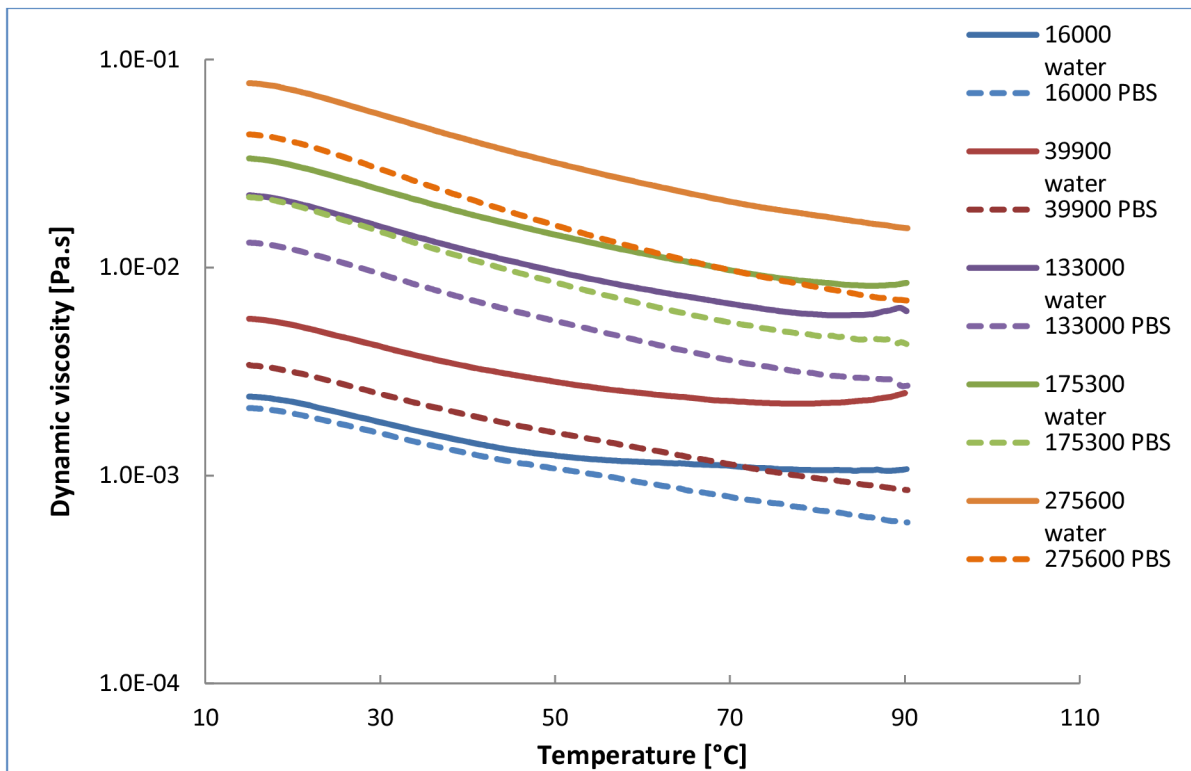


Fig. 42 The comparison of temperature ramp curves of 1% VLMW HA with different molecular weight in phosphate buffer solution, pH = 7.00 and demineralised water. Shear rate $100s^{-1}$, temperature ramp $4^{\circ}C/min$.

4.4.2 HMW HA

HA is temperature unstable biopolymer; it starts to degrade at temperatures around $60^{\circ}C$, which is its big disadvantage during the sterilization process. In an effort to study the behavior of HA solutions during the increasing temperature, the temperature ramps of HA aqueous solutions without and with added different amount of NaCl have been measured.

The aim of this study was to answer the question if the initial concentration of HA or the addition of NaCl does influence the thermal stability of HA during the temperature ramp measurements. The idea was that while molecules of HA in present of NaCl molecules form more rigid structure, such structure may be more resistant of high temperature effect.

The viscosity of HA aqueous solutions of different concentrations and of 1% HA solution with different concentration of NaCl have been measured during the increasing temperature.

This experiment is simpler possibility how to study the effect of different HA concentrations and addition of salt on thermal stability than to autoclave all samples. It is a simplified simulation of degradation HA by increasing temperature and a big advantage of method is the possibility to see the behavior online with the increasing temperature. The disadvantage is that it is impossible to study it at temperatures higher than $90^{\circ}C$, because of

the aqueous solutions evaporation. The small amount of the sample tends to stick to the Peltier plate, thereby increases the viscosity and this effect predominates over the degradation.

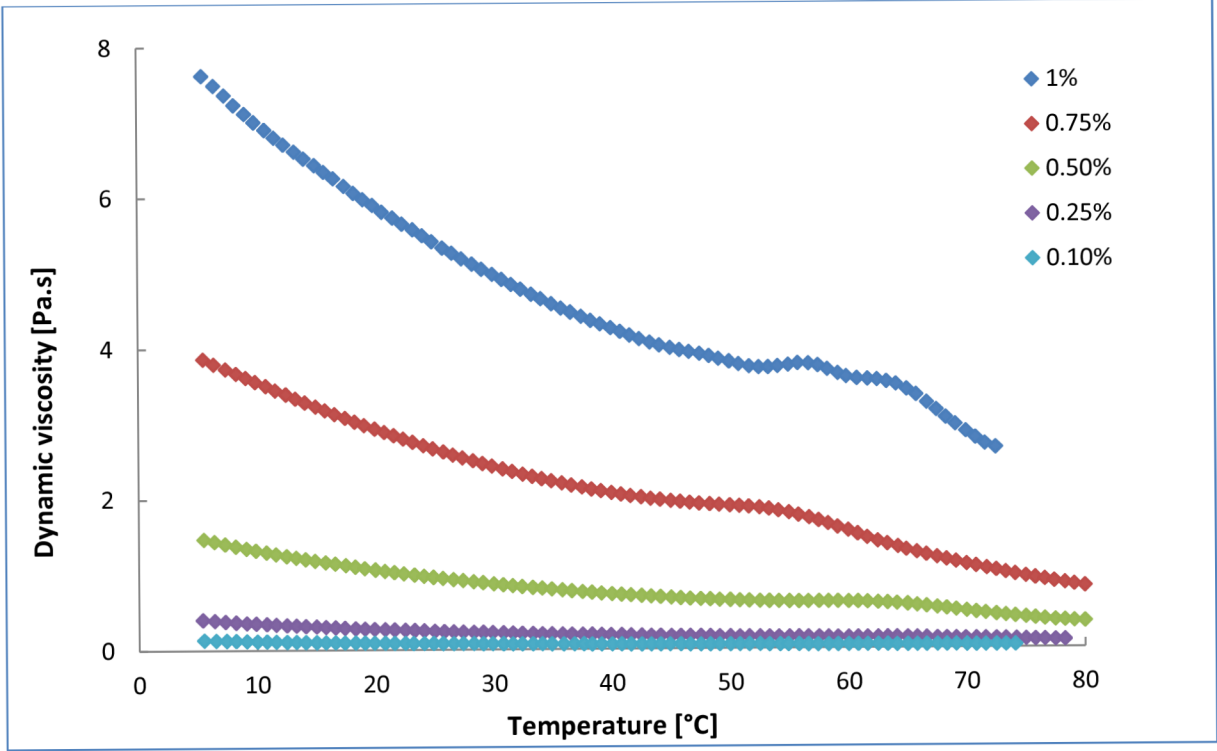


Fig. 43 The temperature ramp curves for different concentration of HA 250205. Shear rate $100s^{-1}$, temperature ramp $4^{\circ}C/min$.

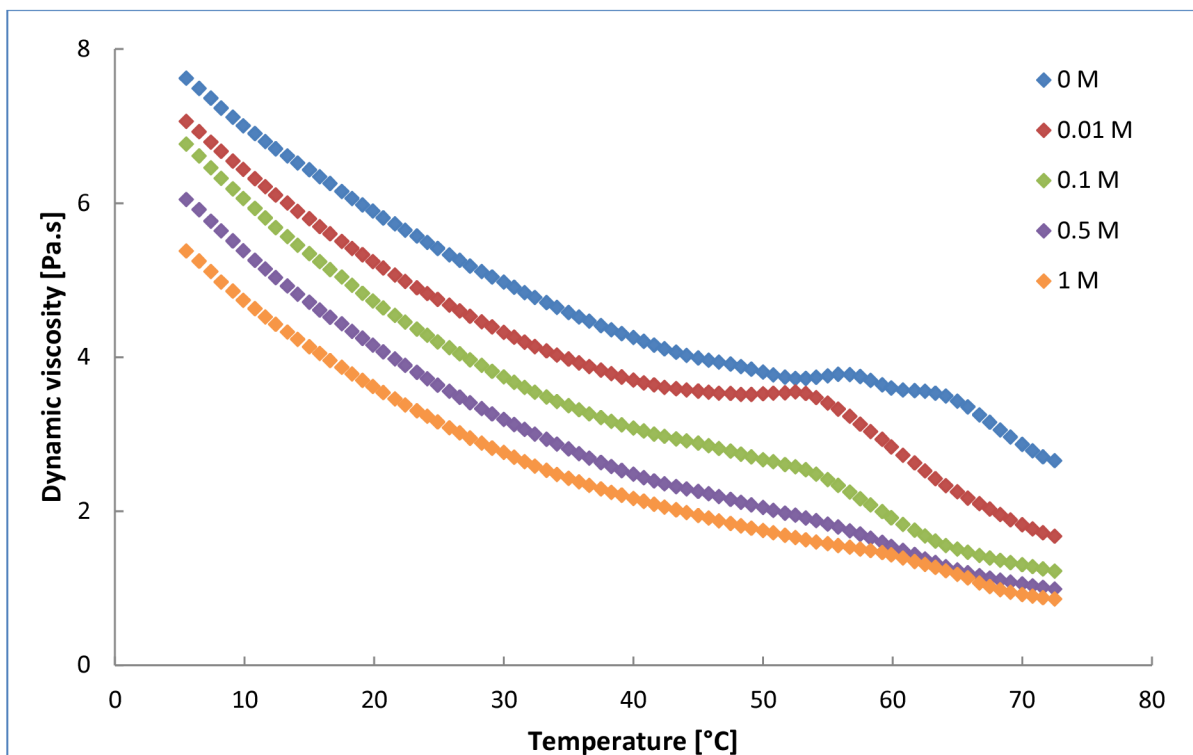


Fig. 44 The temperature ramp curves for 1% aqueous solution of HA 250205 with different concentration of NaCl. Shear rate $100s^{-1}$, temperature ramp $4^{\circ}C/min$.

Surprisingly, the addition of NaCl caused decrease of viscosity of HA samples. One reason may be in negative influence of NaCl on the HA stability, so that with the increasing concentration of the salt the stability decreases rapidly. But the decrease of stability should be also seen in acute decrease of viscosity curve during the temperature increase. Nothing like this was observed during the measurements. More probably explanation is that the decrease of viscosity is caused by changes of conformation after shielding of electrostatic forces after addition of NaCl.

If nothing special happened in the solution, the temperature ramp curves should decrease with increasing temperature. But in our case bold peaks can be observed in temperature region between 50 and 70°C (Figs. 43, 44 and 46). With increasing ionic strength of the solution the peaks heights decrease and also with addition of NaCl the peaks slightly move to lower temperatures. It may be a result of changing interactions between HA chains. The idea is that without any added salt, the conformation of HA chains has modify when the temperature reached approximately 55°C. Because the viscosity is, among other factors, a function of conformation, the changes on the viscosity curves have been observed. But if there is any amount of NaCl added to the solution, the conformation will change in the beginning and the increasing temperature does not affect it so much. These results about forming more resistant structure in region around 60°C correspond with previous assertion about more thermal stable region of HA around this temperature.

The same concentrations of aqueous solutions without and with NaCl have been measured for HA 250205-D1. The results are almost the same (Figs. 45 and 46). The stability also decreases with decreasing concentration of HA and with increasing concentration of sodium salt.

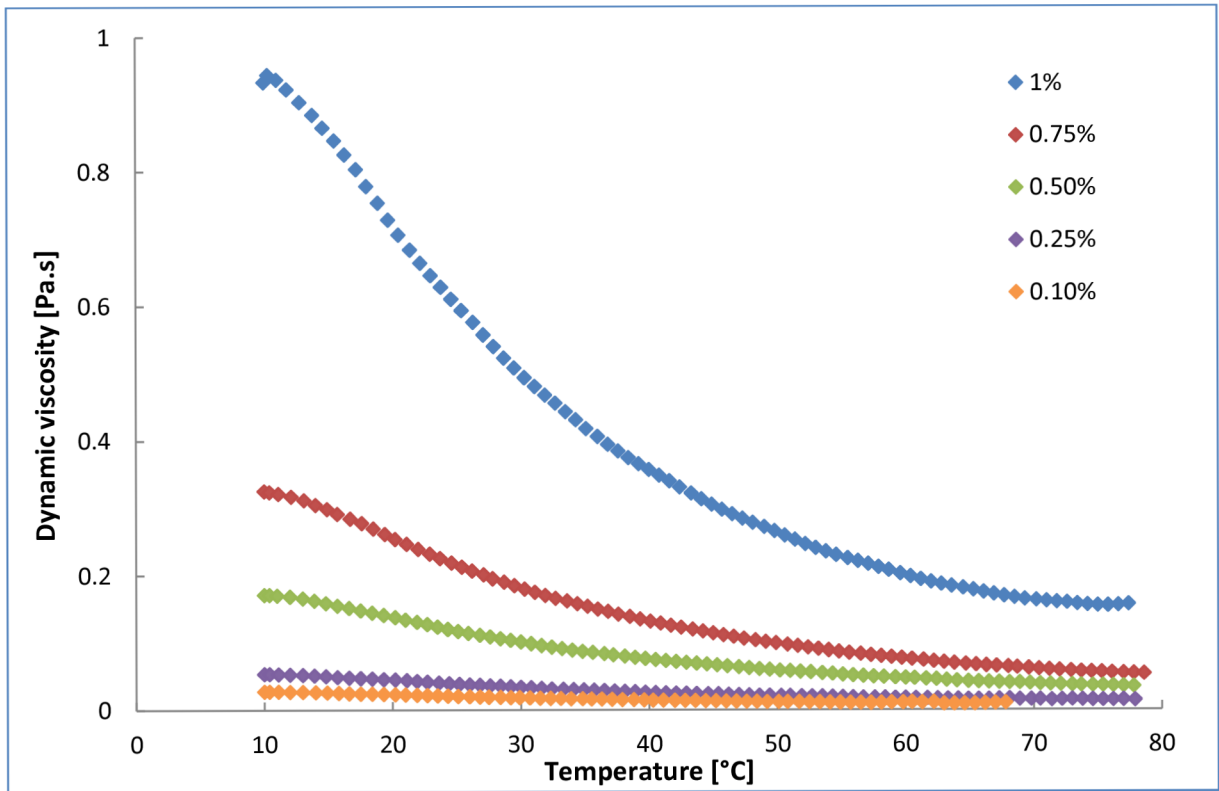


Fig. 45 The temperature ramp curves for different concentration of HA 250205-D1. Shear rate $100s^{-1}$, temperature ramp $4^{\circ}C/min$.

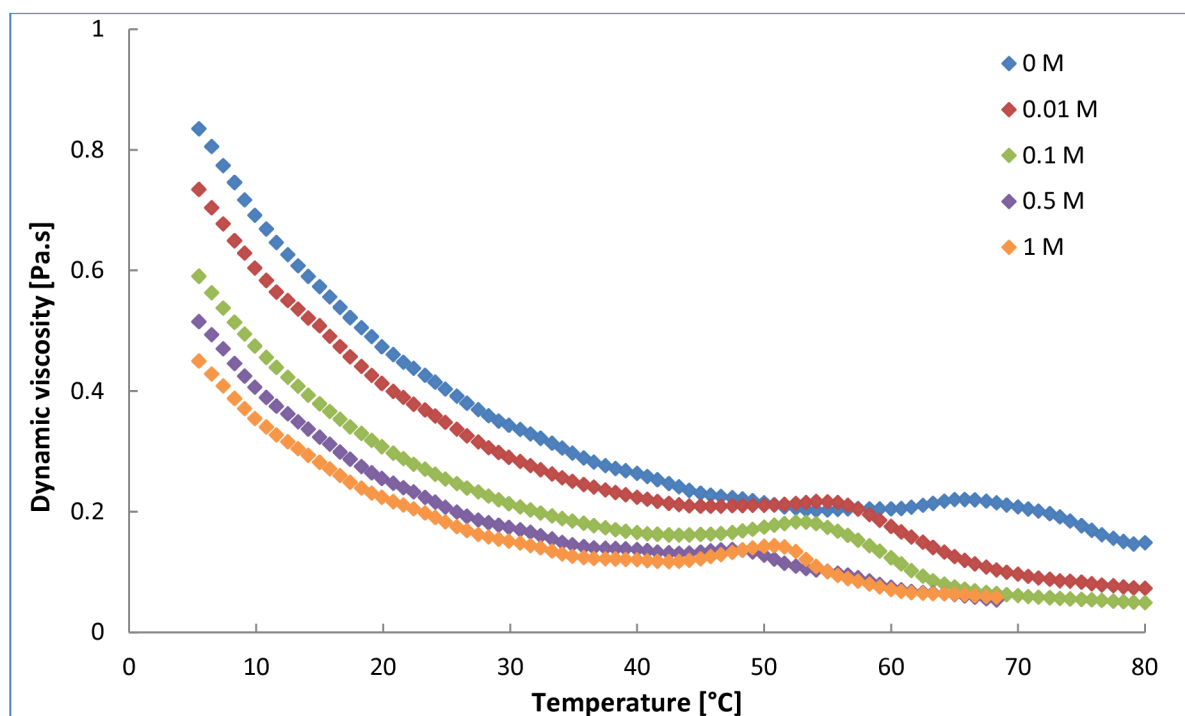


Fig. 46 The temperature ramp curves for 1% aqueous solution of HA 250205-D1 with different concentration of NaCl. Shear rate 100s^{-1} , temperature ramp $4\text{C}/\text{min}$.

In Fig. 45, there are not any marked peaks observed. The reason may be in the measuring geometry. While in the other cases the temperature ramps have been measured by CP geometry, in this case the DCC geometry (because of lower viscosity) has been used. But not only the type of geometry may play the role, either the effect of chains length can not be excluded.

The temperature dependence of the intrinsic viscosity of HA has been investigated by Cleland and Fouissac et al.⁸⁷ Over the temperature range of 25–60 °C, the persistence length decreases, leading to a decrease in intrinsic viscosity. This reflects the increased population of high energy conformers at high temperatures. The bulk solution viscosity was confirmed to decrease as a result. Recently, Hoefling et al.⁸⁸ found that the temperature dependence (25–65 °C) of the viscosity of semi-dilute HA solutions could be predicted from the expected change in intrinsic viscosity, using the four term interaction equation (Eq. 18).

4.5 Other physical chemical methods

To confirm the hyaluronan quality and eliminate the presence of any impurities which can affect the results, other physical methods, such as NMR, UV VIS and dynamic scattering were used. All of those methods were supporting for rheological measurements, that is why are presented in this separate chapter.

4.5.1 1D NMR and UV VIS spectra of VLMW HA

^1H spectra of low molecular weight hyaluronan (Figs. 47 and 48) contain well-resolved anomeric (δ 4.4 - 4.7 ppm) and methyl groups (δ 1.9 - 2.1 ppm). Resonances belonging to skeletal signals are clustered between 3.3-4.0 ppm. The signal between 4.7 – 4.9 ppm belongs to deuterium water, which still contains a small amount of ^1H . In some cases traces of IPA were detected (δ 1.1 - 1.2 ppm).

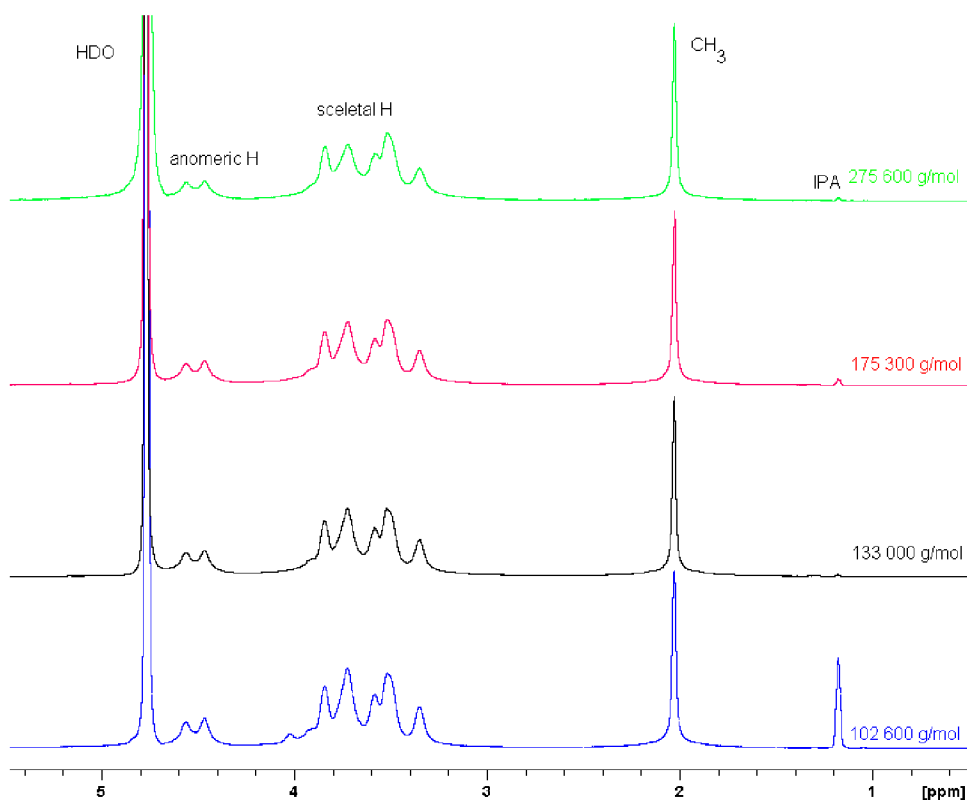


Fig.47 ^1H NMR spectrum of VLMW HA (range of the Mw between 102 600 – 275 600 g/mol).

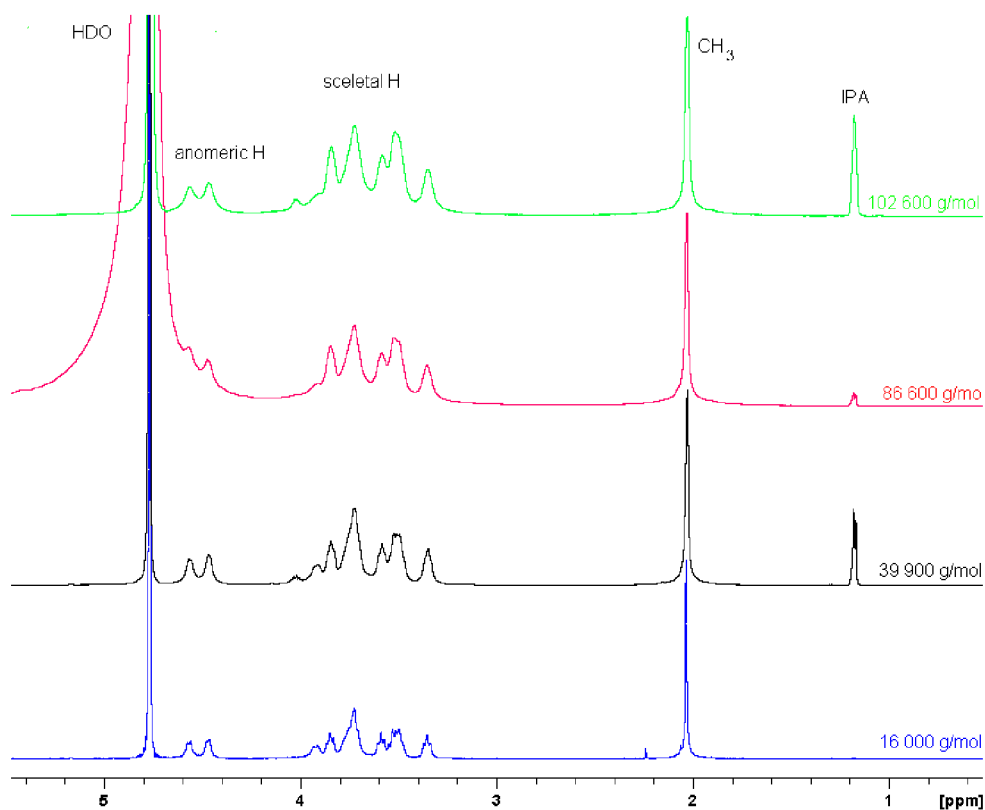


Fig.48 ^1H NMR spectrum of VLMW HA (range of the Mw between 16 000 – 102 600 g/mol).

When comparing the highest and the lowest molecular weight sample (Fig. 49), it could be seen that the signals are at the same position, independently on molecular weight of the sample. While in the case of lower Mw, the peaks are sharp; with the increasing molecular weight peaks are becoming broad. This phenomenon is due to the higher amount of the nuclei, which are present in the sample and thus shorter T_2 (spin-spin relaxation time).

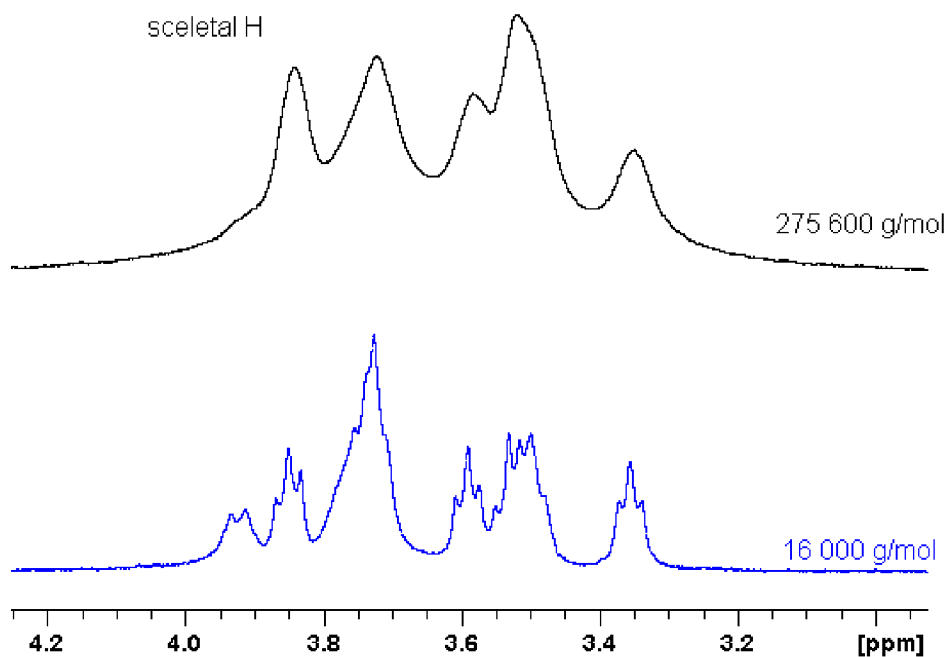


Fig.49 ^1H spectra: Comparison of the lowest and the highest molecular weight samples of HA.

^{13}C spectra of low molecular weight hyaluronan (Figs. 50 and 51) contain also well-resolved anomeric (δ 103 - 107 ppm) and methyl groups (δ 24 - 26 ppm). Resonances belonging to skeletal signals are clustered between 55-90 ppm. The signal about 178 ppm belongs to carbonyl group. Only in cases of HA with Mw 102 600, 86 600 and 39 900 g/mol, traces of IPA were detected (δ 28 and 68 ppm).

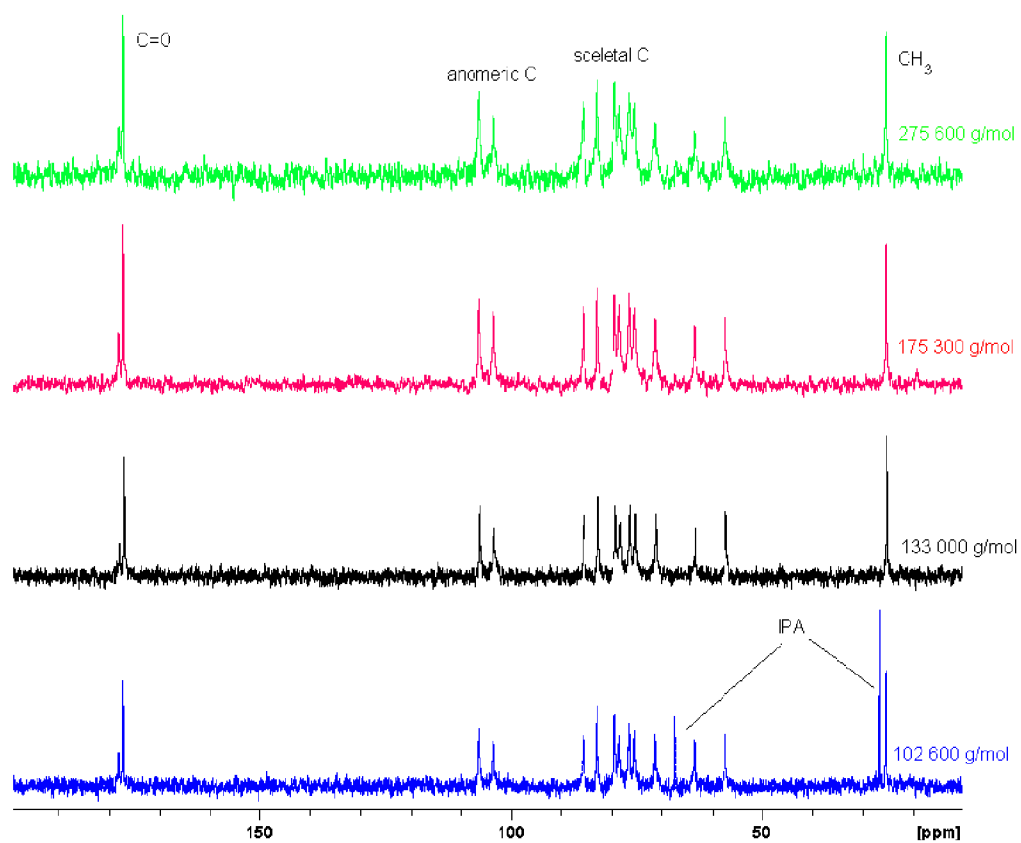


Fig. 50 ^{13}C NMR spectrum of VLMW HA (range of the Mw between 102 600 – 275 600 g/mol)

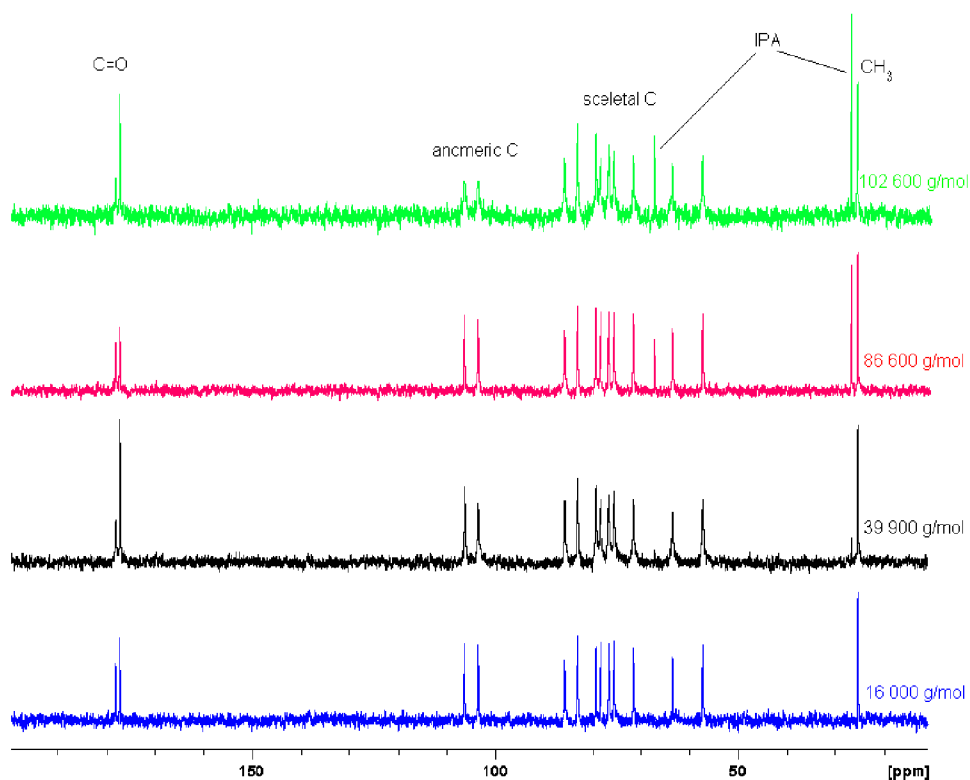


Fig.51 ^{13}C NMR spectrum of VLMW HA (range of the Mw between 16 000 – 102 600 g/mol).

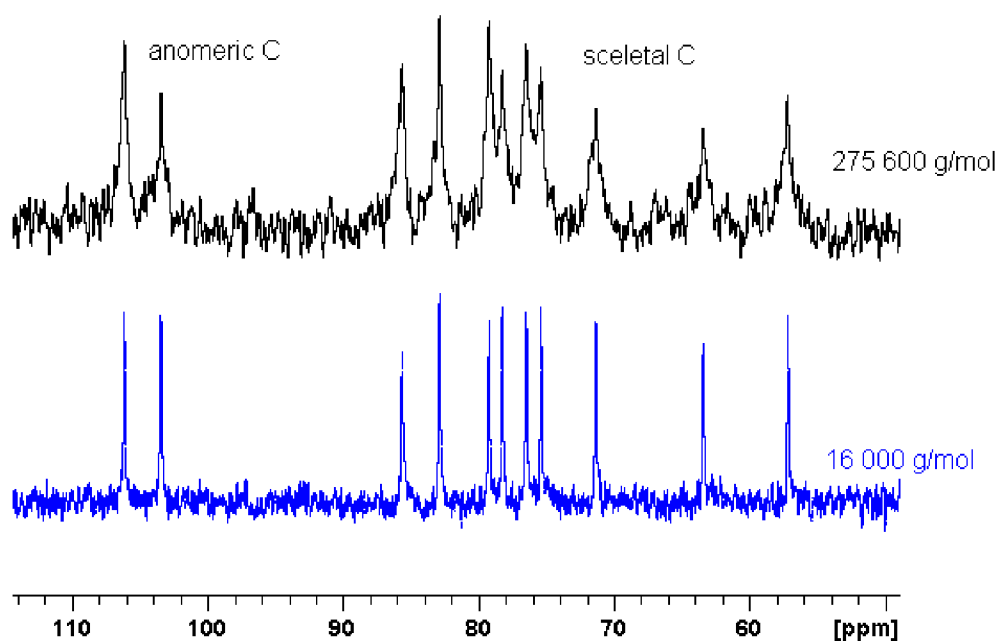


Fig.52 ^{13}C spectra: Comparison of the lowest and the highest molecular weight samples of HA.

By measuring 1D NMR spectra, the purity of all measured HA samples was proved. Only in few cases (Mw 102 600, 86 600 and 39 900 g/mol), traces of IPA were found.

4.5.2 UV-VIS spectra

Typical UV VIS spectra for hyaluronan were obtained by measuring 1% HA solutions in PBS, pH 7.00 (Fig. 53). The peaks at 220 nm correspond with the pure hyaluronan and the second smaller peaks belong to impurities, which increase during the degradation process throughout the produce. With exception of 200409-E2 sample (Mw 175 300 g/mol), intensity of impurities peak increases with decreasing Mw of hyaluronan.

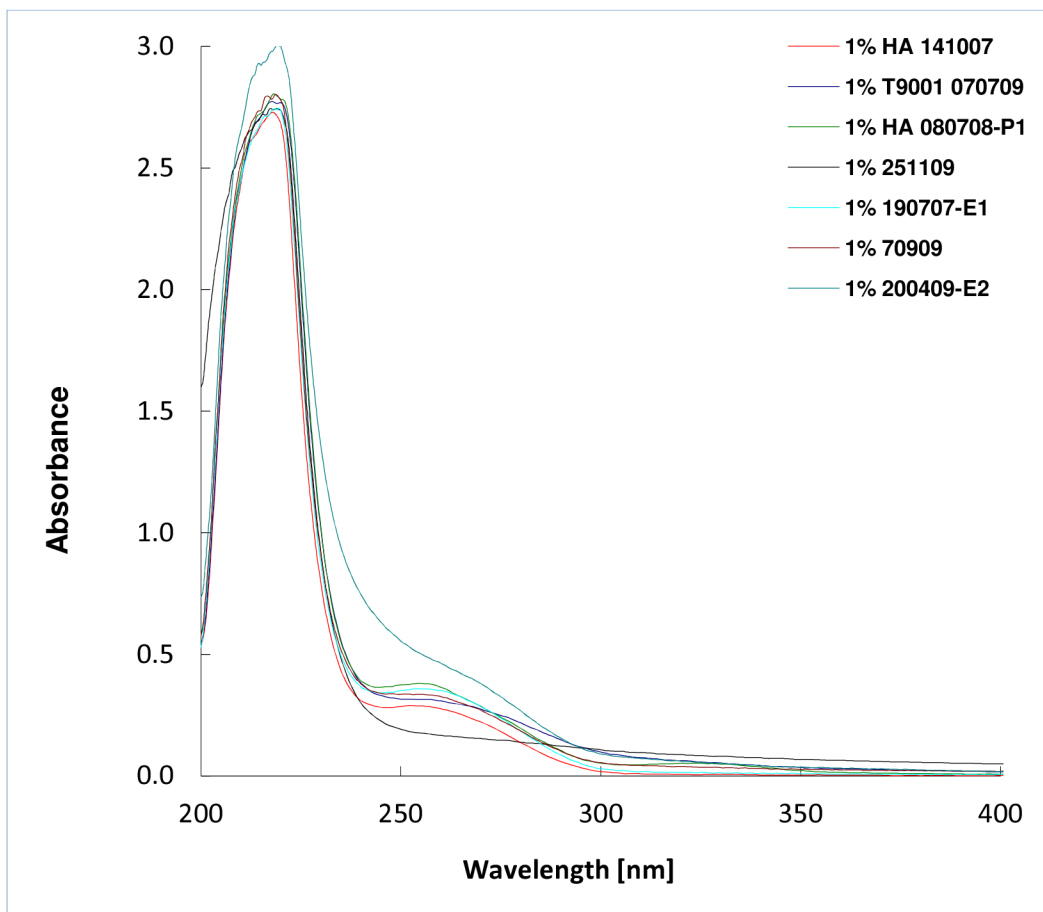


Fig.53 UV-VIS spectra of 1% very low molecular weight HA

4.5.3 The size of particles in VLMW HA solutions

Using the zeta sizer, the size of the HA particles present in 0.1 M PBS, pH 7.00, was measured (Figs. 54 and 55). As described in chapter 3.1.4, the concentration of HA was 1% and all solutions were filtered before the measurement. The necessity of filtration is described in next chapter. Although each sample was measured at least for three times (more often for five times), the results were rather different. The chains of HA in solution are still moving and changing its conformation, the equilibrium is dynamic, and that could caused problems with verification of the results.

The peak of filtered HA is in range 6 -10 nm and the maximum is little shifted with increasing Mw. Peaks in range of 70 – 1000 nm correspond with some bigger particles, probably HA aggregates that had to “grow up” after the filtration.

The sample 200409-E2 (Mw 175 300 g/mol) has higher content of impurities (peak about 4000 nm, Fig. 55) which scattered, because of their size, more light than molecules of HA. This result agrees with the information from measuring UV VIS spectra.

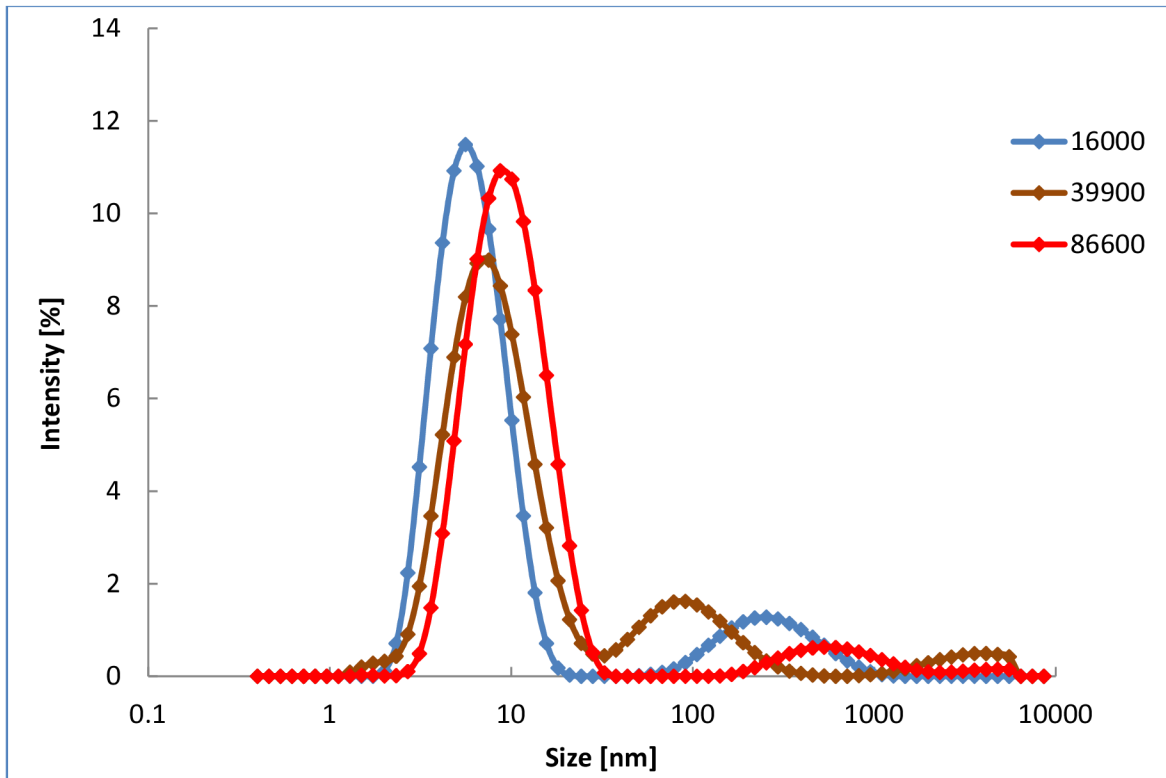


Fig.54 1.0 % filtered solutions of HA (Mw 16 000 – 86 600 g/mol) in PBS (pH 7.00).

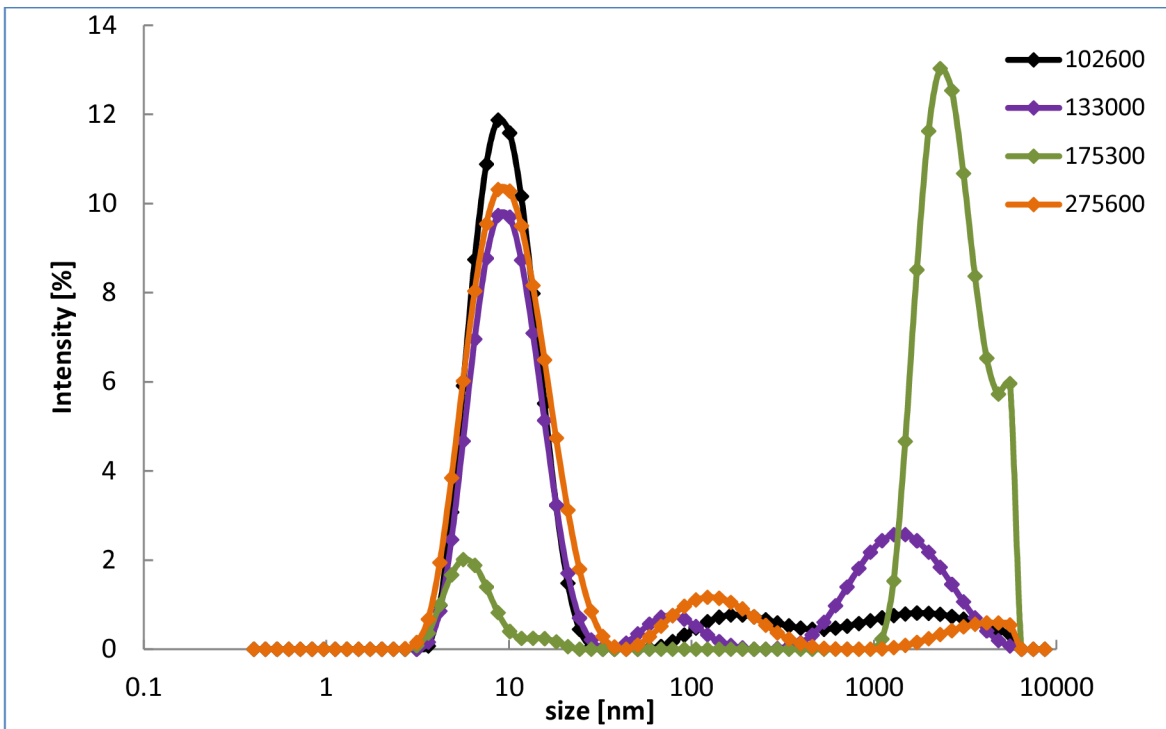


Fig.55 1.0 % filtered solutions of HA (Mw 102 600 – 275 600 g/mol) in PBS (pH 7.00).

4.6 The time stability of hyaluronan

As was mentioned in the beginning of Experimental part, the dissolution of any polysaccharide and especially of hyaluronic acid depends on many factors, such as temperature, speed of rotation, concentration of final solution, Mw of the polysaccharide, the way of adding the powder sample, the size of solution surface and a few others.

The aim of present part of the work is to characterize the dissolution and storage stability of hyaluronan, using some of the physical – chemistry methods. To be specific, the dynamic viscosity, particle size, surface tension and the conductivity of the samples were measured during a few days of mechanical stirring. Also the effect of filtration and ultrasound on the HA aggregates was studied.

4.6.1 Hyaluronan in water

Using Zetasizer Nano ZS, the size of the particles present in the solution may be studied. In case of hyaluronan in demineralised water with addition 0.05% NaN₃ (Figs. 56 and 57) some small, middle and very big particles have been observed. The particles about 400 nm may be classified as hyaluronan aggregates, particles about 60 nm are chains of hyaluronan and the small particles about 4 nm may be probably assigned to molecules of sodium azide. The idea was that during the time of mixing the amount of middle particles will increase, whereas the very big particles (aggregates of HA) will dissolve and the peaks will decrease. Nothing like this theory can be seen on Figs. 56-57.

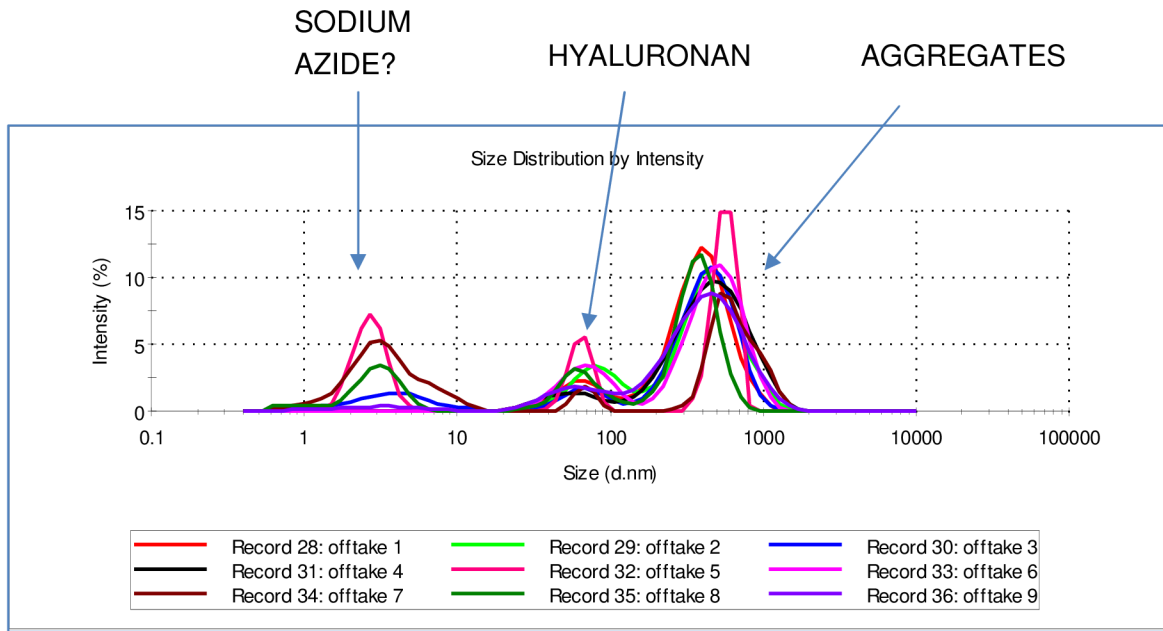


Fig.56 Filtered solutions of HA 250205-D1 in demineralised water with addition of 0.05% NaN_3 . The numbers in the graph legend are numbers of the sampling (red 1st, green 2nd, blue, 3rd sampling ...).

Comparing these two plots (Figs. 56 and 57), means filtrated and non-filtrated solutions, the difference between the peaks of aggregates may be observed. The particles bigger than 1000 nm were filtered out using the filter with size of pores 0.22 μm .

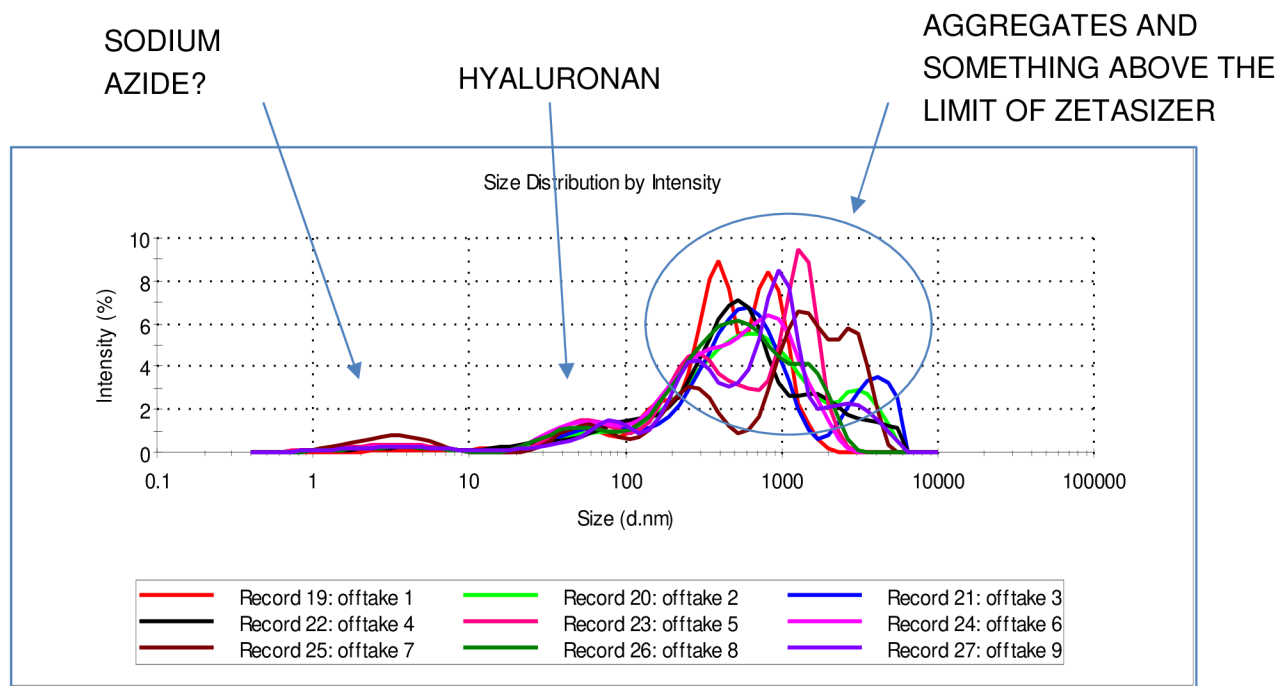


Fig.57 Non-filtered solutions of HA 250205-D1 in demineralised water with addition of 0.05% NaN_3

The original record of flow curves is on the Fig. 58. The zero shear viscosities of different samplings are in the range 0.3 – 0.5 Pa.s, whereas the infinitive rate viscosity is nearly the same for all samples.

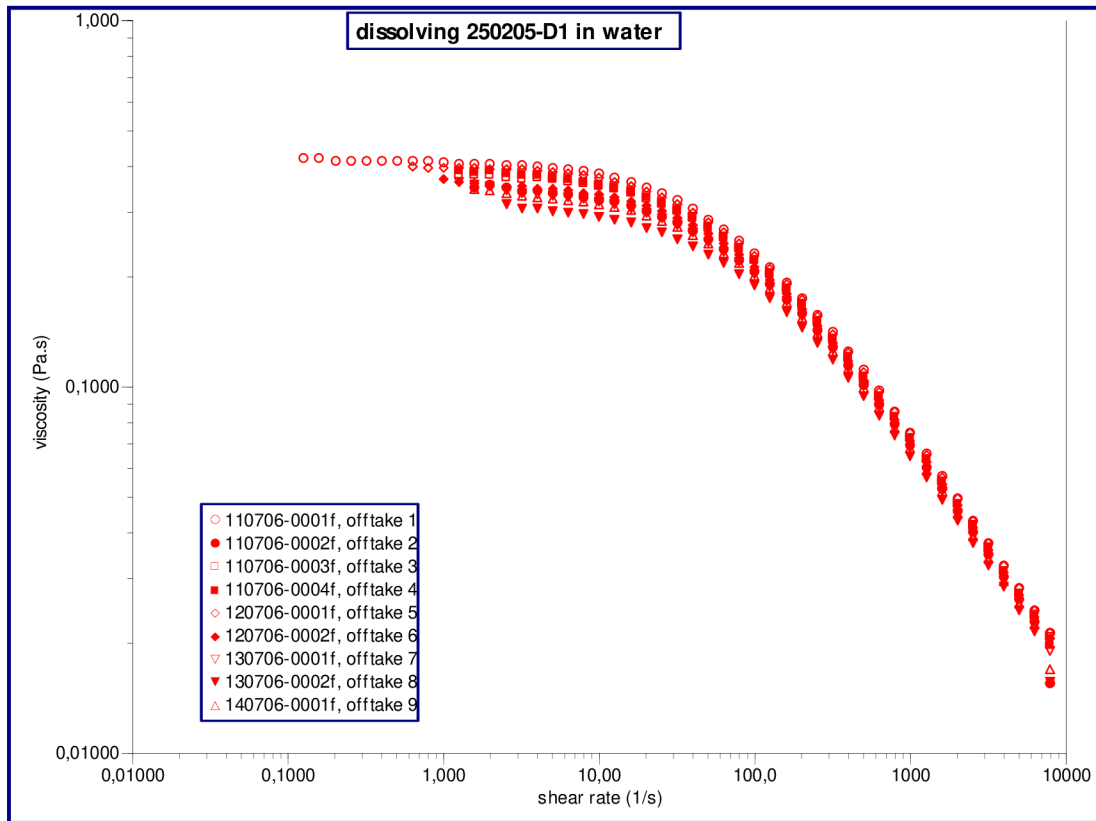


Fig.58 Flow curves of 1% HA 250205-D1 in demineralised water with addition of 0.05% NaN_3 , different sampling.

The results of conductivity and surface tension measurements of 1% HA 250205-D1 in water are shown in Fig. 59. Changes of surface tension during three days testing time period are negligible, the values vary between 29 and 32 mN/m. The conductivity of solution slowly decreases (except one error point) during the time period.

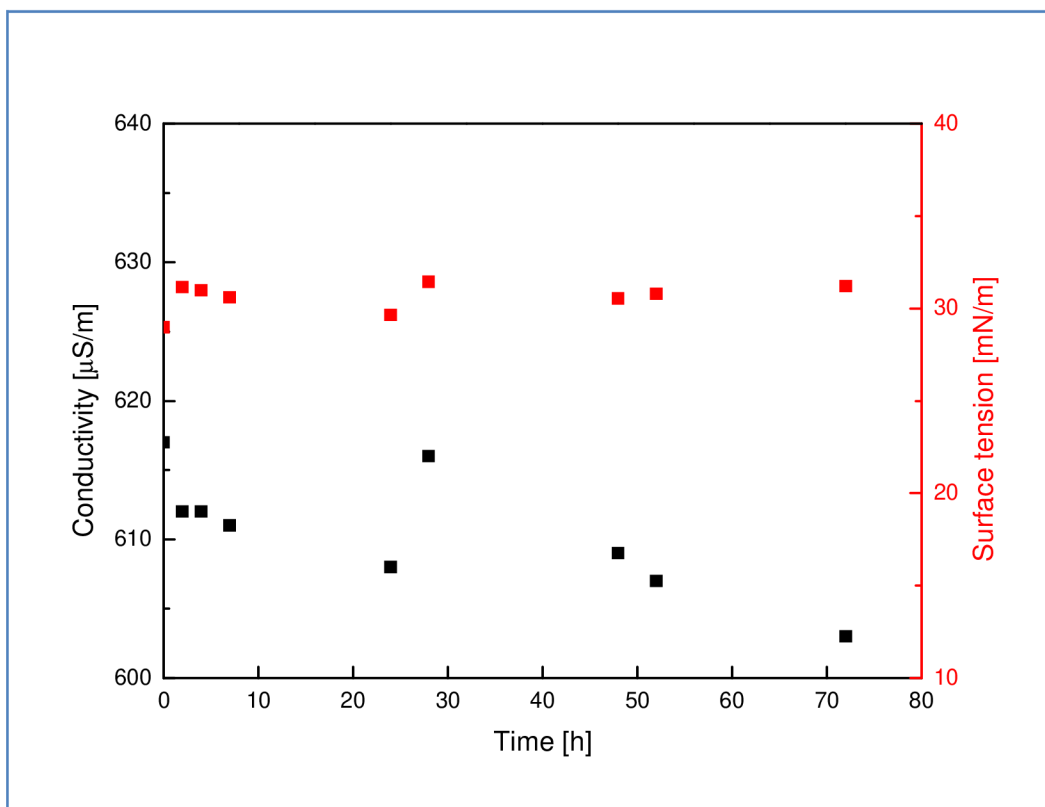


Fig.59 The changes of conductivity and surface tension of 1% HA solution in demineralised water with addition of 0.05% NaN_3 during three days time period.

4.6.2 Hyaluronan in phosphate buffer

Dissolving hyaluronan in 0.1M phosphate buffer and 0.05% NaN_3 , the small particles about 5 nm have disappeared (Figs 60 and 61). After the filtration of solutions through the 0.22 μm filters, only one peak about 60 nm of single hyaluronan chains was observed (Fig. 60). In this case (phosphate buffer solvent), the increase of the peak height may be seen with the increasing time of mixing for filtrated samples. With the elongating time of mixing, the hyaluronan aggregates have dissolved and after the sampling 6 (9 h of mixing, 16 h in fridge, 7 h of mixing – Tab.4) the peak have shown its maximum. So nearly two days are necessary for good dissolution of 1% HA, which corresponds with the result mentioned in Chap.4.1.

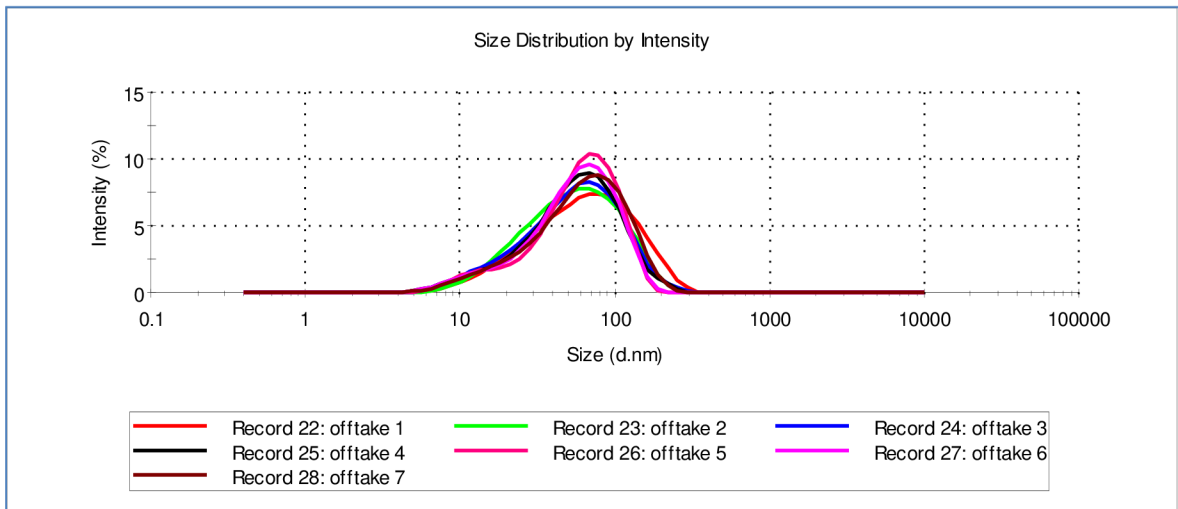


Fig. 60 Filtered solutions of HA 250205-D1 (M_w 750 000 g/mol) in phosphate buffer with addition of 0.05% NaN_3 . The numbers in the graph legend are numbers of the samplings (red 1st, green 2nd, blue, 3rd...offtake).

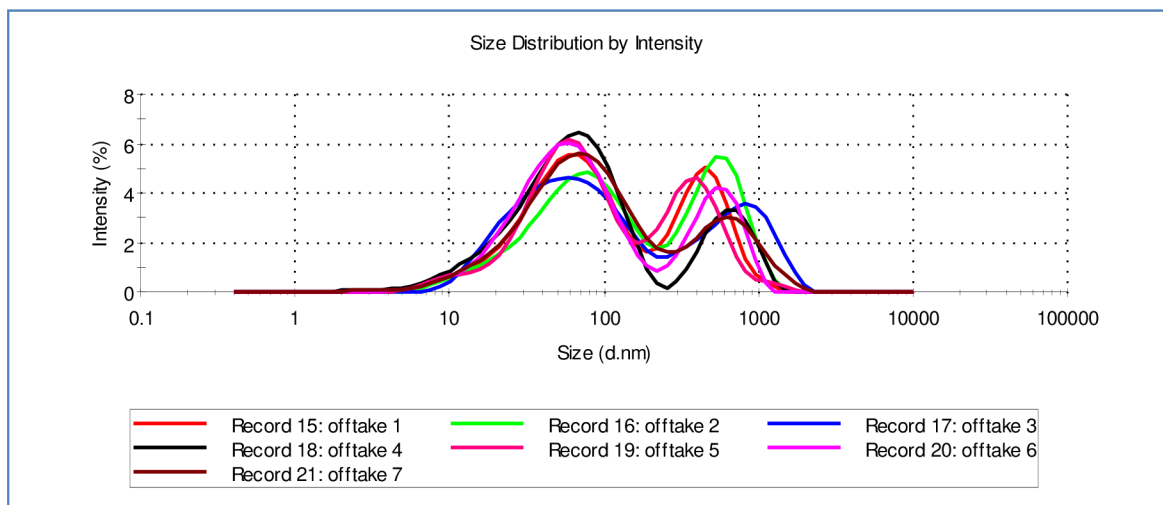


Fig.61 Non-filtered solutions of HA 250205-D1 (M_w 750 000 g/mol) in phosphate buffer with addition of 0.05% NaN_3 . The numbers in the graph legend are numbers of the offtake (red 1st, green 2nd, blue, 3rd... offtake).

4.6.3 Aggregates

The stability of the HA aggregates has been studied using ultrasound waves as a source of force disturbing them. The aqueous and phosphate buffer solutions of HA were prepared as mentioned in chapter “Methods” and were stirred for two hours at room temperature. Then the solutions were put into an ultrasound bath, power about 72 W was used and the samples were taken after 10, 20 and 30 minutes.

The peak of big particles (bigger than 1000 nm) has progressively decreased with the time of ultrasound incidence (Fig. 62), whereas the peaks of smaller particles have increased.

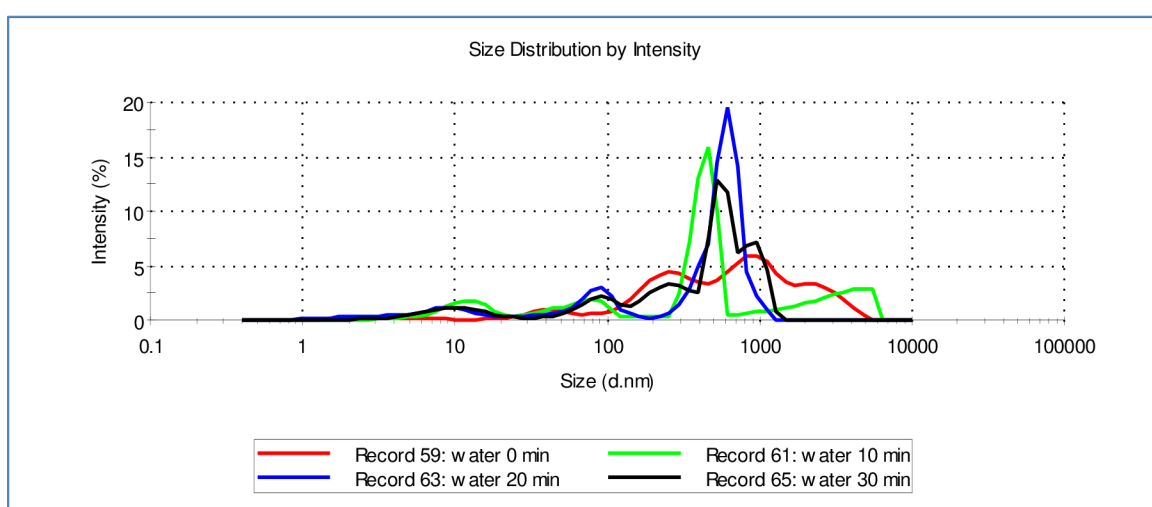


Fig.62 Size of the HA particles in non-filtrated aqueous solutions of HA 250205-D1 (Mw 750 000 g/mol) after 0, 10, 20 and 30 minutes of ultrasound.

There is no evidence of any changes of HA in phosphate solution after the ultrasound (Fig. 63). From the plots, it is clearly seen that the system of HA in water is much more complicated than that in phosphate buffer. In both cases, 30 minutes of ultrasound with such a power is not enough to destroy all aggregates in solution. Maybe it would be better to use higher power or longer time, but it may cause degradation of the single chain of HA.

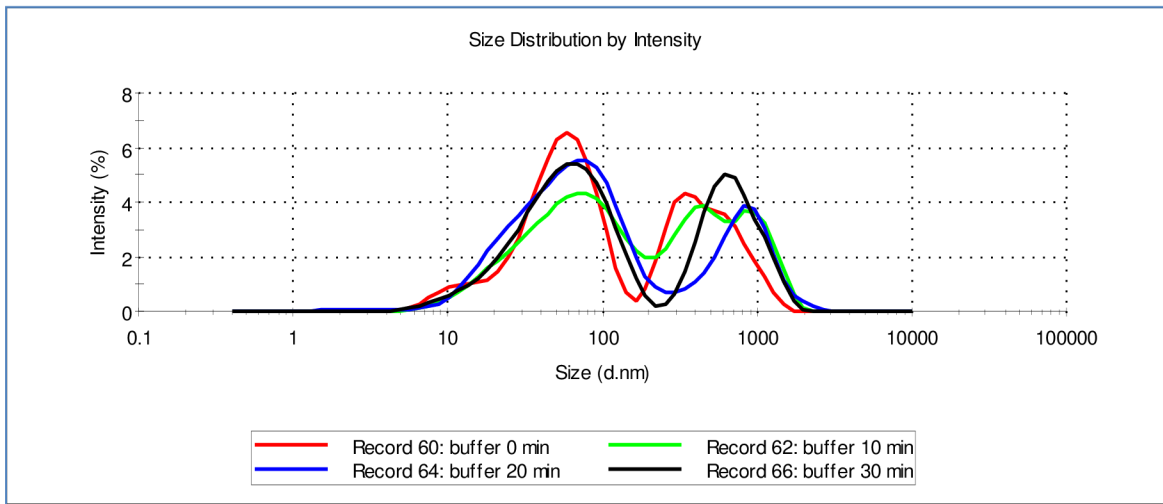


Fig.63 Size of the HA particles in non-filtrated solutions of HA 250205-D1 (Mw 750 000 g/mol) in 0.1M phosphate buffer after 0, 10, 20 and 30 minutes of ultrasound.

The ultrasound has no effect on the viscosity of HA (Fig. 64). The differences in the flow curves are caused only by solvents.

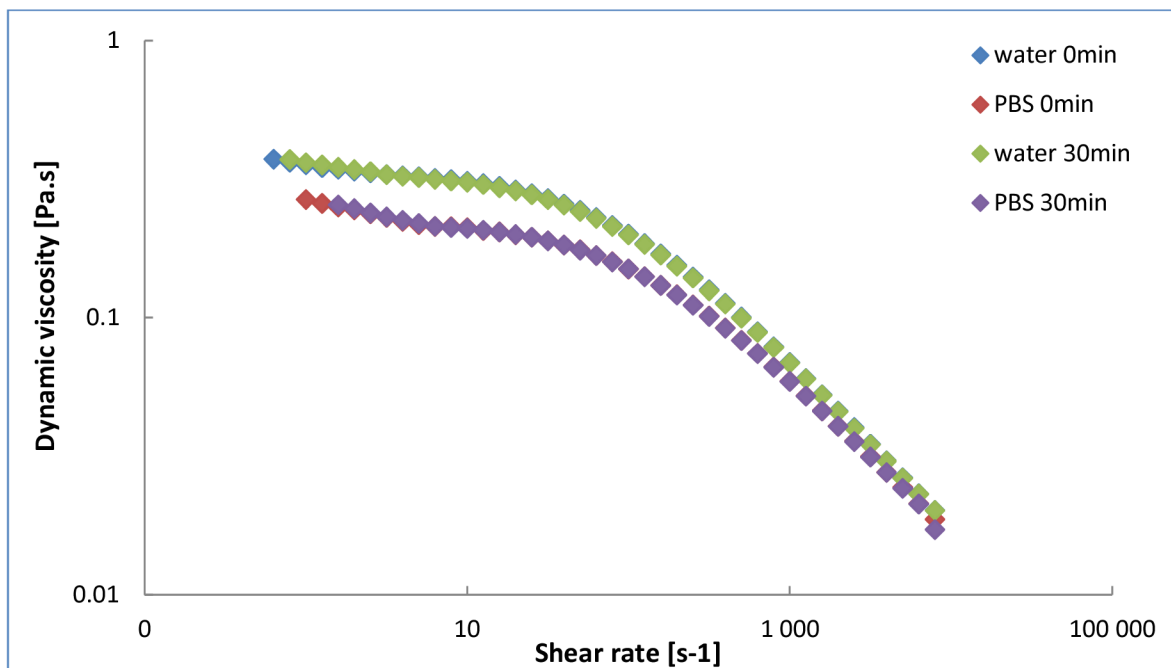


Fig.64 Flow curves of HA 250205-D1 (Mw 750 000 g/mol) in 0.1M phosphate buffer or water after 0 and 30 minutes of ultrasound.

The influence of filtration on the presence of hyaluronan aggregates was mentioned earlier. After the filtration through the 0.22 μm filters, the aggregates in demineralised water did not disappear but they were more uniform (show more Gaussian distribution) than without

any filtration (Figs. 60-61). On the other hand, using phosphate buffer solution, the aggregates were completely filtered out and only peaks of hyaluronan chains were measured (Figs. 62-63).

5 CONCLUSION

Presented work is focused on rheology of hyaluronan solutions. It studies hyaluronan dissolved in different solvents, effect of pH, temperature, time of storage. Nearly 600 samples were measured to have enough of high-quality data, their distribution is shown in Fig. 65.

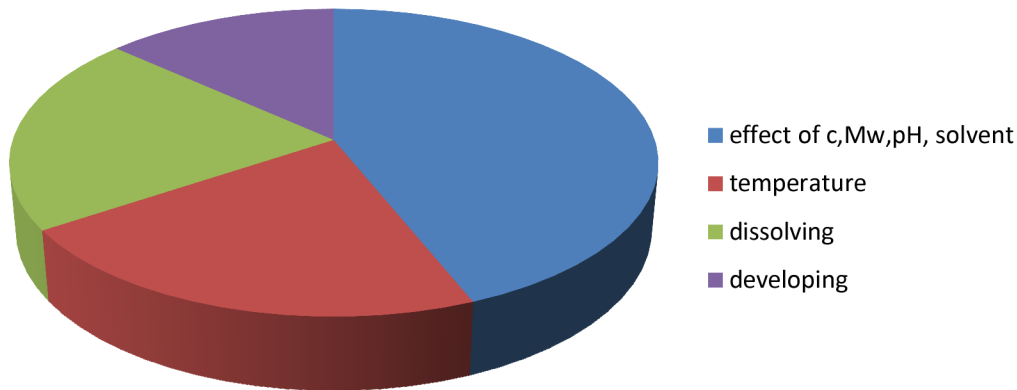


Fig. 65 Distribution of all rheological measurements between particular chapters

The biggest benefit of this work is particularly in very detailed study of hyaluronan behavior using so many different samples. The part dealing with hyaluronan dissolution and solvents temperature dependence show completely new results that can not be find in any literature. The part dedicated to hyaluronan flow curves describes mainly VLMW HA behavior in great detail, the results are in great agreement with data known from the literature. Although the known outcomes are in this work extended of the results of pH and solvent dependences.

Equally important are the detected conclusions in terms of practical point of view. This was first complete study of rheological properties of bacterial hyaluronan produced by the Contipro Holding a.s. that needed to examine their products for simplified RaD department work and to have detailed information for costumers.

To be concrete, at first, the dissolution of HA powder was studied to get the good solution. It was concluded, the best method of dissolution of HA is to mix it at least for two days.

In next step, the usable rheological methods were developed to get the best picture of HA behavior in solution. More than 240 flow curves and 130 temperature ramps were measured using the rotational rheometer to obtain such a complete review on physical properties of VLMW HA solutions. Seven different molecular weight samples were chosen and five concentration of each sample in six different solvents were measured. The values of zero shear viscosity were compared depending on molecular weight, concentration, used solvent

or pH of measured samples. At low molecular weights and concentrations, VLMW HA behaves as Newtonian solution, and the pseudoplasticity, common characteristic of polysaccharides, is observed at higher molecular weights and concentrations. This study found $\eta_{sp} \sim c \cdot Mw$ 1.33 in dilute solution and $\eta_{sp} \sim c \cdot Mw$ 3.26 in concentrated solution, which is in excellent agreement with the results in literature.

It was achieved that in water the HA chains are in a form of random coil, whereas in presence of ions (in PB or PBS), VLMW HA chains formed more rigid conformation. There was no effect of pH (in range 5-8) on conformation of VLMW HA.

Also HMW HA samples were measured. For HMW HA data η_0 correlates very well with HA (concentration · molecular weight) and the HA solution η_0 can be predicted from the relationship: $\eta_0 = 6 \cdot 10^{-6} (c \cdot Mw)^{0.853}$.

The kinematic viscosity was also determined and it was concluded that the difference between zero shear viscosity and kinematic viscosity is negligible for all samples.

The second part is focused on temperature dependence of HA viscosity. The effect of increasing temperature on viscosity of HA solution was measured. According to expectation, the viscosity decreases during the increasing temperature, but there were dissimilarities between VLMW HA in PBS and water at higher temperatures.

Interesting results showed the thermal curves of HMW HA. To stabilize HA solutions NaCl was added, but no effect of stabilization was observed. Whereas the viscosity of hyaluronan solution in presence of NaCl molecules decreased equally, solutions of HA without the presence of NaCl showed significant peaks between 50-70°C.

The purity of used VLMW HA samples was verified by the spectral (1D NMR and UV-VIS) methods. 1H and ^{13}C spectra showed, in addition to characteristic hyaluronan peaks, traces of residual IPA in three cases. Also some impurities in UV-VIS spectra were visible and their peak intensity increases with decreasing molecular weight.

The third part of the work is focused on the dissolution of hyaluronan in water and in phosphate buffer and to characterize the aggregates if there are any. Trials with two hyaluronan batches were performed and the dissolution has been studied using rheology, particle size measurements, measuring of conductivity and finally surface tension. It was achieved that nearly two days of mixing and filtration through 0.22 μm filters are necessary for good dissolution of 1% HA with Mw about 10^6 g/mol.

6 LIST OF ABBREVIATIONS AND SYMBOLS

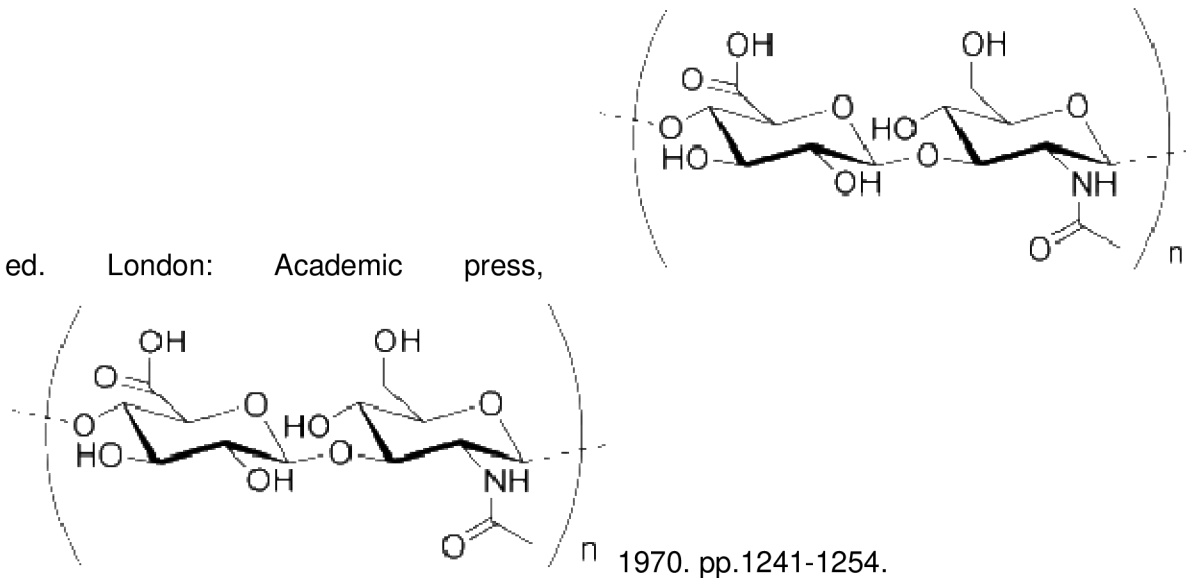
a	radius of the plate [cm]
a_1	radius of inner cylinder [cm]
a_2	radius of outer cylinder [cm]
c	concentration [kg/m^3]
C^*	overlap (critical) concentration [kg/m^3]
CP	cone and plate geometry
DCC	double concentric cylinder geometry
EM	electron microscopy
Eur. Ph.	European Pharmacopoeia
F	Farady constant
FRAP	fluorescence recovery after photobleaching
G'	dynamic modulus [Pa]
G''	dynamic modulus [Pa]
H	cylinder height [cm]
HA	hyaluronan
LS	light scattering
K	consistency coefficient
NMR	Nuclear magnetic resonance
PB	physiological buffer
PBS	phosphate buffer solution
R	gas constant
R_H	hydrodynamic radius [nm]
SLS	static light scattering

T	torque on the inner cylinder [Nm]
T_C	critical temperature [K]
TMAFM	taping mode atomic force microscopy
u_B	electric mobility of species B
VLMW	very low molecular weight
z_B	charge number of the ionic species B
Γ	surface concentration [mol·m ⁻²]
γ	surface tension [N·m]
$\dot{\gamma}$	shear rate [s ⁻¹]
η	dynamic viscosity [Pa.s]
$[\eta]$	intrinsic viscosity
η_{rel}	relative viscosity
η_{red}	reduced viscosity [ml/g]
η_s	solvent viscosity [Pa.s]
η_{sp}	specific viscosity
η'	viscous component of the complex viscosity [Pa.s]
η''	elastic component of the complex viscosity [Pa.s]
λ	ionic conductivity [S·m ⁻¹]
ν	kinematic viscosity [cm ² /s]
ρ	density [kg/m ³]
σ	shear stress [Pa]
ω	rotational rate of outer cylinder [rad/s]
ϕ	the angle between the cone and plate [rad]

7 LITERATURE

¹ Balazs, E. A., Gibbs, D. A. The rheological properties and the biological function of hyaluronic acid. *Chemistry and Molecular Biology of the Intercellular Matrix*. Balazs E. A,

ed. London: Academic press,



² Saari, H., Konttinen, Y. T., Friman, C., et al. Differential effects of reactive oxygen species on native synovial fluid and purified human umbilical cord hyaluronate. *Inflammation*, 1993, vol. 17, pp. 403-415.

³ Meyer, K., Palmer, J. W. The Polysaccharide of the Vitreous Humor. *J. Biol. Chem.*, 1934, vol. 107, pp. 629-634.

⁴ Ogston, A. G., Stanier, J. E. Further observations on the preparation and composition of the hyaluronic acid complex from ox synovial fluid. *Biochem. J.*, 1952, vol. 52, pp. 149-156.

⁵ Laurent, T. C. Studies on hyaluronic acid in the vitreous body. *J. Biol. Chem.*, 1955, vol. 216, pp. 263-271.

⁶ Swann, D. A. Studies on hyaluronic acid: II. The protein component of rooster comb hyaluronic acid. *Biochem. Biophys. Acta*, 1968, vol. 160, pp. 96-105.

⁷ Simoni, R. D., Hill, R. L., Vaughan, M. et al. The discovery of Hyaluronan by Karl Meyer. *Jour. Biol. Chem.*, 2002, 277. Available at:

http://www.jbc.org/content/277/39/e27.full?maxtoshow=&HITS=10&hits=10&RESULTFOR=MAT=&searchid=1130442887043_7599&stored_search=&FIRSTINDEX=60&tocsectionid=Classics&sortspec=PUBDATE_SORTDATE+desc. [cit. 29.03.2010].

- ⁸ Prehm, P. Synthesis of hyaluronic acid in differentiated teratocarcinoma cells – mechanism of chain growth. *Biochem. J.*, 1983, vol. 220, pp. 597-600.
- ⁹ De Angelis, P. L., Papaconstantinou, J., Weigel, P. H. Molecular cloning, identification and sequence of the hyaluronic acid synthase gene from Group A *Streptococcus pyogenes*. *J. Biol. Chem.*, 1993, vol. 268, pp.19181-19184.
- ¹⁰ Ogston, A. G., Stanier, J. E. Further observations on the preparation and composition of the hyaluronic acid complex from ox synovial fluid. *Biochem. J.*, 1952, vol. 52, pp. 149-156.
- ¹¹ Laurent, T. C. Studies on hyaluronic acid in the vitreous body. *J. Biol. Chem.*, 1955, vol. 216, pp. 263-271.
- ¹² Balazs, E. A., Laurent, T. C. Viscosity function of hyaluronic acid as a polyelectrolyte. *J. Polym. Sci.*, 1951, vol. 6, pp. 665-667.
- ¹³ Balazs, E. A. Physical chemistry of hyaluronic acid. *Fed. Proc.*, 1958, vol. 17, pp. 1086-1093.
- ¹⁴ Laurent, T. C., Ryan, M., Pietruszkiewicz, A. Fractionation of hyaluronic acid. The polydispersity of hyaluronic acid from the vitreous body. *Biochem. Biophys. Acta*, 1960, vol. 42, pp. 476-485.
- ¹⁵ Ogston, A. G. Some thermodynamic relationships in ternary systems with special reference to the properties of systems containing hyaluronic acid and protein. *Arch. Biochem. Biophys.*, 1962, vol. 1, pp. 39-51.
- ¹⁶ Balazs, EA. Sediment volume and viscoelastic behaviour of hyaluronic acid solutions. *Fed Proc* 1966; 25:1817-1822.
- ¹⁷ Cleland, R. L., Wang, J. L. Ionic polysaccharides: III. Dilute solution properties of hyaluronic acid fractions. *Biopolymers*, 1970, vol. 9, pp. 799-810.
- ¹⁸ Sheenan, J., Almond, A. Hyaluronan: static, hydrodynamic and molecular dynamic view. Last update 1.11.2011. Available at:
<http://www.glycoforum.gr.jp/science/hyaluronan/HA21/HA21E.html>. [cit. 12.4.2010].
- ¹⁹ Guss, J. M., Hukins, D. W. L., Smith, J. P. C., et al. Hyaluronic acid: molecular conformations and interactions in two sodium salts. *J. Mol. Biol.*, 1975, vol. 95, pp. 359-384.

- ²⁰ Mitra, A. K., Arnott, S., Sheehan, J. K. Hyaluronic acid: molecular conformations and interaction in the tetragonal form of the potassium salt containing extended chains. *J. Mol. Biol.*, 1983, vol. 169, pp. 813-827.
- ²¹ Winter, W. T., Arnott, S. Hyaluronic acid: the role of divalent cations in conformation and packing. *J. Mol. Biol.*, 1977, vol. 117, pp. 761-784.
- ²² Sheehan, J. K., Gardner, K. H., Atkins, E. D. T. Hyaluronic acid, a double helical structure in the presence of potassium at low pH and found also with the cations ammonium, rubidium and caesium. *J. Mol. Biol.*, 1977, vol. 117, pp. 113-135.
- ²³ Scott, J. E., Tigwell, M. J. Periodate oxidation and the shapes of glycosaminoglycuronans in solution. *Biochem. J.*, 1978, vol. 173, pp. 103-114.
- ²⁴ Morris, E. R., Rees, D. A., Welsh, E. J. Conformation and dynamic interactions in HA solutions. *J. Mol. Biol.*, 1980, vol. 138, pp. 383-400.
- ²⁵ Wil, K. O., Comper, W. D. Hyaluronate diffusion in semi-dilute solutions. *Biopolymers*, 1982, vol. 21, pp. 583-599.
- ²⁶ Sheehan, J. K., Atkins, E. D. T. X-ray fiber diffraction study of the conformational changes in hyaluronic acid induced in the presence of sodium, potassium and calcium cations. *Int. J. Biol. Macromol.*, 1983, vol. 5, pp. 215-221.
- ²⁷ Almond, A., Sheehan, J. K., Brass, A. Molecular dynamics simulations of the disaccharides of hyaluronan in solution. *Glycobiology*, 1997, vol. 7, pp. 597-604.
- ²⁸ Hardingham, T. E., Gribbon, P., Heng, B. C. New approaches to the investigation of hyaluronan networks. *Biochem. Soc. Trans.*, 1999, vol. 27, pp. 124-127.
- ²⁹ Gribbon, P., Heng, B. C., Hardingham, T. E. The molecular basis of the solution properties of hyaluronan investigated by confocal fluorescence recovery after photobleaching. *Biophys. J.*, 1999, vol. 77, pp. 2210-2216.
- ³⁰ Gribbon, P., Heng, B. C., Hardingham, T. E. The analysis of intermolecular interactions in concentrated hyaluronan solutions suggest no evidence for chain-chain association. *Biochem. J.*, 2000, vol. 350, pp. 329-335.
- ³¹ Hascall, V. C., Laurent, T.C. Hyaluronan: Structure and physical properties. [HTML dokument]. Last update: 15.12.1997. Available at :
<http://www.glycoforum.gr.jp/science/hyaluronan/HA01/HA01E.html>. [cit. 12.12.2011]

- ³² Engel, J. The biology of hyaluronan. *Ciba Found. Symp.*, 1989, vol. 143, pp. 18-19.
- ³³ Scott, J. E., Cummings, C., Brass, A., Chen, Y. Secondary and tertiary structures of HA in aqueous solution, investigation by rotary shadowing electron microscopy and computer simulation. *Biochem. J.*, 1991, vol. 274, pp. 699-705.
- ³⁴ Scott, J. E., Heatley, F. Hyaluronan forms specific stable tertiary structures in aqueous solution: a C-13 NMR study. *Proc. Natl. Acad. Sci.*, 1999, vol. 96, pp. 4850-4855.
- ³⁵ Scott, J. E., Heatley, F. Biological properties of hyaluronan in aqueous solution are controlled and sequestered by reversible tertiary structures defined by NMR spectroscopy. *Biomacromolecules*, 2002, vol. 3, pp. 547-553.
- ³⁶ Hardingham, T. E., Gribbon, P. Confocal-FRAP analysis of ECM molecular interactions. *Methods in Molecular Biology, Extracellular Matrix Protocols*. Strueli, C., Grant, M., eds., Totowa, NJ: Humana Press, 2000, vol. 139, pp. 83-93.
- ³⁷ Gribbon, P., Hardingham, T. E. Macromolecular diffusion of biological polymers measured by confocal fluorescence recovery after photobleaching. *Biophys. J.*, 1998, vol. 75, pp. 1032-1039.
- ³⁸ Sheehan, J. K., Arundel, C., Phelps, C. F. Effect of the cations sodium potassium and calcium on the interactions of hyaluronate chains: a light scattering and viscometric study. *Int. J. Biol. Macromol.*, 1983, vol. 5, pp. 222-228.
- ³⁹ Cowman, M. K., Hittner, D. M., Feder-Davies, J. ¹³C NMR studies of hyaluronan: conformational sensitivity to various environments. *Macromolecules*, 1996, vol. 29, pp. 2894-2902.
- ⁴⁰ Geciavo, R., Flaibani, A., Delben, F., Liut, G., Urbani, R., Cesaro, A. Physico-chemical properties of hyaluronan and its hydrophobic derivatives: a calorimetric study. *Macromol. Chem. Phys.*, 1995, vol. 196, pp. 2891-2903.
- ⁴¹ Cowman, M. K., Cozart, D., Nakanishi, K., Balazs, E. A. ¹H NMR of glycosaminoglycans and hyaluronic acid oligosaccharides in aqueous solutions: the amide proton environment. *Arch. Biochem. Biophys.*, 1984, vol. 230, pp. 203-212.
- ⁴² Fujii, K., Kawate, M., Kobayashi, Y., Okamoto, A. Effects of the addition of hyaluronate segments with different chain lengths on the viscoelasticity of hyaluronic acid solutions. *Biopolymers*, 1996, vol. 38, pp. 583-591.

- ⁴³ Ambrosio, L., Borzacchiello, A., Netti, P. A., et al. Rheological study on hyaluronic acid and its derivative solutions. *J. Macromol. Sci. Pure*, 1999, vol. A36, pp. 991–1000.
- ⁴⁴ Smedt, S.C., Dekeyser, P., Ribitsch, V., et al. Viscoelastic and transient network properties of hyaluronic acid as a function of the concentration. *Biorheology*, 1993, vol. 30, pp. 31–41.
- ⁴⁵ Lapcik, L., Lapcik, L., De Smedt, S., et al. Hyaluronan: Preparation, structure, properties, and applications. *Chem. Rev.*, 1998, vol. 98, pp. 2663–2684.
- ⁴⁶ Miyazaki, T., Yomota, C., Okada, S. Change in molecular weight of hyaluronic acid during measurement with a coneplate rotational viscometer. *J. Appl. Polym. Sci.*, 1998, vol. 67, pp. 2199–2206.
- ⁴⁷ Krause, W. E., Bellomo, E. G., Colby, R. H. Rheology of sodium hyaluronate under physiological conditions. *Biomacromolecules*, 2001, vol. 2, pp. 65–69.
- ⁴⁸ Murakami, T., Higaki, H., Sawae, Y., et al. Adaptive multimode lubrication in natural synovial joints and artificial joints. *Proc. Inst. Mech. Eng.*, 1998, vol. 212, pp. 23–35.
- ⁴⁹ Rainer, Katzer, H., Ribitsch, V. Correlation between molecular parameters of hyaluronic acid and viscoelasticity of synovia. *Acta Med. Austriaca*, 1996, vol. 23, pp. 133–136.
- ⁵⁰ Kobayashi, Y., Okamoto A., Nishinari, K. Viscoelasticity of hyaluronic acid with different molecular weights. *Biorheology*. 1994, vol. 31, pp. 235–244.
- ⁵¹ Schurz, J. Rheology of synovial fluids and substitute polymers. *J. Macromol. Sci. Pure*, 1996, vol. A33, pp. 1249–1262.
- ⁵² Chaplin, M. Water structure and science. Last update 10.4.2012 Available at: www.lsbu.ac.uk/water/hydrat.html [cit.10.05.2012]
- ⁵³ Kirschner, K. N., Woods, R. J. Solvent interactions determine carbohydrate conformation, *Proc. Natl. Acad. Sci. USA*, 2001, 98, 10541-10545.
- ⁵⁴ Pashley, R. M., Rzechowicz, M., Pashley, L. R. et al. De-gassed water is a better cleaning agent, *J. Phys. Chem. B*, 2004, 109, 1231-1238.
- ⁵⁵ Ribitsch, G., Schurz, J., Ribitsch, V. Investigation of the solution structure of hyaluronic acid by light scattering, SAXS, and viscosity measurements, *Colloid and Polymer Sci.*1980, 258(12), 1322-1334.
- ⁵⁶ Ghosh, S., Kopal, I., Zanette, D. et al. Conformational contraction and hydrolysis of hyaluronate in sodium hydroxide solutions. *Macromolecules*, 1993, 26(17), 4685-4693.

- ⁵⁷ Milas, M., Rinaudo, M., Roure, I. et al. Comparative rheological behaviour of hyaluronan from bacterial and animal sources with cross-linked hyaluronan (Hylan) in aqueous solution. *Biopolymers*, 2001, 59, 191-204.
- ⁵⁸ Fouissac, E., Milas, M., Rinaudo M. Shear-rate, concentration, molecular weight, and temperature viscosity dependences of hyaluronate, a wormlike polyelectrolyte. *Macromolecules*, 1993, 26(25), 6945-6951.
- ⁵⁹ Reed, C. E., Li, X., Reed, W. F. The effects of pH on hyaluronate as observed by light scattering. *Biopolymers*, 1989, 28, 1981-2000.
- ⁶⁰ Schurz, V. J., Hemmetsberger, H., Sashofer, F. et al. Studies on hyaluronic acid solutions. *Z. Phys. Chem.*, 1967, 348, 711-719.
- ⁶¹ Sheenan, J. K., Arundel, C., Phelps, C. F. Effect of the cations sodium, potassium and calcium on the interaction of hyaluronate chains: a light scattering and viscometric study. *Int. J. Biol. Macromol.*, 1983, 5 (4), 222-228.
- ⁶² Månsson, P., Jacobsson, Ö., Granath, K. A. Effect of the cations sodium and potassium on the molecular weight of hyaluronate. *Int. J. Biol. Macromol.*, 1985, 7 (1), 30-32.
- ⁶³ Welsh, E. J., Rees, D. A., Morris, E. R. et al. Competitive inhibition evidence for specific intermolecular interactions in hyaluronate solutions. *J.Mol.Biol.*, 1980, 138(2), 375-382.
- ⁶⁴ Cowman, M. K., Li, M., Balazs, E. A. Tapping mode atomic force microscopy of hyaluronan: extended and intramolecularly interacting chains. *Biophysical Journal*, 1998, 75(4), 2030-2037.
- ⁶⁵ Gribbon, P., Heng, B., Hardingham, T. E. The molecular basis of the solution properties of hyaluronan investigated by confocal fluorescence recovery after photobleaching. *Biophys. J.*, 1999, 77, 2210-2216.
- ⁶⁶ Ghosh, S., Li, X., Reed, C. E. et al. Apparent persistence lengths and diffusion behavior of high molecular weight hyaluronate. *Biopolymers*, 1990, 30, 1101-1112.
- ⁶⁷ Barnes, H. A. A handbook of elementary rheology. Institute of Non-Newtonian Fluid Mechanics, University of Wales, 2000, pp. 204, ISBN 978-0953803200.
- ⁶⁸ AR-G2 Rheometer – operator's manual. TA Instruments, revision A, May 2005.
- ⁶⁹ Gibbs, D. A., Merrill, E. W., Smith, K. A., Balazs, E. A. Rheology of hyaluronic acid. *Biopolymers*, 1968, vol. 6, pp. 777-791.
- ⁷⁰ Morris, E. R., Rees, D. A., Welsh, E. J. Conformation and Dynamic Interactions in Hyaluronate Solutions. *J. Mol. Biol.*, 1980, vol. 138, pp. 383-400.
- ⁷¹ Milas, M., Rinaudo, M., Roure, I. et al. Rheological behaviour of hyaluronan, healon and hylan in aqueous solutions. *Hyaluronan – Chemical, biochemical and biological aspects*. 2000, vol. 1, pp.181-193.

- ⁷² Mo, Y., Takaya, T., Nishinari, K., Kubota, K., Okamoto, A. Effects of sodium chloride, guanidine hydrochloride, and sucrose on the viscoelastic properties of sodium hyaluronate solutions. *Biopolymers*, 1999, vol. 50, pp. 23–34.
- ⁷³ Mo, Y., Nishinari, K. Rheology of hyaluronan solutions under extensional flow. *Biorheology*, 2001, vol. 38, pp. 379-387
- ⁷⁴ Knill, C. J., Kennedy, J. F., Latif, Y. et al. Effect of metal ions on the rheological flow profiles of hyaluronate solutions. *Hyaluronan – Chemical, biochemical and biological aspects*, 2000, vol. 1, pp. 175-180.
- ⁷⁵ Maleki, A., Kjøniksen, A. L., Nyström, B. Anomalous Viscosity Behavior in Aqueous Solutions of Hyaluronic Acid. *Polymer Bulletin*, 2007, vol. 59, pp. 217–226.
- ⁷⁶ Arshinoff, S. A., Hofman, I. Prospective, randomized trial comparing Micro Visc Plus and Healon GV in routine phacoemulsification, *J. Cataract Refract. Surg.*, 1998, vol. 24, pp. 814-820.
- ⁷⁷ Bothner, H. and Wik, O., Rheology of hyaluronate, *Acta Otolaryngol. Suppl.*, 1987, vol. 442, pp. 25-30.
- ⁷⁸ Welsh, E. J., Rees, D. A., Morris, E. R., Madden, J. K., Competitive inhibition evidence for specific intermolecular interactions in hyaluronate solutions, *J. Mol. Biol.*, 1980, vol. 138, pp. 375-382.
- ⁷⁹ Hardings, E., Vårum, K. M., Stoke, B. T. et al. Molecular weight determination of polysaccharides, *Advances in carbohydrate analysis*, 1991, vol. 1, pp. 63-144.
- ⁸⁰ Linder, H., Glatter, O. Determination of absolute intensity and molecular weight of small colloidal particles in the presence of some large aggregates. A combined study using static and dynamic light scattering. *Part. Syst. Charact.*, 2000, vol. 17, pp. 89-95.
- ⁸¹ Takahashi, R., Kubota, K., Kawada, M., et al. Effect of molecular weight distribution on the solution properties of sodium hyaluronate in 0,2M NaCl solution. *Biopolymers*, 1999, vol. 50, pp. 87-98.
- ⁸² Månsson, P., Jacobsson, Ö., Granath, K. A. Effect of the cations sodium and potassium on the molecular weight of hyaluronate. *Int. J. Biol. Macromol.*, 1985, vol. 7, n. 1, pp. 30-32.
- ⁸³ http://www.tf.uni-kiel.de/matwis/amat/elmat_en/kap_2/backbone/r2_4_1.html
[cit.17.07.2006].
- ⁸⁴ <http://www.iupac.org/goldbook/I03175.pdf> [cit.17.07.2006].

⁸⁵ http://en.wikipedia.org/wiki/Surface_tension [cit.17.09.2011].

⁸⁶ Balazs, E. A., Cowman, M. K., Briller, S. O., et al. On the limiting viscosity number of hyaluronate in potassium phosphate buffers between pH 6.5 and 8. *Biopolymers*, 1983, vol. 22, pp. 589–591.

⁸⁷ Cleland, R. L. Effect of temperature on the limiting viscosity number of hyaluronic acid and chondroitin 4-sulfate. *Biopolymers*, 1979, vol. 18, pp. 1821–1828.

⁸⁸ Barrett, T. W., Harrington, R. E. Low velocity gradient flow birefringence and viscosity changes in hyaluronate solutions as a function of pH. *Biopolymers*, 1977, vol. 16, pp. 2167–2188.

8 APPENDIX 1 - STATISTICAL EVALUATION OF EXPERIMENTAL DATA

8.1 Basic principles

Analysis of variance is based on comparing pairs of models. One model is complex and assumes that a statistically significant effect has more characters, the second model is simpler and assumes that an effect has less or no characters. For each measurement model is divided into groups according to the major characters in each group to estimate the mean and then add up the squared deviations of random variables from the mean. The fewer parameters, the less groups and the larger deviations from the mean values. Using a special variant of the F test determines whether the sum of deviations for various models differ from each other so that both models can not be declared as equivalent. In this case, rejected the model with a larger sum of deviations. If the sums of deviations significantly different, it is possible to adopt a simpler model, that can accept the assumption that a character does not matter.

The sum of the squares reflects on what number goes in more complex model (after inclusion of the character or its combination) the sum of the squares of the deviations from the estimated mean values.

Degrees of freedom reflect the number of parameters in addition to the more complex model is used.

F value is a dummy value criterion, which compares the two models.

p value indicates significance level at which it is possible to reject the hypothesis that the both used models are equivalent. Compared with a predetermined number (most commonly with 0.05) and if less, the equivalence of models is rejected.


8.2 Interpretation of analysis of variance table

For the interpretation of the table are the most important values of p. We proceed from the bottom up from the most complex model and try to get to the simpler model. The characters

represented in the simplest usable model is then declared statistically significant. If the p value is greater than 0.05, both models can be considered equivalent to a move from model to an additive interaction model. Because there is always p value less than 0.05, it is impossible to go to the simplest model, a character can not be discarded.

8.3 Flow curves of hyaluronan

In that unit I have focused on statistics of individual measurements of shear stress which are specific to each Mw and were measured at various pH conditions. Therefore I do not give a complete account of analytical models that can be used to approximation with Cross model but only testing of data exactness and rightness in case of linearity described with Newton model (in interval where the Hyaluronan is look like Newtonian fluid)

Statistical data processing was done via using software Minitab v.16  Minitab[®] 16
Statistical Software

Sigma in the plots is the shear stress [Pa] and gama is the shear rate [s^{-1}].

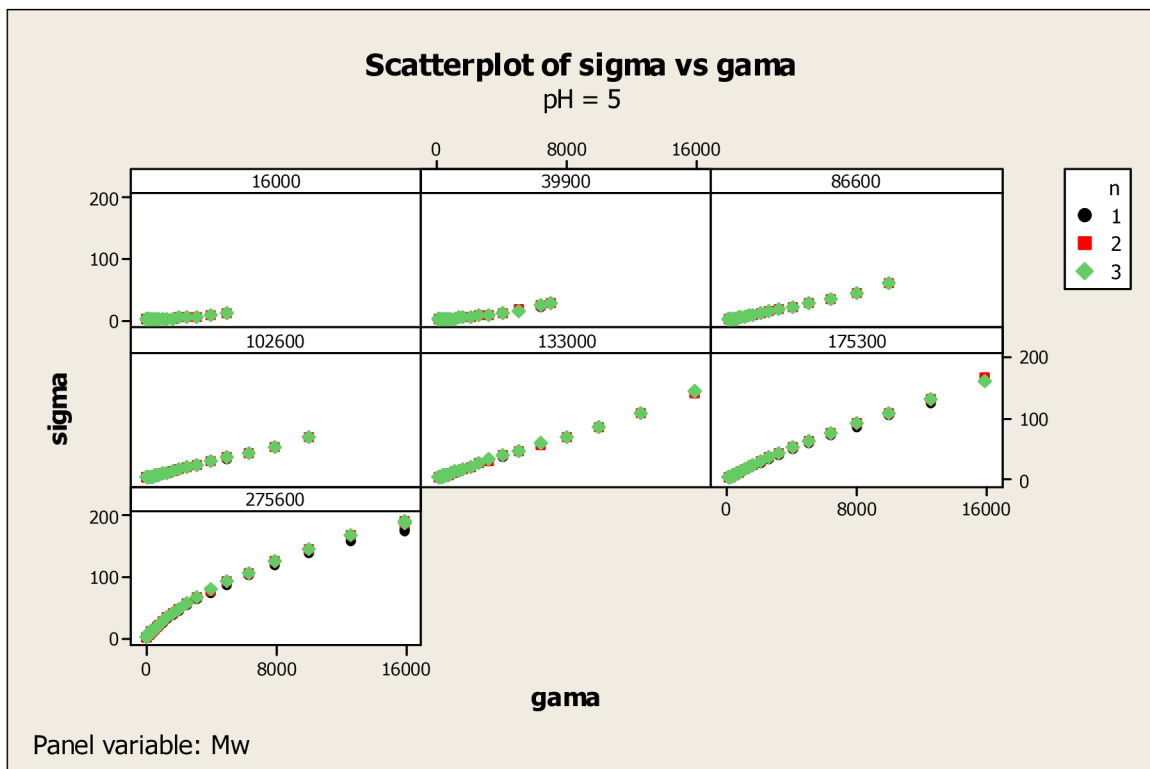


Fig. 1a – plot of shear stress versus shear rate for different Mw at pH = 5, where n is number of measurement (measured raw data)

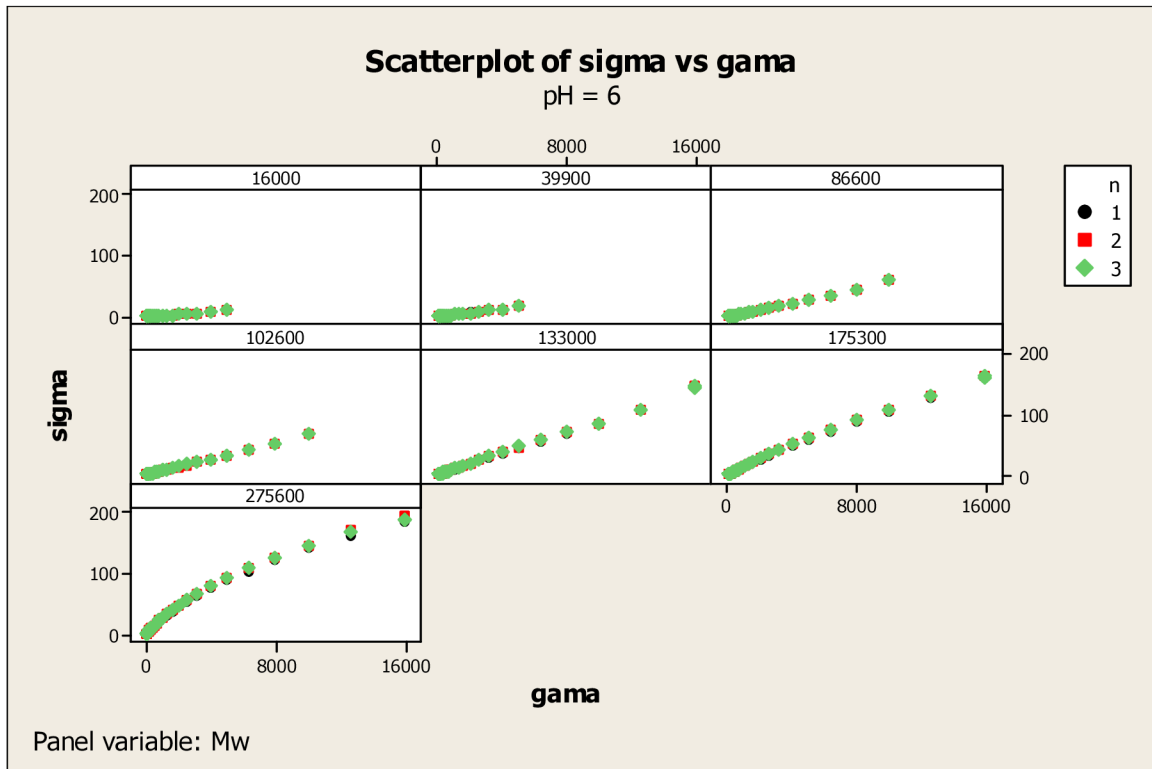


Fig. 1b – plot of shear stress versus shear rate for different Mw at pH = 6, where n is number of measurement (measured raw data)

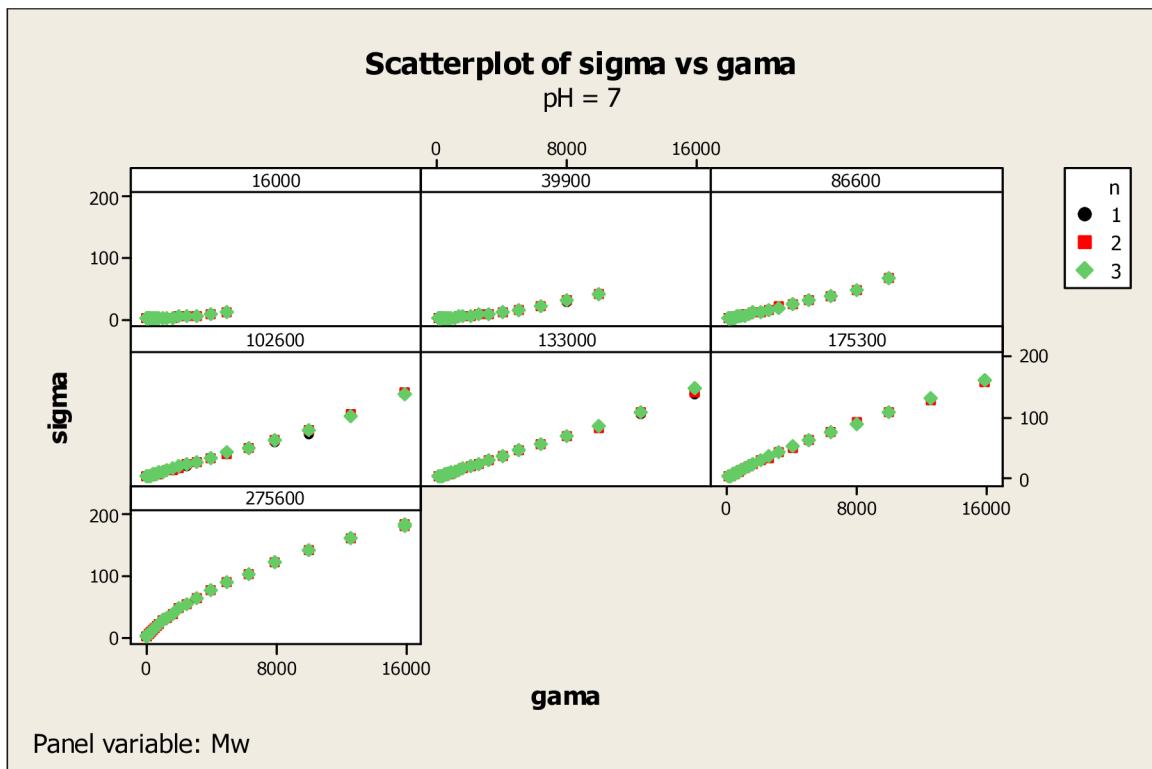


Fig. 1c – plot of shear stress versus shear rate for different Mw at pH = 7, where n is number of measurement (measured raw data)

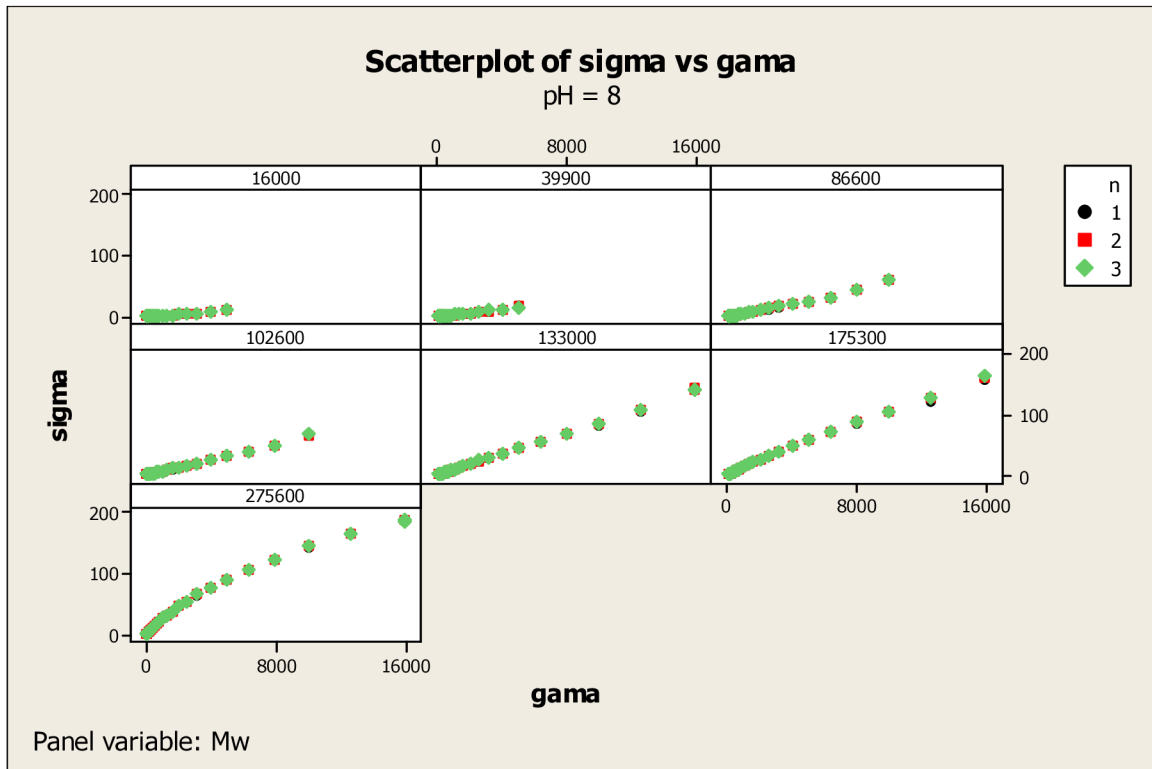


Fig. 1d – plot of shear stress versus shear rate for different Mw at pH = 8, where n is number of measurement (measured raw data)

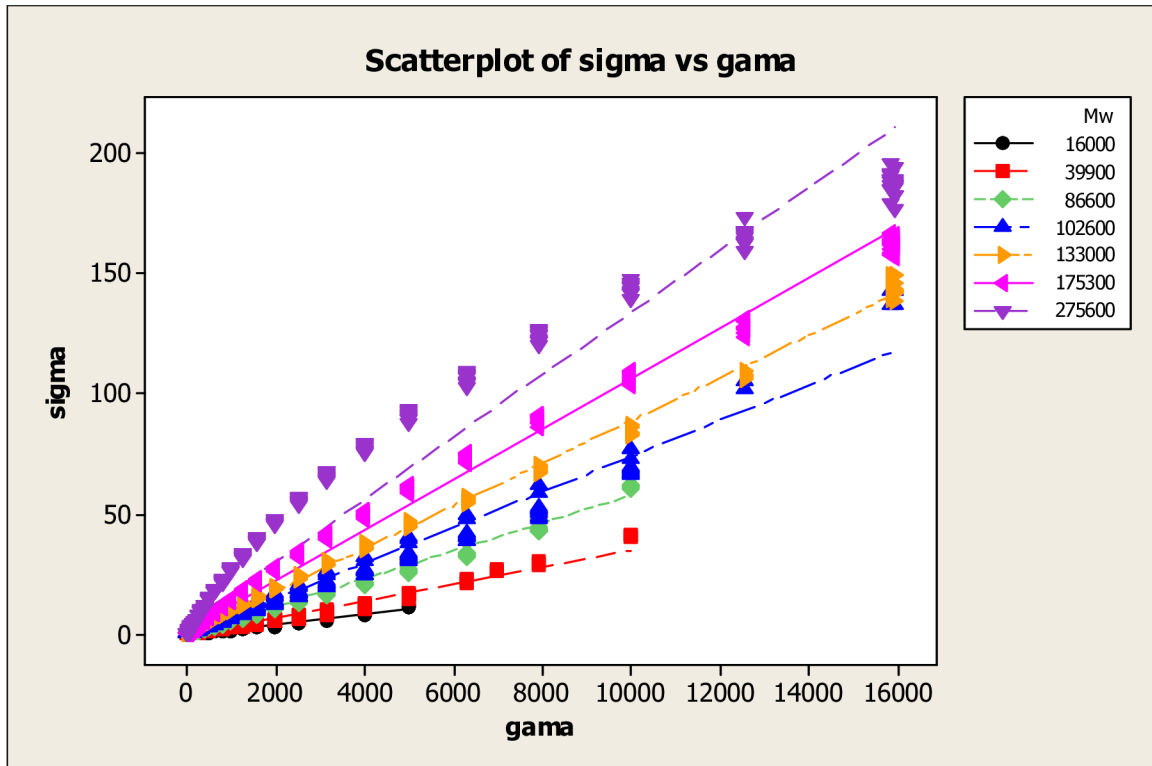


Fig. 2a – plot of shear stress versus shear rate for different Mw (measured raw data – i.e. various pH and various measurements)

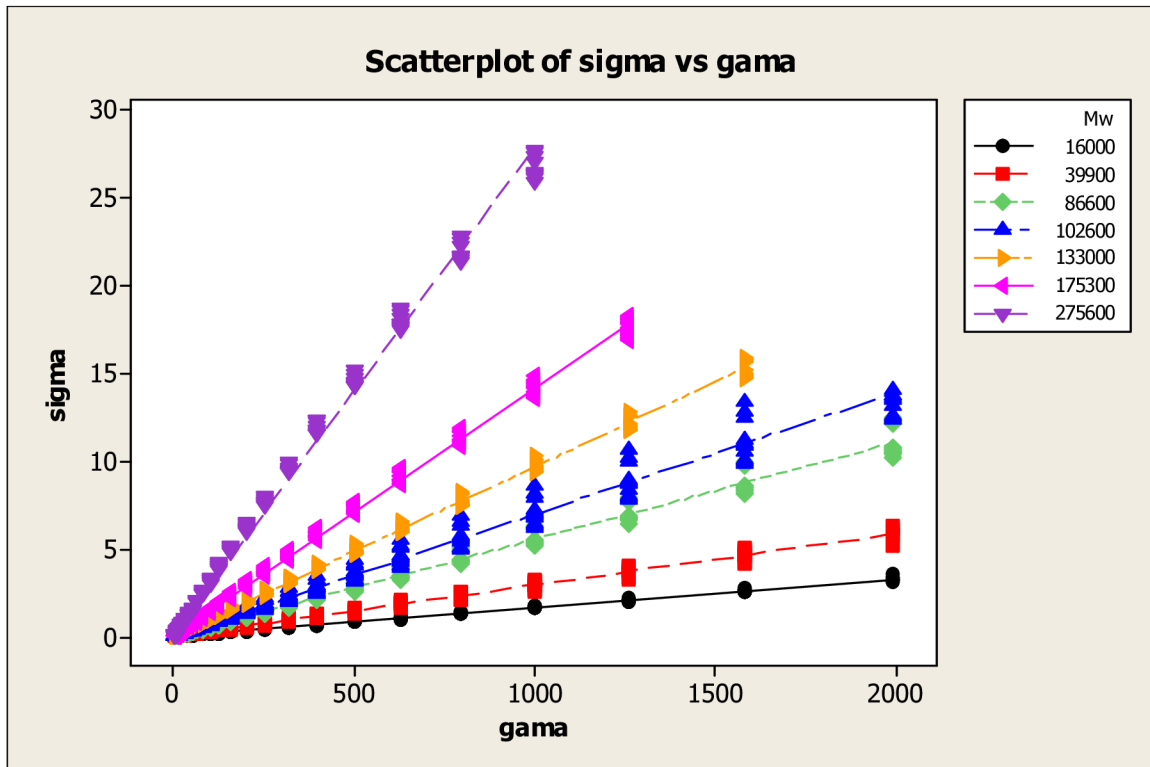


Fig. 2b – plot of shear stress versus shear rate for different Mw (measured raw data – i.e. various pH and various measurements) and following limitations: $\sigma \cdot \gamma$ must be lower than 30.000 and γ must be lower than 2.000 simultaneously.

In that limited area is experimental data strictly linear for all tested molecular weights (Mw = 16.000 – 275.000) and the same concentration. From the point of statistical tests view it can be said that the influence of pH is not statistically significant. Detailed report of statistical data processing via linear regression analysis is showed below in tab. 1 – 7.

Tab. 1

Mw=16000					
	value	StDev	t_Test	Part.r	
intercept	4.88E-02	5.53E-03			
pH	-7.26E-03	8.36E-04	8.686	0.323	
gama	1.63E-03	2.28E-06	717.981	0.999	

t(646)=1.964

Explained variability [%] 99.87

Multiple correlation coefficient 0.9994

Acaic's inf. criterion -4.85E+03

MEP 5.82E-04

Tab. 2

Mw=39900					
	value	StDev	t_Test	Part.r	
intercept	2.62E-02	2.92E-02			
pH	-2.81E-03	4.41E-03	0.637	0.025	
gama	2.88E-03	8.32E-06	345.884	0.997	

t(658)=1.964

Explained variability [%] 99.45

Multiple correlation coefficient 0.9973

Acaic's inf. criterion -2.73E+03

MEP 1.67E-02

Tab. 3

Mw=86600					
	value	StDev	t_Test	Part.r	
intercept	-3.44E-02	4.11E-02			
pH	6.45E-03	6.21E-03	1.038	0.041	
gama	5.53E-03	1.69E-05	326.798	0.997	

t(643)=1.964

Explained variability [%] 99.40

Multiple correlation coefficient 0.9970

Acaic's inf. criterion -2.24E+03

MEP 3.21E-02

Tab. 4

Mw=102600					
	value	StDev	t_Test	Part.r	
intercept	1.55E-01	6.47E-02			
pH	-2.01E-02	9.76E-03	2.058	0.081	
gama	6.93E-03	2.79E-05	248.693	0.995	

t(639)=1.964

Explained variability [%] 98.98

Multiple correlation coefficient 0.9949

Acaic's inf. criterion -1.65E+03

MEP 7.88E-02

Tab. 5

Mw=133000					
	value	StDev	t_Test	Part.r	
intercept	2.07E-01	2.77E-02			
pH	-2.93E-02	4.20E-03	6.985	0.269	
gama	9.64E-03	1.43E-05	676.667	0.999	

t(627)=1.964

Explained variability [%] 99.86

Multiple correlation coefficient 0.9993

Acaic's inf. criterion -2.69E+03

MEP 1.43E-02

Tab. 6

Mw=175300					
	value	StDev	t_Test	Part.r	
intercept	1.66E-01	3.38E-02			
pH	-2.06E-02	5.10E-03	4.027	0.16	
gama	1.41E-02	2.17E-05	653.065	0.999	

t(616)=1.964

Explained variability [%] 99.86

Multiple correlation coefficient 0.9993

Acaic's inf. criterion -2.42E+03

MEP 2.07E-02

Tab. 7

Mw=275600					
		value	StDev	t_Test	Part.r
intercept		-1.64E-01	7.59E-01		
pH		-2.92E-02	1.15E-01	0.254	0.004
gama		9.77E-03	4.77E-05	205.048	0.944

t(646)=1.964

Explained variability [%] 89.11

Multiple correlation coefficient 0.944

Acaic's inf. criterion 2.28E+04

MEP 8.48E+01

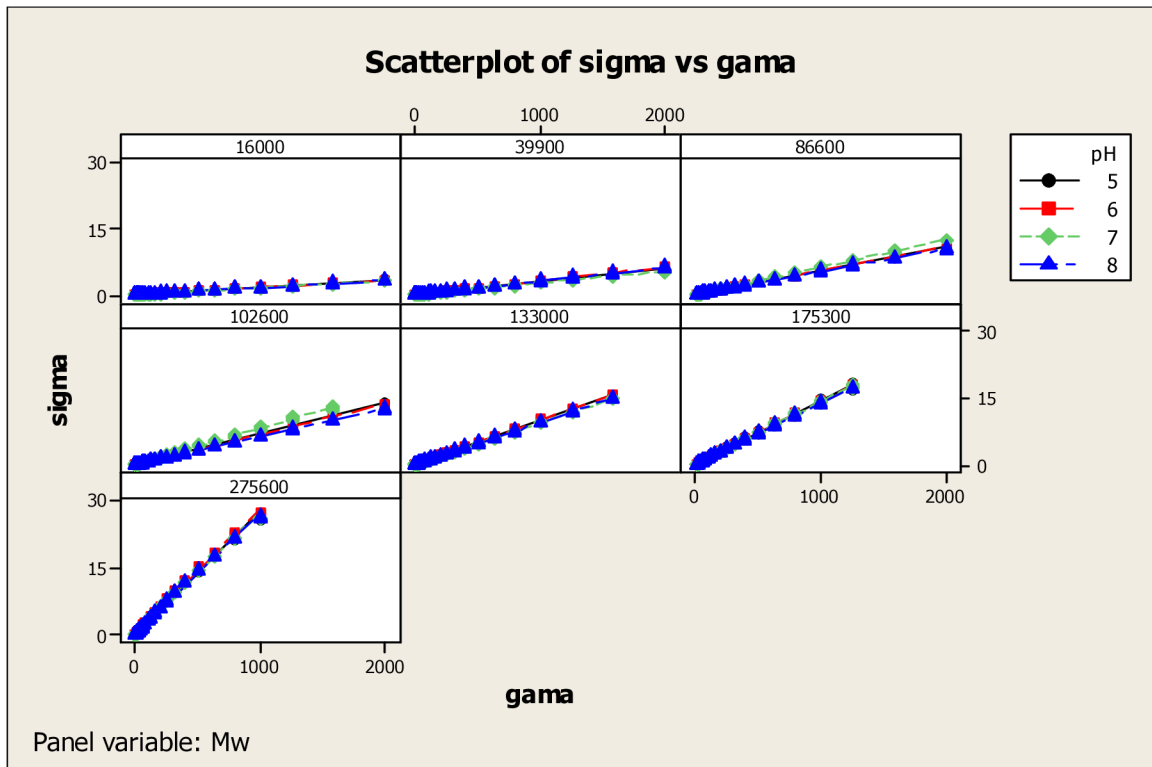


Fig. 3a – plot of shear stress versus shear rate for different Mw, where pH is 5 – 8 (measured raw data)

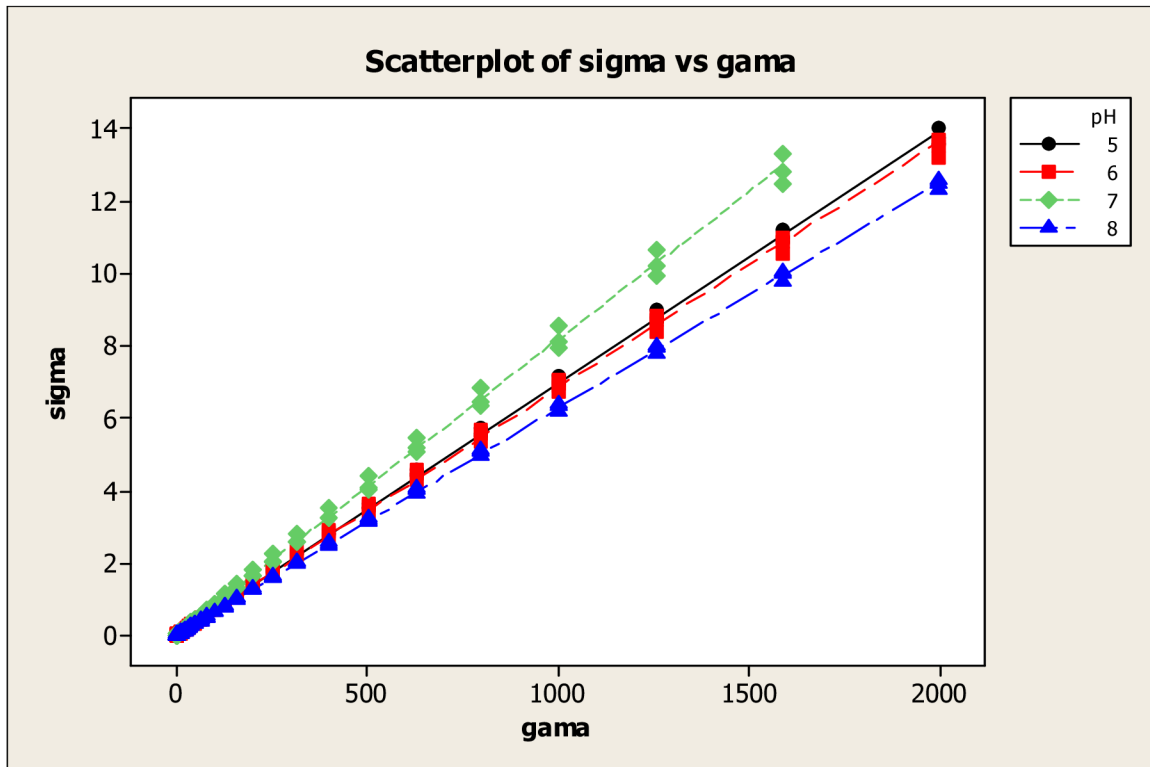



Fig. 3b – plot of shear stress versus shear rate for $M_w = 102.600$, where pH is 5 – 8 (measured raw data).

In case of measurements of Hyaluronan with molecular weight of 102.600 was detected different dependency of shear rate at pH = 5 – 8 in comparison of other molecular weights. (it is shown on Fig. 3a and 3b). The curve at pH = 7 must be between curves for pH = 6 and pH = 8. The reason is in separate preparation of this sample, so it shows on a manual mistake during the preparation.

8.4 Temperature curves

In that unit I have focused on statistics of individual measurements of dynamic viscosity which are specific to each solvent conditions (i.e. PBS7 and water) and temperature. For statistical data processing of two means (way) is the best way via using analysis of variance (ANOVA).

ANOVA provides a statistical test of whether or not the means of several groups are all equal, and therefore generalizes t-test to more than two groups. Doing multiple two-sample t-tests would result in an increased chance of committing a type I error. For this reason, ANOVAs are useful in comparing two, three, or more means.

Statistical data processing was done via using software Minitab v.16  Minitab[®] 16
Statistical Software

Ny vs T in the plots is the dependence viscosity, shear rate versus temperature.

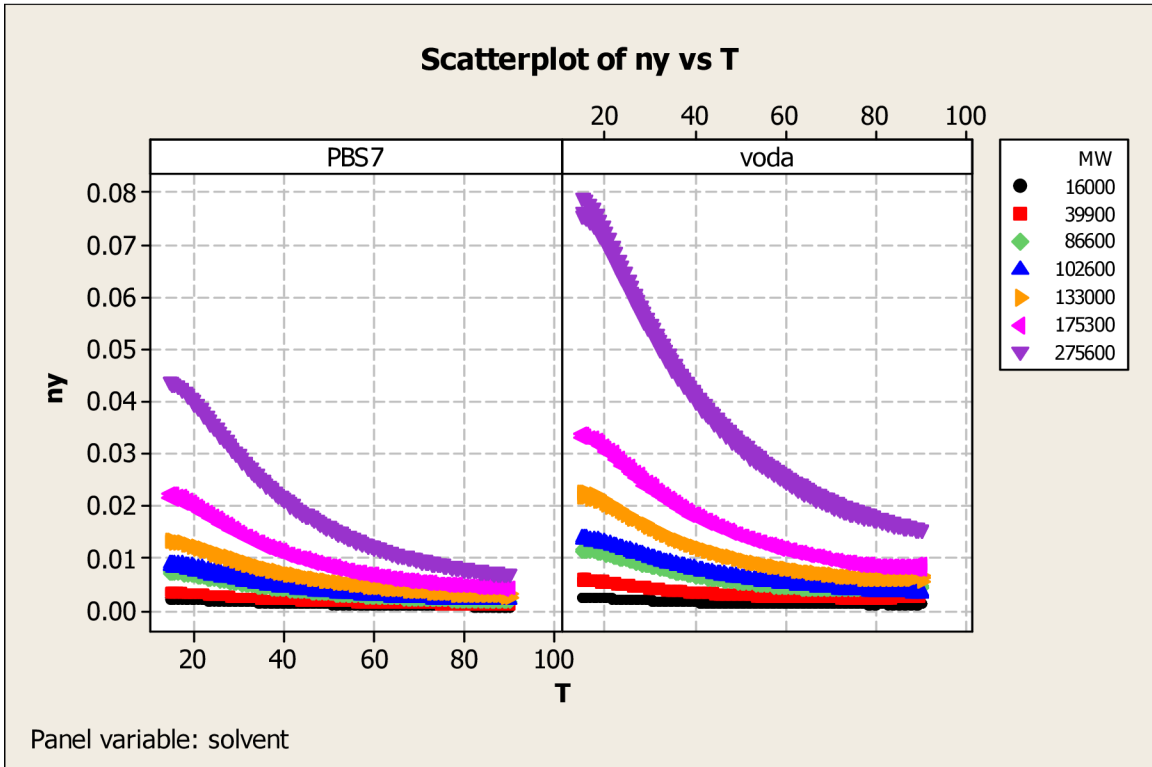


Fig. 4 – plot of dynamic viscosity versus temperature for different solvent (PBS7 and water), where $M_w = 16.000 - 275.600$ (measured raw data).

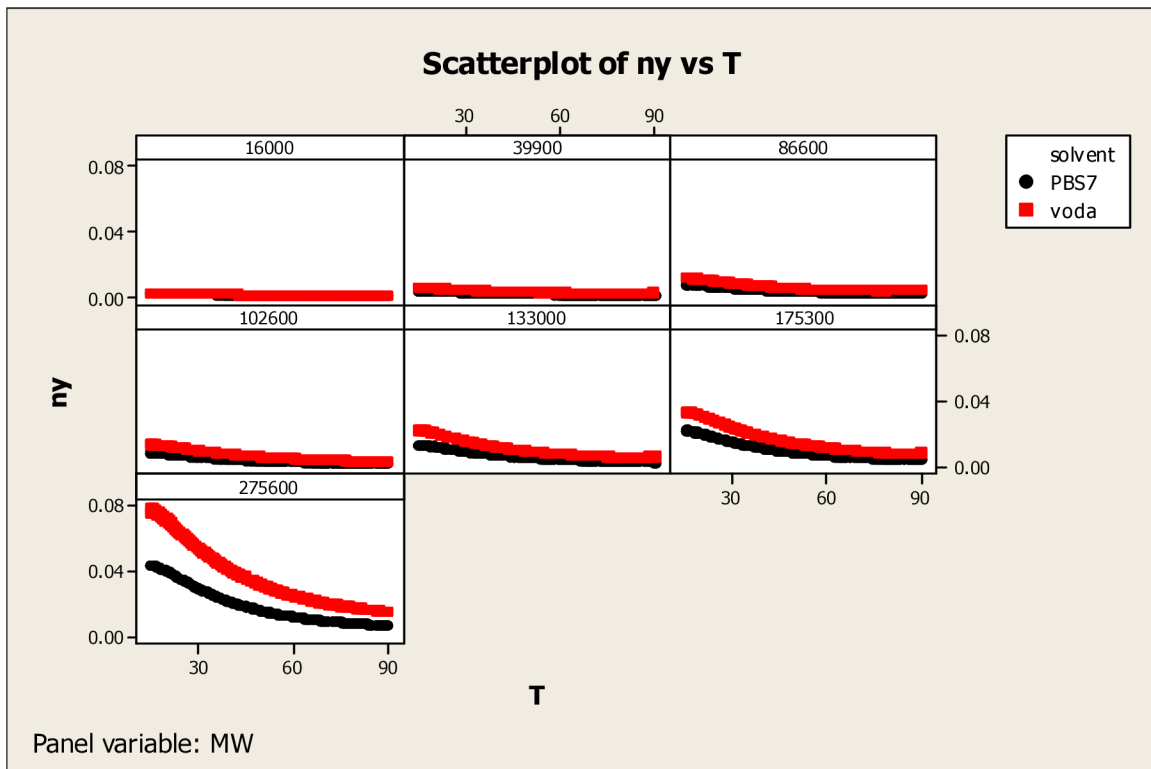


Fig. 5 – plot of dynamic viscosity versus temperature for different molecular weights, where solvent is PBS7 or water (measured raw data).

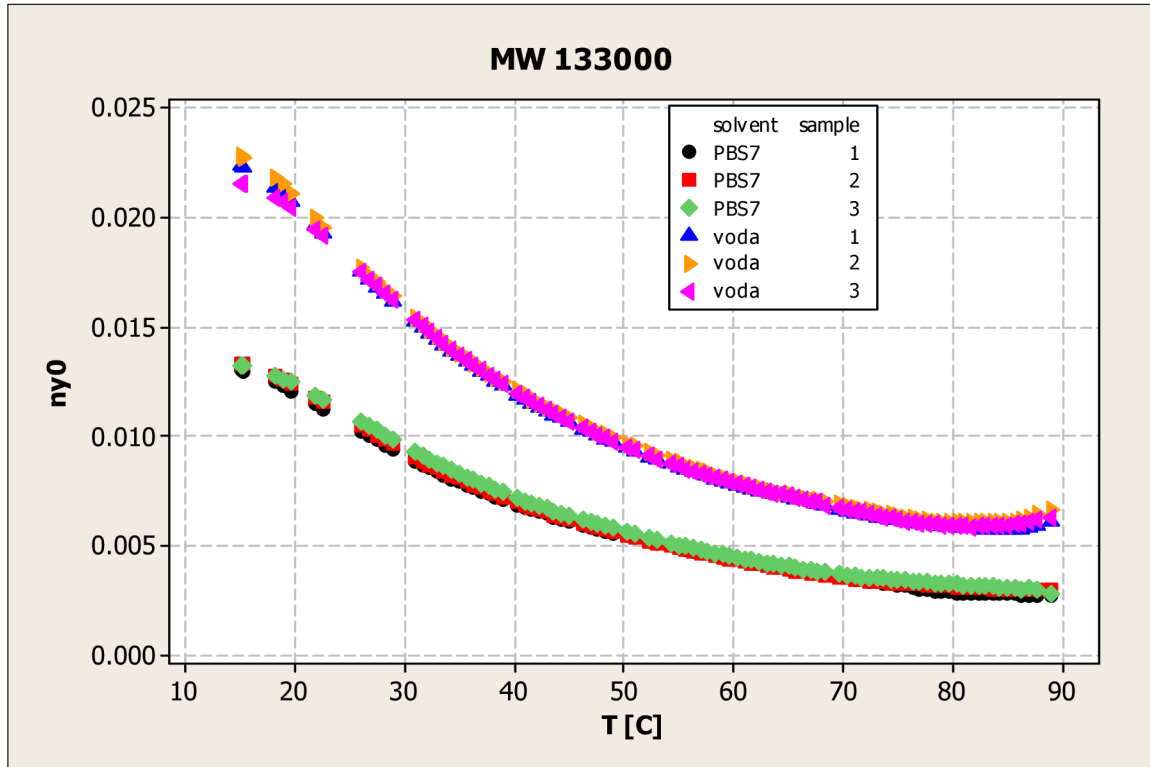


Fig. 6a – plot of dynamic viscosity versus temperature for Mw = 133.000, where solvent is PBS7 or water (measured raw data) and results of ANOVA is shown below in Tab. 8

Tab. 8 Two-way ANOVA: ny versus solvent; T

Source	DF	SS	MS	F	P
Solvent	1	0.0026551	0.0026551	105612.12	0.000
T	92	0.0073888	0.0000803	3194.64	0.000
Interaction	92	0.0003816	0.0000041	165.01	0.000
Error	372	0.0000094	0.0000000		
Total	557	0.0104349			

S = 0.0001586 R-Sq = 99.91% R-Sq(adj) = 99.87%

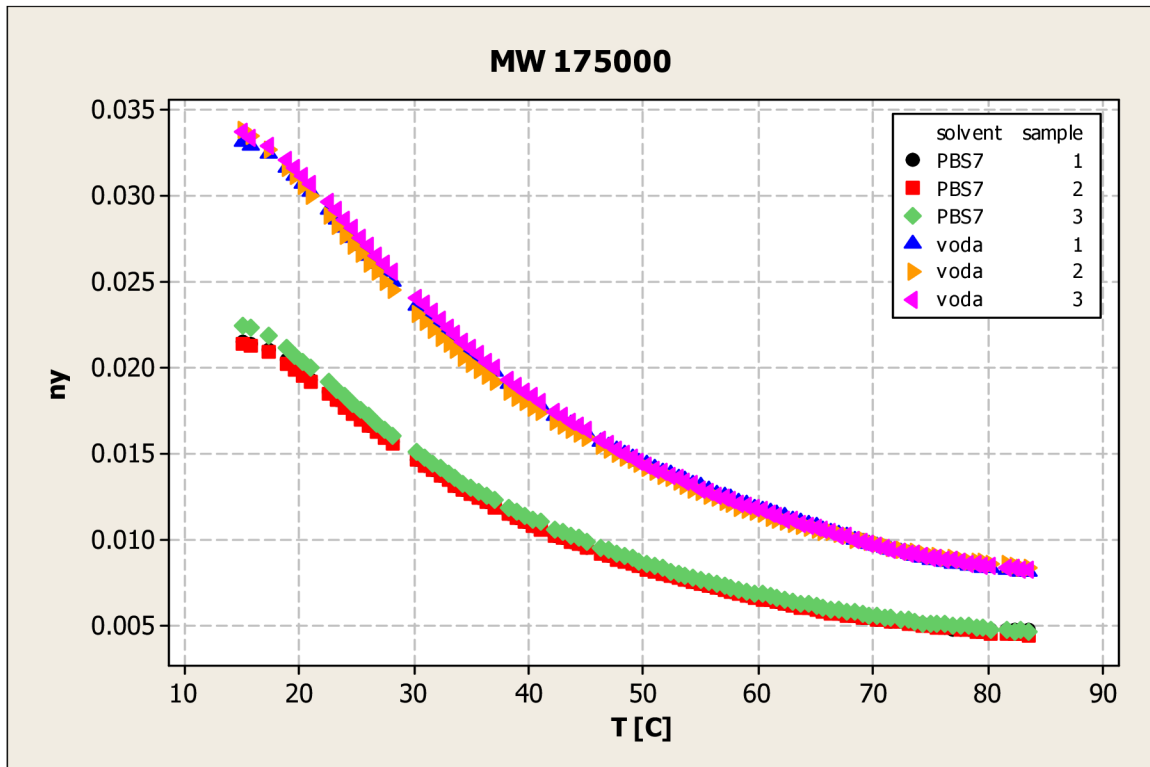


Fig. 6b – plot of dynamic viscosity versus temperature for Mw = 175.000, where solvent is PBS7 or water (measured raw data) and results of ANOVA is shown below in Tab. 9

Tab.9 Two-way ANOVA: ny versus solvent; T

Source	DF	SS	MS	F	P
Solvent	1	0.0056845	0.0056845	90890.23	0.000
T	92	0.0207778	0.0002258	3611.06	0.000
Interaction	92	0.0007552	0.0000082	131.26	0.000
Error	372	0.0000233	0.0000001		
Total	557	0.0272408			

S = 0.0002501 R-Sq = 99.91% R-Sq(adj) = 99.87%

Previous results of ANOVA (Tab. 8 and 9) leads to conclusion that influence of solvent and influence of temperature is statistically significant and moreover the interaction of solvent and temperature is statistically significant too.

9 APPENDIX 2 – PUBLICATION ACTIVITY

9.1 Hyaluronan

9.1.1 Publication

Podzimek, S., Hermannová, M., Bilerová, H., Bezáková, Z., Velebný, V. Solution properties of hyaluronic acid and comparison of SEC-MALS-VIS data with off-line capillary viscometry. *Journal of Applied Polymer Science*, 5 June 2010, Volume 116, Issue 5, Pages: 3013-3020

9.1.2 Conferences

Bilerová, H., Dolník, M., Velebný, V., Pekař M. New view on dissolution and ageing of Hyaluronan solutions. 7th International conference on Hyaluronan in Charleston, USA, 2007.

Bilerová, H., Hánošová, V., Velebný, V. Physical properties of native hyaluronan solutions for preparation nanofibres. Nanocon 2nd International Conference, Olomouc, Czech Republic, 2010. Conference Proceedings ISBN 978-80-87294-18-5

9.1.3 Utility model

Bilerová, H., Velebný, V. Přípravek pro hojení ran a prevenci adheze bandáže na ránu obsahující polysacharidy. A61K 9/70. 2006.

9.1.4 Patent

Valentová, Z., Bilerová, H., Šuláková, R., Velebný, V. Preparation for wound healing and prevention of bandage adhesion to the wound, containing chitosan-glucan. WO/2009/043319.

9.1.5 Book

Pekař, M., Velebný, V., Bilerová, H. Hyaluronan – based nanofibers. Colloids in biotechnology, Ed. Fanun, M. CRC Press, 2011, pp.437-453. ISBN 978-1-4398-3080-2

9.2 Others

Biler, M., Vrbová, H., Nešpůrek, S.^G Poly[(ethylenedioxy)thiophene] conductive films: a new preparative method. *Abstracts. Cargese* : University of Angers and Institute of Scientific Studies, 2005, P30. [International Conference Erpos on Electrical and Related Properties of Solids and Polymers /10./ 10.7.2005-15.7.2005, Cargese]

Biler, M., Vrbová, H., Nešpůrek, S. Conductive poly[(ethylenedioxy)thiophene] films. *Proceedings*. Lanškroun : IMAPS, Brno University of Technology, 2004 - (Šikula, J.) s. 642-647. ISBN 80-239-2835-X. [European Microelectronics and Packaging Symposium /3./. Prague (CZ), 16.06.2004-18.06.2004]

Biler, M., Vrbová, H., Nešpůrek, S., Glezos, N. Poly[(ethylenedioxy)thiophene] conductive films. *Congress Proceedings*. Paris : International Union of Pure and Applied Chemistry, 2004, 2.3.5.1-2.3.5.2. [IUPAC International Symposium on Macromolecules, World Polymer Congress MACRO /40./. Paris (FR), 04.07.2004-09.07.2004]